

AD-R171 875

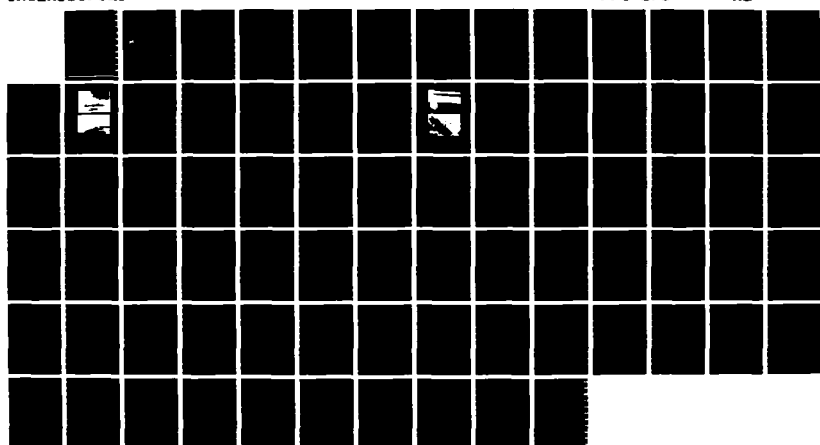
EXTERIOR ELECTROMAGNETIC RESPONSE OF NASA F-106
AIRCRAFT(U) DIKEWOOD ALBUQUERQUE NM V V LIEPA ET AL.
JUN 86 DC-FR-1026. 330-3 AFML-TR-85-95 F29681-82-C-0027

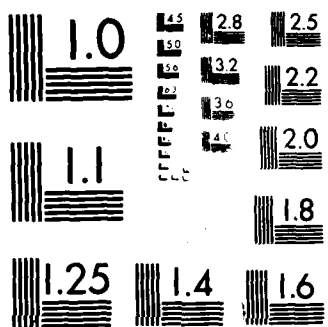
1/1

UNCLASSIFIED

F/G 1/3

NL





MICROCOPY RESOLUTION TEST CHART
NATIONAL BUREAU OF STANDARDS-1963-A

AD-A171 875

EXTERIOR ELECTROMAGNETIC RESPONSE OF NASA F-106 AIRCRAFT

V. V. Liepa
S. T. Pennock

Dikewood, Division of Kaman Sciences Corporation
1613 University Boulevard, N.E.
Albuquerque, New Mexico 87102

June 1986

Final Report

Approved for public release; distribution unlimited.

DTIC
SELECTED
SEP 25 1986
S B D

DTIC FILE COPY

AIR FORCE WEAPONS LABORATORY
Air Force Systems Command
Kirtland Air Force Base, NM 87117-6008

This final report was prepared by Dikewood, Division of Kaman Sciences Corporation, Albuquerque, New Mexico, under Contract F29601-82-C-0027, Job Order 37630131, with the Air Force Weapons Laboratory, Kirtland Air Force Base, New Mexico. Captain Dennis J. Andersh (NTAA) was the Laboratory Project Officer-in-Charge.

When Government drawings, specifications, or other data are used for any purpose other than in connection with a definitely Government-related procurement, the United States Government incurs no responsibility or any obligation whatsoever. The fact that the Government may have formulated or in any way supplied the said drawings, specifications, or other data, is not to be regarded by implication, or otherwise in any manner construed, as licensing the holder, or any other person or corporation; or as conveying any rights or permission to manufacture, use, or sell any patented invention that may in any way be related thereto.

This report has been authored by a contractor of the United States Government. Accordingly, the United States Government retains a nonexclusive, royalty-free license to publish or reproduce the material contained herein, or allow others to do so, for the United States Government purposes.

This report has been reviewed by the Public Affairs Office and is releasable to the National Technical Information Service (NTIS). At NTIS, it will be available to the general public, including foreign nationals.

If your address has changed, if you wish to be removed from our mailing list, or if your organization no longer employs the addressee, please notify AFWL/NTAA, Kirtland AFB, NM 87117 to help us maintain a current mailing list.

This report has been reviewed and is approved for publication.

Dennis J. Andersh
DENNIS J. ANDERSH
Captain, USAF
Project Officer

James F. Young
JAMES F. YOUNG
Maj, USAF
Chief, Applications Branch

FOR THE COMMANDER
Philip J. Messuri
PHILIP J. MESSURI
Maj, USAF
Chief, Aircraft and Missiles Division

DO NOT RETURN COPIES OF THIS REPORT UNLESS CONTRACTUAL OBLIGATIONS OR NOTICE ON A SPECIFIC DOCUMENT REQUIRES THAT IT BE RETURNED.

UNCLASSIFIED

SECURITY CLASSIFICATION OF THIS PAGE

REPORT DOCUMENTATION PAGE

A171875

1a. REPORT SECURITY CLASSIFICATION Unclassified		1b. RESTRICTIVE MARKINGS										
2a. SECURITY CLASSIFICATION AUTHORITY		3. DISTRIBUTION / AVAILABILITY OF REPORT Approved for public release; distribution unlimited.										
2b. DECLASSIFICATION / DOWNGRADING SCHEDULE												
4. PERFORMING ORGANIZATION REPORT NUMBER(S) DC-FR-1026.330-3		5. MONITORING ORGANIZATION REPORT NUMBER(S) AFWL-TR-85-95										
6a. NAME OF PERFORMING ORGANIZATION DIKEWOOD, Division of Kaman Sciences Corporation	6b. OFFICE SYMBOL (If applicable)	7a. NAME OF MONITORING ORGANIZATION Air Force Weapons Laboratory										
6c. ADDRESS (City, State, and ZIP Code) 1613 University Boulevard, NE Albuquerque, New Mexico 87102		7b. ADDRESS (City, State, and ZIP Code) Kirtland AFB, New Mexico 87117-6008										
8a. NAME OF FUNDING / SPONSORING ORGANIZATION	8b. OFFICE SYMBOL (If applicable)	9. PROCUREMENT INSTRUMENT IDENTIFICATION NUMBER F29601-82-C-0027										
8c. ADDRESS (City, State, and ZIP Code)		10. SOURCE OF FUNDING NUMBERS <table border="1"><tr><td>PROGRAM ELEMENT NO. 64711F</td><td>PROJECT NO. 3763</td><td>TASK NO. 01</td><td>WORK UNIT ACCESSION NO. 31</td></tr></table>		PROGRAM ELEMENT NO. 64711F	PROJECT NO. 3763	TASK NO. 01	WORK UNIT ACCESSION NO. 31					
PROGRAM ELEMENT NO. 64711F	PROJECT NO. 3763	TASK NO. 01	WORK UNIT ACCESSION NO. 31									
11. TITLE (Include Security Classification) EXTERIOR ELECTROMAGNETIC RESPONSE OF NASA F-106 AIRCRAFT												
12. PERSONAL AUTHOR(S) Liepa, V.V.; Pennock, S.T.												
13a. TYPE OF REPORT Final	13b. TIME COVERED FROM 83-01 TO 85-04	14. DATE OF REPORT (Year, Month, Day) 1986 June	15. PAGE COUNT 78									
16. SUPPLEMENTARY NOTATION												
17. COSATI CODES <table border="1"><tr><th>FIELD</th><th>GROUP</th><th>SUB-GROUP</th></tr><tr><td>01</td><td>03</td><td></td></tr><tr><td>20</td><td>14</td><td></td></tr></table>		FIELD	GROUP	SUB-GROUP	01	03		20	14		18. SUBJECT TERMS (Continue on reverse if necessary and identify by block number) Electromagnetic (EM) Response NASA F106B Aircraft, EM Coupling Scale F106A Model EM Tests	
FIELD	GROUP	SUB-GROUP										
01	03											
20	14											
19. ABSTRACT (Continue on reverse if necessary and identify by block number) Frequency domain surface current and charge data are presented for the NASA F-106B aircraft when illuminated with a plane electromagnetic wave. Measurements were made on a 1:48 scale F-106A model that had been modified to represent the NASA F-106B. The measurement locations and the field quantities measured correspond to those on the NASA aircraft. Nine different excitations were used including those corresponding to the situations in HPD, VPD-II, and VPD-II fly-by tests performed at Kirtland Air Force Base. The amplitude and phase measurements on the models were performed over 100 to 4770 MHz and for the full-scale aircraft this corresponds to 2.1 to 100 MHz coverage.												
20. DISTRIBUTION / AVAILABILITY OF ABSTRACT <input checked="" type="checkbox"/> UNCLASSIFIED/UNLIMITED <input type="checkbox"/> SAME AS RPT <input type="checkbox"/> DTIC USERS		21. ABSTRACT SECURITY CLASSIFICATION Unclassified										
22a. NAME OF RESPONSIBLE INDIVIDUAL Capt Dennis J. Andersh		22b. TELEPHONE (Include Area Code) (505) 844-0327	22c. OFFICE SYMBOL NTAA									

UNCLASSIFIED

SECURITY CLASSIFICATION OF THIS PAGE

UNCLASSIFIED

SECURITY CLASSIFICATION OF THIS PAGE

CONTENTS

<u>Section</u>		<u>Page</u>
I.	INTRODUCTION	1
II.	FACILITY	3
III.	MODEL	6
IV.	MEASUREMENTS AND DATA	9
	1. MEASUREMENTS	9
	2. INTERPRETATION OF DATA	15
V.	CONCLUSIONS AND RECOMMENDATIONS	22
VI.	DATA PLOTS	23

Acceptance Date		
NTIS	Serial	
DTIC	Number	
Unannounced		
Justification		
By _____		
Distribution		
Availability		
Dist	Available for	
	Special	
A-1	23	6/65

DISCLAIMER NOTICE

**THIS DOCUMENT IS BEST QUALITY
PRACTICABLE. THE COPY FURNISHED
TO DTIC CONTAINED A SIGNIFICANT
NUMBER OF PAGES WHICH DO NOT
REPRODUCE LEGIBLY.**

I. INTRODUCTION

The data presented here were obtained to support the lightning measurement program in which the NASA F-106B aircraft is used for collection of direct strike and near miss lightning data (Ref. 1). These data are recorded as output from current and charge sensors mounted on the aircraft and, since the spectrum of the lightning falls well within the range of the aircraft natural resonances, the recorded data may be appreciably affected by these resonances.

The measurements presented here provide the exterior electromagnetic response of the aircraft when illuminated by a plane wave. These are frequency domain data for the surface current and charge (amplitude and phase) normalized to the incident field and, as such, can be referred to as transfer functions for the exterior coupling. A cursory look at the data immediately provides the aircraft resonant frequencies and the enhancement of the surface field at the resonances. Transformation of the data to time domain will provide the impulse response which, when convoluted with an appropriate driving waveform, would give the time domain field on the aircraft.

Some of these data have already been used to determine expected signal amplitudes and accordingly preset the recorder gain settings for the full-scale ground and fly-by tests performed at Kirtland Air Force Base*. A too-high (gain) setting of the digitizers can result in saturation of the signal, or a low setting can result in a low dynamic range or a noisy signal. Other applications of these data include the comparison of scale model data (frequency domain) with the data obtained in full-scale simulator (time domain) tests and, eventually, as a data base for correction of the measured lightning data by NASA F-106B.

1. Baum, C. E., E. L. Breen, F. L. Pitts, G. D. Sower and M. E. Thomas, "The measurement of lightning environmental parameters related to interaction with electronic systems, IEE Trans., Electromagnetic Compatibility, Vol. 24, pp.123-137, 1982.

* Lee, K.S.H., Dikewood, personal communication, March 1984.

The data presented herein were measured for the same locations and field components for which the NASA F-106B has been instrumented. The measurements of charge and current are presented for eight locations or stations on the model under up to nine excitation conditions which include

- top incidence, E-parallel to the fuselage
- top incidence, E-perpendicular to the fuselage
- side incidence, E-vertical, etc

These excitations were selected to simulate the HPD, VPD-II and VPD-II fly-by test situations as well as lightning measurement situations such as bottom incidence (Ref. 2).

The data are presented in the form of amplitude and phase plots as a function of the full-scale frequency. In total there are 48 transfer functions presented. The data have also been stored on magnetic tape for future availability.

2. Riffe, L. G., Detailed Test Requirements in Comparison of Natural Direct Strike Lightning and Simulated NEMP on NASA F-106, TRW Report No. 42156-6011-UT-00, Albuquerque, N.M., December 1983 (DRAFT).

II. FACILITY

The measurements were made in the University of Michigan Radiation Laboratory's surface (and near) field facility (Ref. 3), a block diagram of which is shown in Figure 1. The system is a CW one in which the frequency is swept (stepped) over a 100 to 4770 MHz range. A key part of the facility is a tapered anechoic chamber approximately 50 ft in length. The rectangular test region is 18 ft wide and 12 ft high. The rear wall is covered with 72-in high-performance pyramidal absorber, with 18-in material used on the side walls, floor and ceiling. The material in the tapered section (or throat) is 2-in hairflex absorber. In a way the chamber can be thought of as a lossy-wall horn antenna terminated by the rear wall. The excitation signal is launched from a single exponentially tapered broadband antenna located at the apex of the chamber. The antenna is fixed and since the radiated signal is horizontally polarized, the pseudoplane wave in the center ('quiet zone') portion of the test region is also horizontally polarized.

The instrumentation is centered around a Hewlett-Packard 8410B network analyzer that has been modified to operate as an HP8409 which phase locks the measurement frequency (r.f.) to the network analyzer local oscillator signal provided by a synthesizer. An HP9830A calculator controls the frequency to be measured, switches in the appropriate power amplifiers and low-pass filters, and reads and stores the amplitude and phase of the signal picked up by the sensor. During a run, the frequencies are stepped from 100 to 4770 MHz in 500 steps. Because of the limited memory size of the calculator, the data are recorded in four bands: 100 to 410 MHz (in 2.5 MHz steps), 415 to 1035 MHz (in 5.0 MHz steps), 1030 to 2280 MHz (in 10.0 MHz steps), and 2290 to 4770 MHz (in 20.0 MHz steps). The data from each band are stored by the HP9830A calculator on standard audio cassettes and later are transferred to an HP9845B calculator for processing and plotting the data. If substantial processing or computation is involved, or if a need exists to write the data on standard computer tape, or to make it available on file to other users via computer nets, the data are transmitted to the central University of Michigan AMDAHL (IBM compatible) computer system.

3. Lee, K.S.H. (ed.), EMP Interaction: Principles, Techniques and Reference Data, AFWL-TR-80-402, pp. 267-276, December 1980.

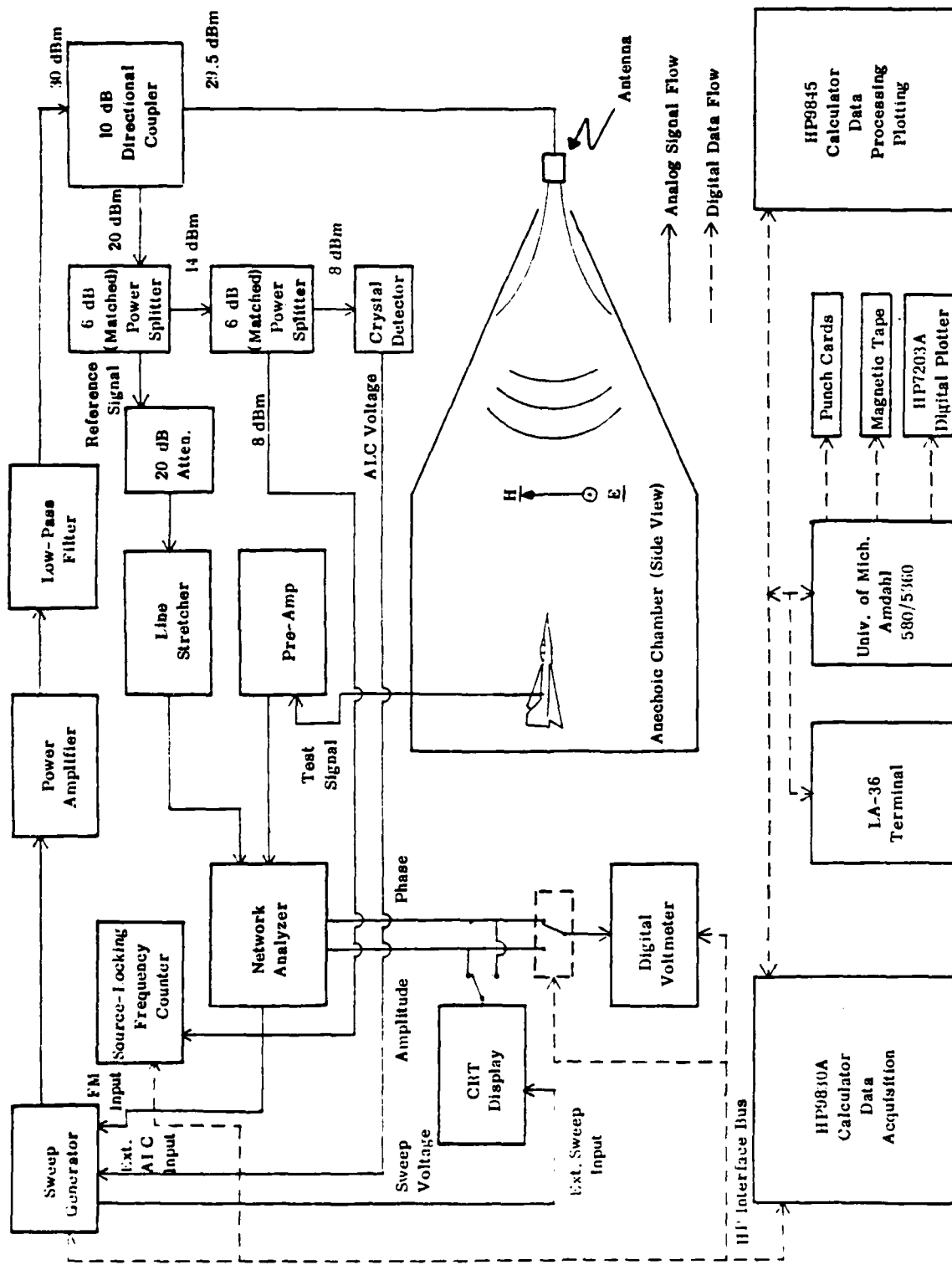


Figure 1. Block diagram of the facility.

The signal that is measured by the network analyzer is a function not only of the surface field but also of the entire facility, including the probe, chamber, antenna, amplifiers and cabling; it would be virtually impossible to separate and to correct for the contribution of each. The approach taken is to apply an appropriate calibration or normalization to the entire system whereby the response of the facility and the instrumentation are, in principle and practice, removed from the test object. In short, a measurement is made on an airplane model (test measurement) and then repeated on a metal sphere of known diameter (calibration); the ratio of the two plus additional correction for the sphere response gives the required data.

III. MODEL

Since F-106B models were not readily available, we used a 1:48 scale F-106A kit (Monogram, No. 5809) and built it into a NASA F-106. The model was constructed in the wheels-up position and without any external stores. The basic difference between the F-106A and NASA F-106B is that the F-106A is a single seater and the NASA F-106B is a two seater. Hence, the canopy for the NASA F-106B is slightly higher and extended toward the back over the copilot's seat. In our model, the original F-106A canopy was used, but by deleting the coating or metallization of the rear portion that normally would be metal, an effect of a larger canopy was simulated. To simulate the metal framing of the canopy, narrow strips of copper tape were used. On the model the joints and other surface imperfections were filled in with automotive body putty, sanded to a smooth finish, and the entire model apart from the radome and canopy were painted with several coats of high grade silver paint (DuPont No. 4817, or equivalent).

The fuselage (from the bulkhead to the top of the vertical stabilizer) and the wingspan were measured and by slight sanding (shortening) of the wingtips the same length-to-wingspan ratio was achieved as for the full scale dimensions. To simulate the NASA boom a 0.8 mm (0.032 inch) diameter brass wire was extended from the bulkhead forward through the tip of the plastic radome. The resultant scale factor for both the fuselage and the wingspan came to 1:47.667 and was used in changing the laboratory frequencies to the full-scale frequencies simply by dividing the laboratory frequency by 47.667.

Figure 2 shows the full scale and the model dimensions needed for scaling. Also shown in the figure are the measurement locations or stations. In Figure 3 are two photographs of the model showing the overall view and the canopy detail.

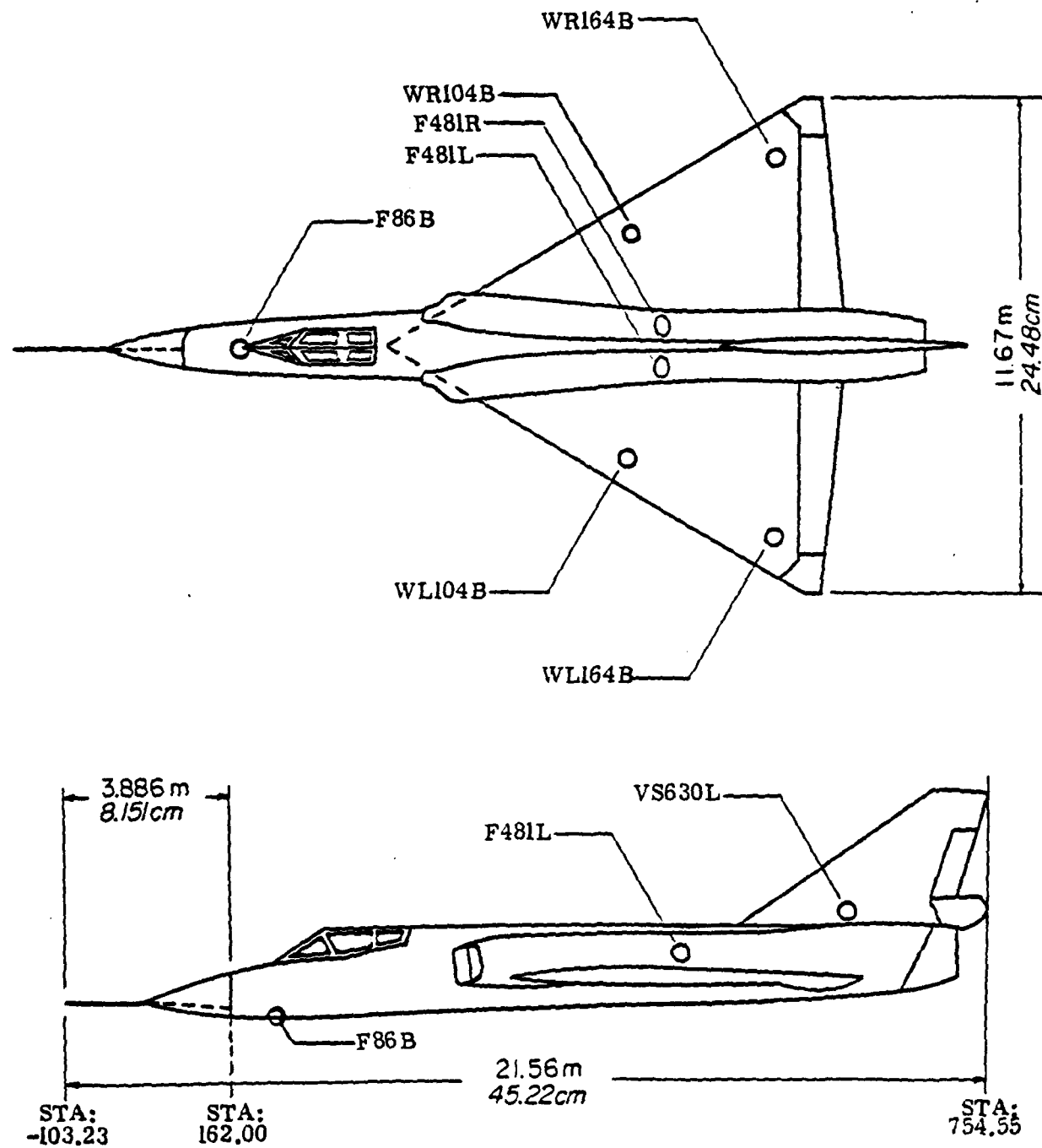


Figure 2. Locations of measurement stations and dimensions of model and full-scale aircraft. (Dimensions in meters: full-scale; dimensions in centimeters: model.)

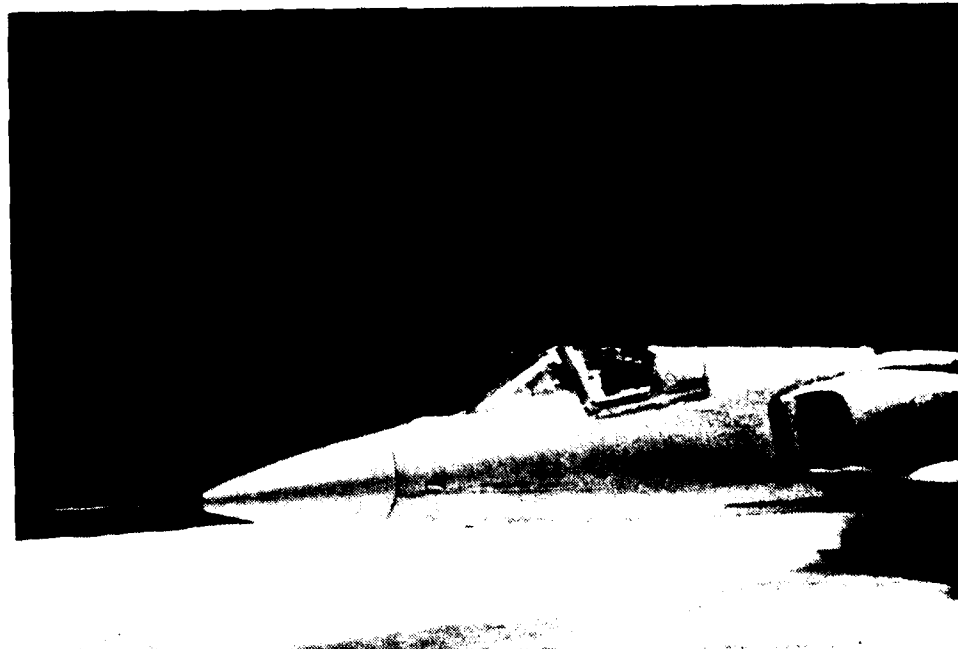
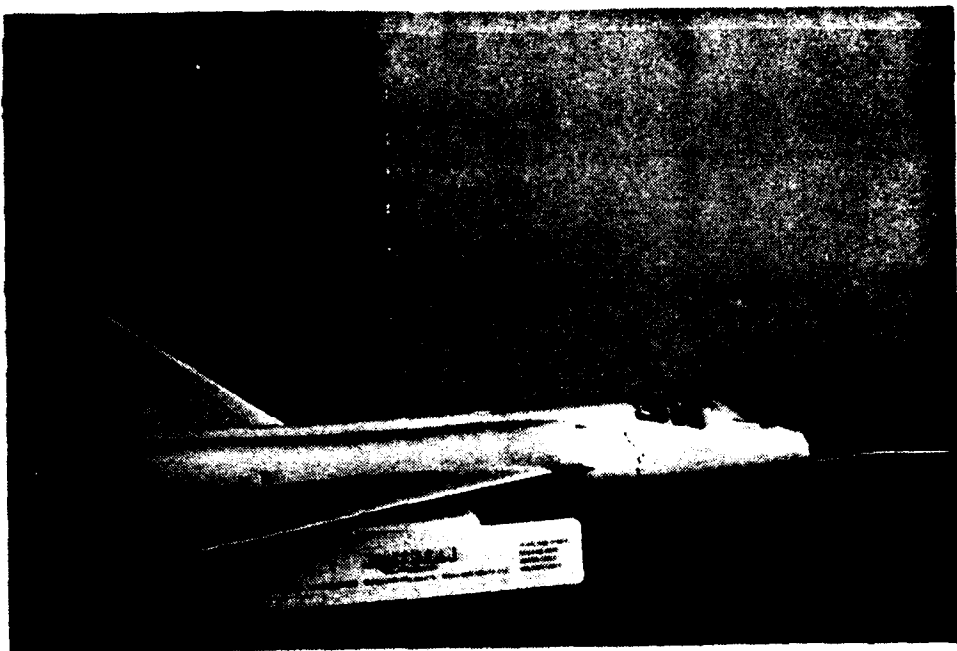


Figure 3. Photographs of the model used. Upper photo: model after assembly and painting with silver paint. Lower photo: plastic radome and canopy.

IV. MEASUREMENTS AND DATA

1. MEASUREMENTS

The procedures used to make the measurements were similar to those of previous programs that have included measurement of surface fields on E-3A, F-16A, B-52, A-7E and, most recently, F-111B aircraft (Ref. 4). In the anechoic chamber, the model was supported on a Styrofoam pedestal, simulating for all practical purposes the free space or in-flight condition. The measurements of the surface currents and charges were made at locations on the model indicated in Figure 2. The locations are further described in Table 1. On the fuselage the locations are identified by station numbers corresponding to inches on the full-scale aircraft measured from an imaginary plane on the radome located 103.23 in from the tip of the boom (Fig. 2). For example, a designation F86B refers to fuselage (F), Bottom (B) 86 in from the imaginary reference. The wing stations are identified by 'W' and the vertical stabilizer by 'VS'. Letters 'L' and 'R' refer to the left (port) or right (starboard) side, respectively.

Figure 4 shows the nine illuminations for which the measurements were made and the convention used to define the directions of the surface field components. The excitations are further described in Table 2. On the fuselage the axial current component, J_a , is defined in the direction of the fuselage axis, and on the wings it is in the directional normal to the fuselage. The circumferential component, J_c , is always perpendicular to J_a , and the normal electric field component (charge) is always defined to be in the outward direction.

Of the eight measurement locations and the nine excitations indicated in Figures 2 and 4, respectively, not all of the possible combinations were measured or presented. Excluded were cases which were of no interest for the full-scale measurements program and cases where the data were bad, for reasons such as broken cable or loose connections. The measurements were made using laboratory-constructed miniature (current) loops and (charge) monopoles as

4. Liepa, Valdis V., Free Space Model FB-111A Scale Model Measurements,
University of Michigan Radiation Laboratory Report No. 017463-5-T;
Interaction Application Memo 39, July 1982.

TABLE 1. F-106 MEASUREMENT STATIONS

Station	Sensor Location	Measurement	Sensor Location Boundaries
F86B	Panel on bottom of forward fuselage	Q	On centerline, between STA:77.00 and STA:94.76
F481L	Panel on upper fuselage, port side	JC	Between STA:472.00 and STA:487.80
F481R	Panel on upper fuselage, starboard side	JA	Between STA:472.00 and STA:487.80
VS630L	Panel on port side of vertical stabilizer	Q	Between STA:614.80 and STA:645.28, above WL34.70, through WL49.50
WL104B	Panel on bottom of port wing	JA	Between STA:431.00 and STA:472:00 between BL160.44 and BL107.50
WL164B	Panel on bottom of port wing	Q	Between STA:556.75 and STA:593.46, between BL160.44 and BL167.94
WR104B	Panel on bottom of starboard wing	JA	Between STA:431.00 and STA:472.00 between BL99.94 and BL107.50
WR164B	Panel on bottom of starboard wing	0	Between STA:445.75 and STA:593.46, between BL160.44 and BL167.94

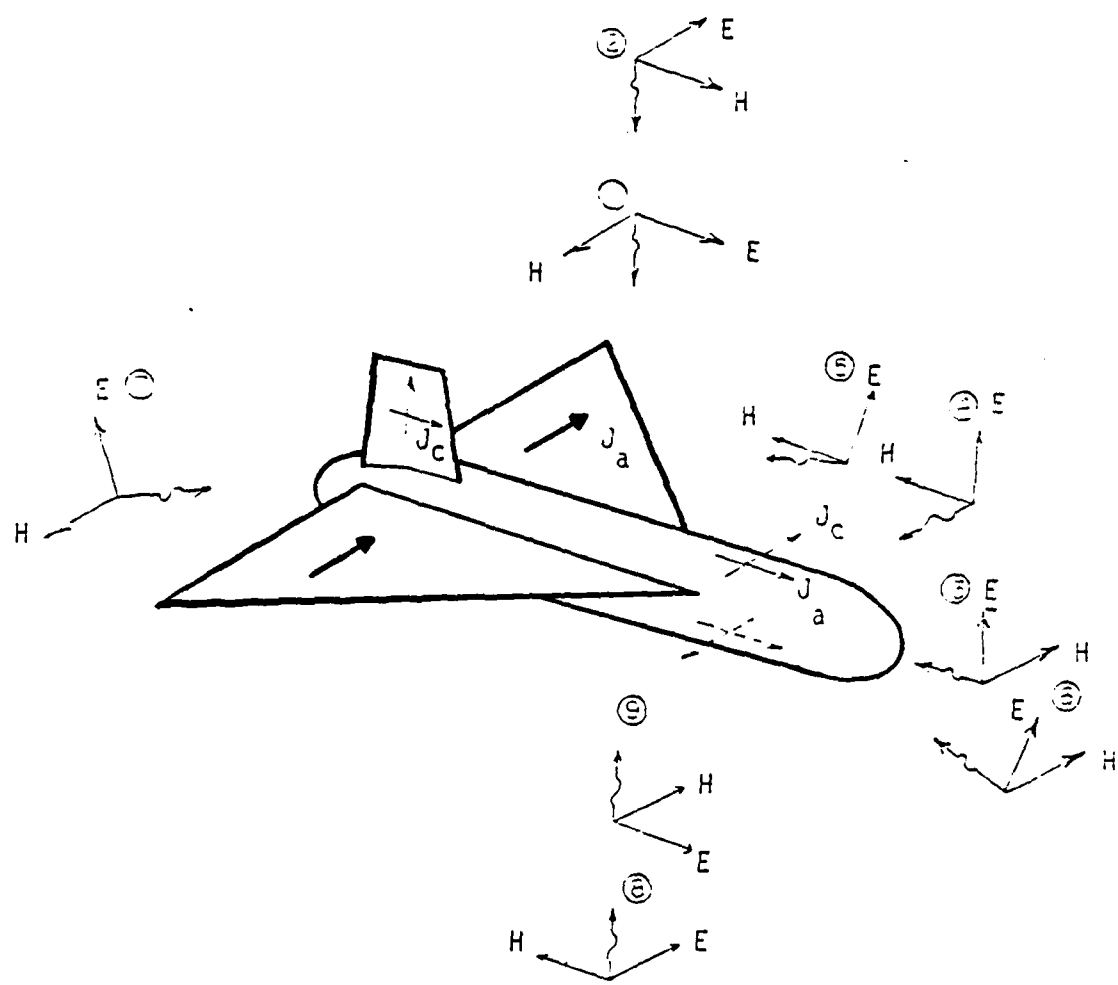


Figure 4. Excitation field and surface current directions on the model.

TABLE 2. EXCITATION DESCRIPTIONS

Number	Description
1	Top incidence, E parallel to fuselage; E direction from tail to nose
2	Top incidence, E perpendicular to fuselage; E direction from right to left wing
3	Nose-on incidence, E vertical
4	Left-side incidence; E vertical
5	Left-side incidence, 30 degrees below; E vertical
6	Nose-on incidence, 30 degrees below; E vertical
7	Tail-on incidence, 30 degrees below; E vertical
8	Bottom incidence, E perpendicular to fuselage; E direction from right to left wing
0	Bottom incidence, E parallel to fuselage; E direction from tail to nose

Also refer to Fig. 2

shown mounted on the model in Figure 5. In the top photo is the current sensor mounted at F481R to measure the axial current J_a . The sensor was constructed using a 0.020-in-dia 50- Ω semirigid coaxial cable and an OSSM-series (Omni-Spectra, Inc.) output connector. It is a half-loop, ground plane sensor, about 3 mm-dia attached to a 10-mm square ground plane. The lower photo shows a charge probe mounted on the far left side of the vertical stabilizer at VS630L to measure the charge. It is also built on a 10-mm square plate and the sensing element is simply a 3-mm extension of the center conductor (with the dielectric) of the coaxial above the plate. The dielectric is left on strictly for rigidity.

Due to the excellent detail of the model it was easy to identify the panels on which the sensors are mounted on the actual aircraft. To mount the probes on the model, a 1/4 in-dia hole is drilled at the center of the appropriate panel, through which the connector and the cable are passed, and the probe is then taped down with conducting adhesive copper tape (No. 1181, 3-M Co.). Only one probe is mounted on the model at a time, and after the measurement the probe is moved to the next location and the previous hole taped over with copper tape.

A typical measurement consists of two parts: the calibration and the test measurement. For the calibration the signal is measured with the same probe on a body whose surface field is known--usually a sphere 3.133 in-dia that can be parted into two hemispheres to allow a surface probe to be mounted. The probe is then removed from the sphere and remounted on the model. The (test) measurement is repeated without any other changes. The ratio of the test data to the sphere data, plus a correction to relate the sphere data to the incident field, gives the field on the body relative to the incident field value, i.e., the transfer function.

How accurately the sphere and the model can be placed in the chamber relative to some reference plane determines the phase accuracy of the measurement. Our goal is to be accurate in placement within 1 mm, but in practice the difference may be 2 or 3 mm, which for full scale translates to 0.15 deg at 1.0 MHz and increasing to 7.5 deg at 50 MHz.

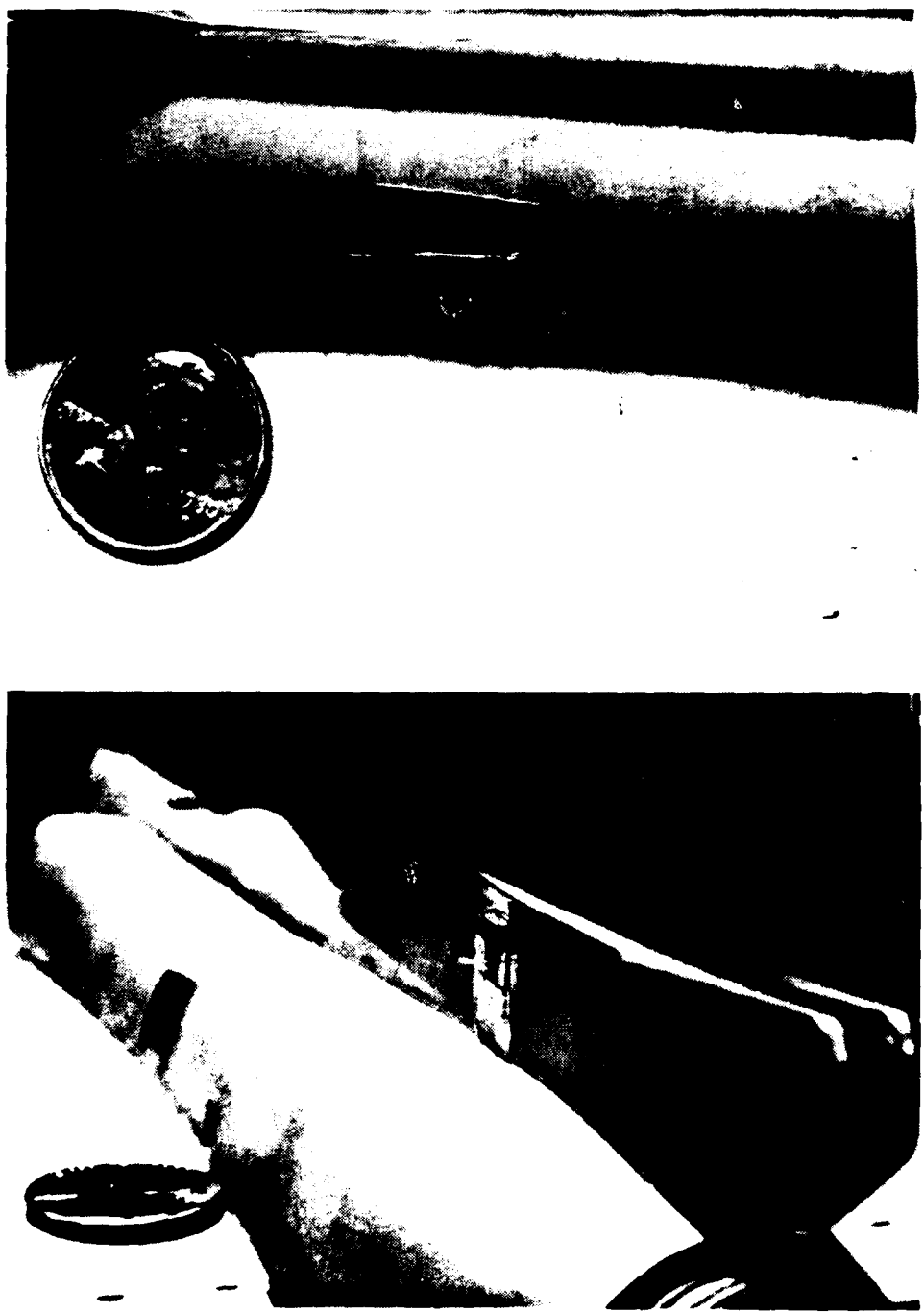


Figure 5. Probes used in measurements. Top photo: current loop mounted on the right side of the fuselage at STA:F481R to measure axial current. Bottom photo: charge probe mounted on the left side of the vertical stabilizer at STA:VS630L.

2. INTERPRETATION OF DATA

For an illustration of the data measured, Figure 6 shows the charge measured on the bottom of the wing for top incidence with the electric field parallel to the fuselage. In the upper right-hand corners of this (and other) plots there is an abbreviated title of form

F-106A, STA:WL164B,1,Q;FT1617

which identifies the particular measurement. The abbreviations are as follows:

F-106A	model used (modified to represent F-106B)
STA:WL164B	measurement station, wing, left, bottom (c.f. Fig. 2)
1	excitation, top incidence, E-parallel to fuselage (c.f. Fig. 4)
Q	field component measured
FT1617	data filename

The raw data from a measurement is usually somewhat noisy near the low end (2 - 20 MHz) and on many measurements takes off above 95 MHz, as shown by the dotted line in Figure 6. This can be attributed to the noisy low level signal in calibration measurements due to low available excitation power. Since such rise at the high frequency end, as well as a similar one at the low frequency end, can be attributed to the measurement noise, ends of the curves are often cut and, consequently, one will find that not all data cover the same frequency range. For example, the highest frequency measured is $4770/47.667 = 100.1$ MHz, but when processed it may be 95.6 MHz due to the cutting off the top end of the curve.

To remove the noise or rapid oscillation that appears to be caused by chamber reflection and cable mismatches, the data are processed through the FILTR5 program that gives slight filtering or smoothing based on convolution and convolves $\text{sinc}(= \sin x/x)$ functions with the frequency data. The program was developed for the FB-111A measurements (Ref. 4) and was then called FILTR2. Minor changes have been added to FILTR5. The convolution of the sinc function with frequency data is equivalent to gating or multiplying the time domain signal by a window function. The filtering that has been applied to the data presented has an equivalent window 300 m long, or about 15 aircraft

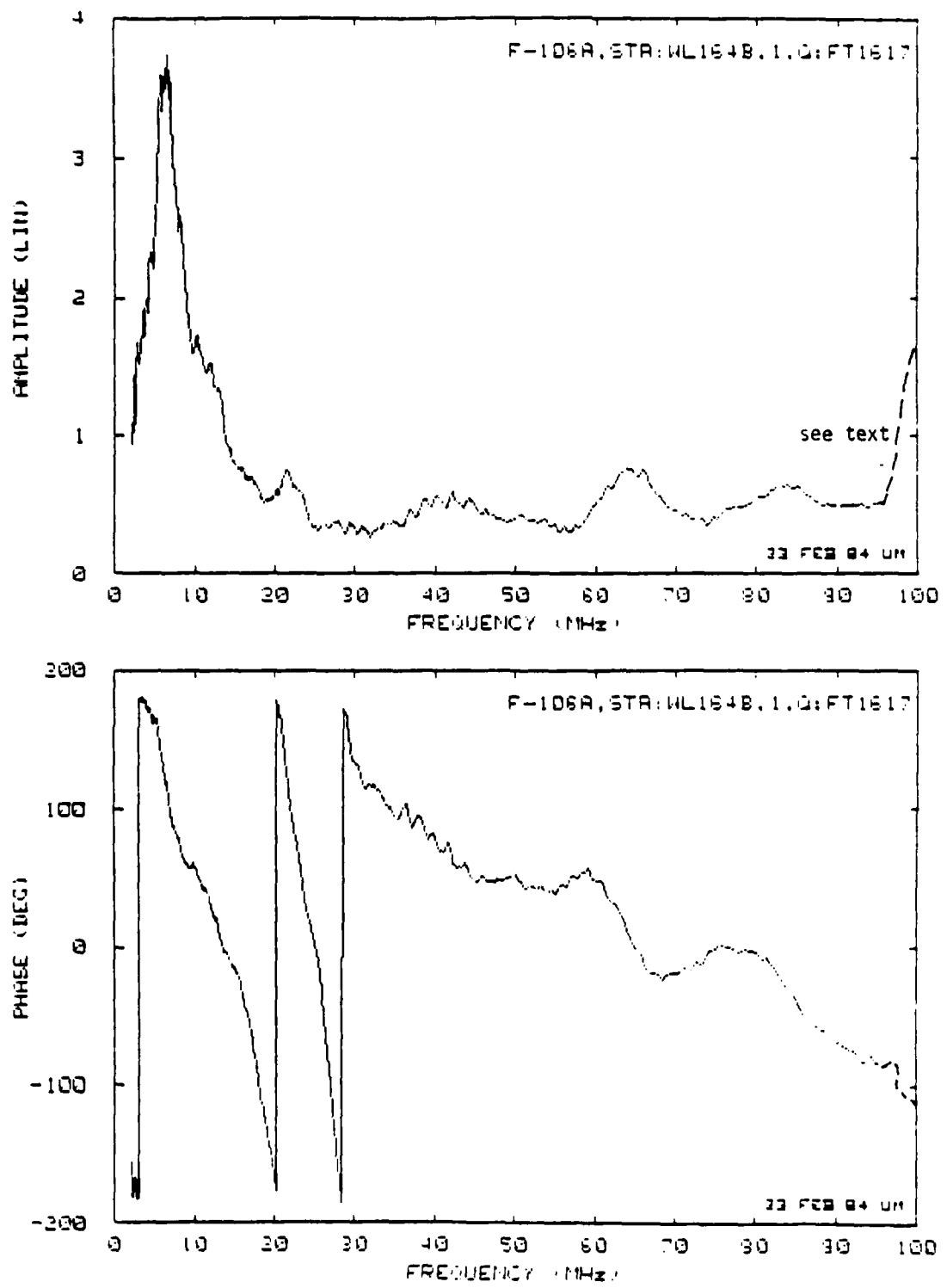


Figure 6. Illustration data (unfiltered).

lengths. As seen in Figure 7, such filtering removes the noise, but still retains even the fine oscillation seen in the 30 to 50 MHz range of the curve. Such oscillations are estimated to be coming from a scatterer some 150 m from the aircraft, or about seven aircraft lengths. In the new measurements such is a distance from the model to the chamber ceiling, for example. Decreasing the window size would remove these oscillations, but at the same time would also lower the resonant peak.

All data presented have been filtered or gated with a 300-m window and in the process the filenames changed from FT to FX prefixes.

The data presented are all normalized to the incident field value, i.e., J/H_0 for the surface current and E_n/E_0 for the charge. The phase is referenced to that of the incident field at the location where the measurement is made, based on the $\exp(j\omega t)$ time convention. In Figure 7, for example, E_n/E_0 or charge starts from about unity at 2.0 MHz, rises to a peak value of about 3.6 at 6.3 MHz and then wanders about a value of 0.5 up to 95.0 MHz. The phase starts at -180 deg and keeps on decreasing with frequency, which is consistent with the particular situation since for the top incidence the energy must travel around the wing to get to the bottom at the measurement point, which is a longer path than a direct line used in defining the phase reference.

Table 3 summarizes the cases for which the data are presented in Section 4 and is useful for identifying a particular measurement by a file number such as FX1309 appearing in the upper corner of the first data plot. The filename numbers were assigned in the order in which the measurements were made and, since not all measurements yielded usable data, the numbers are not sequential. There are also some files where multiple measurements were taken and the data averaged. The plots are arranged in increasing numerical order for the files.

The data for both the filtered (FX-files) and unfiltered (FT-files) have also been stored on IBM compatible tape. The file format is:

- 1 Line 1 FILENAME (4A4)
- 2 Line 2 Comments (18A4)
- 3 Line 3 Comments (18A4)
- 4 Line 4 TITLE used in plotting ('8A4)

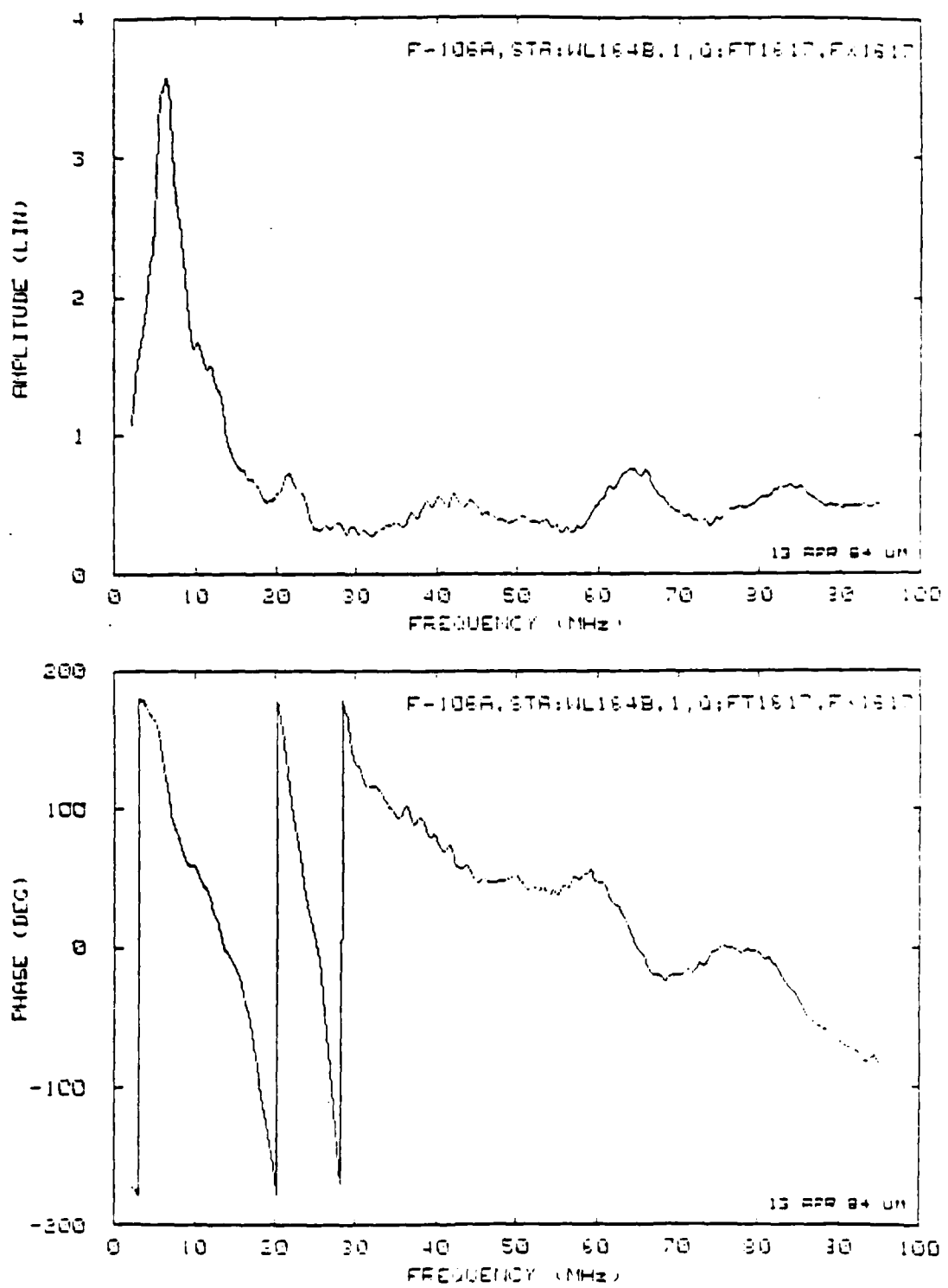


Figure 7. Illustration of data (filtered).

TABLE 3. MEASUREMENT MATRIX

Orientation Station	1	2	3	4	5	6	7	8	9
F86B Q	FX1757		FX1773	FX1817	FX1825	FX1765	FX1801		FX1809
F481L JC		FX2325	FX2373	FX2341	FX2401	FX2409	FX2333	FX2349	FX2365
F481R JA			FX2433	FX2501	FX2449	FX2509	FX2517	FX2441	FX2457
VS630L Q				FX1409	FX1465 ¹	FX1417	FX1425	FX1433	
WL104B JA			FX1925	FX1857	FX1949	FX1865	FX1873	FX1933	FX1941
WL164B Q								FX1849 ³	FX1917
WL104B JA									FX1601

(1) Average of FT1441 and FT1465
 (2) Average of FT1549 and FT1573
 (3) Average of FT1265 and FT1849

5 FMIN, FMAX, AMPMIN, PHASEMIN, PHASEMAX, NN
(4F8.3, 2F8.2, 15)
6 F(1) AMP(1) PHASE(1) F(2) AMP(2) PHASE(2) F(3) AMP(3)
PHASE(3) 3(2F8.3, F8.2)

+
data

+F(NN) AMP(NN) PHASE(NN)

where NN is the number of data points in the set. Table 4 is an example of a data set from file FX1425.

TABLE 4. SAMPLE OF TYPICAL DATA

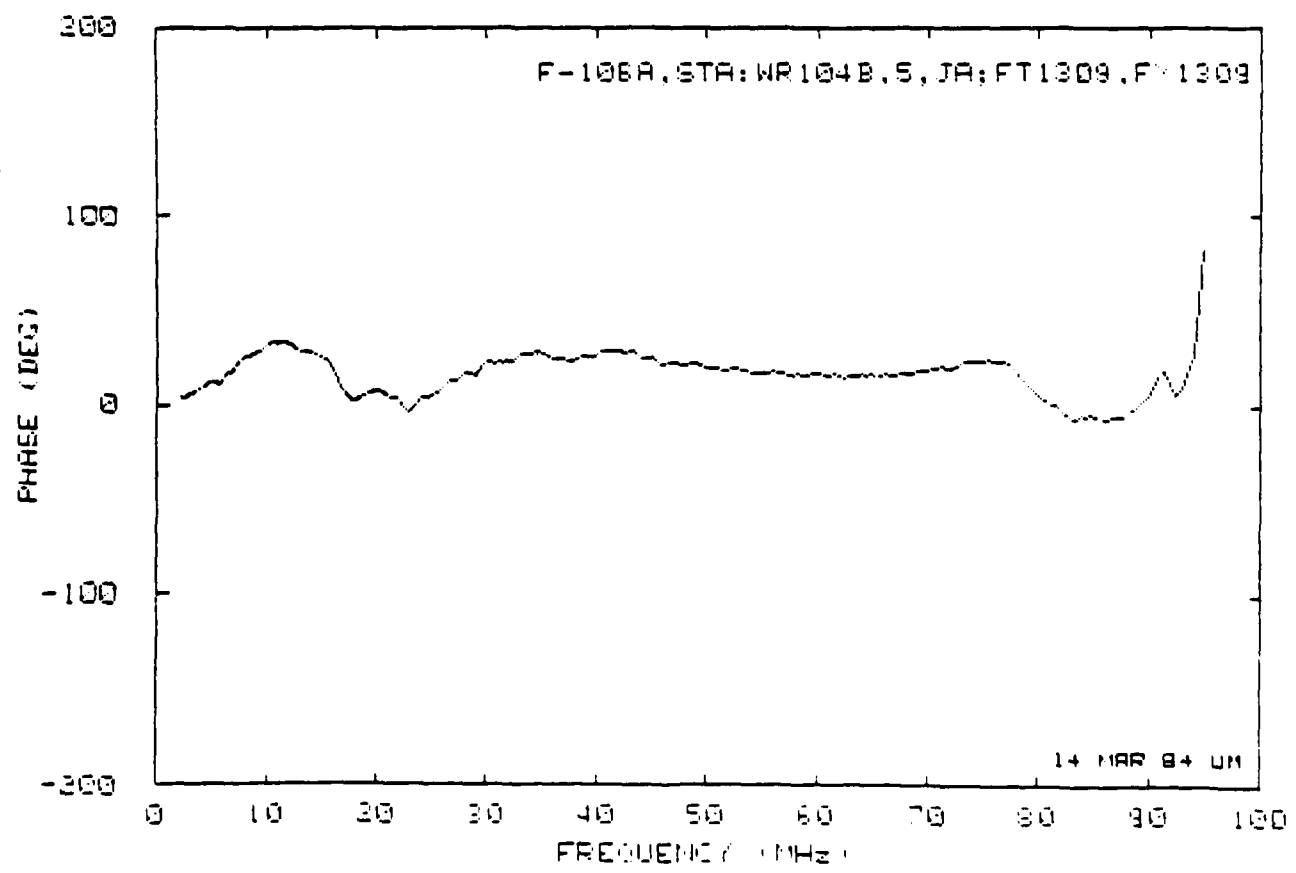
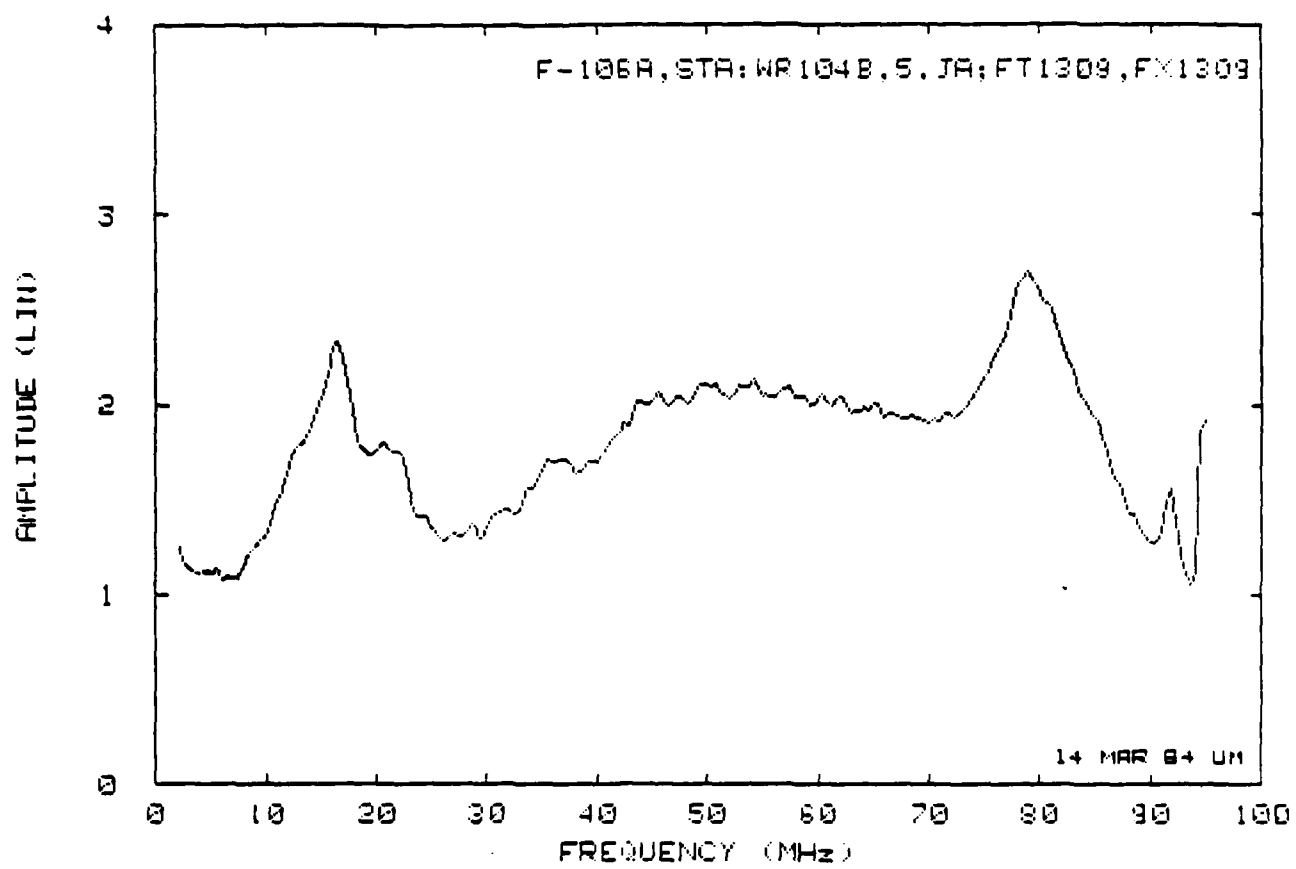
1	FX1425									
2	F-106, VS630L, LFT SIDE INC/ -30, 0, C-03, 1 31 84JB...BAND1									
3	Data filtered by FILTR5 Prgm.; Cycles=100									
4	Filtered F-106A, STA: VS630L, 5, 0; FT1425, FX1425									
5	3.513	95.644	.084	2.573	-183.70	182.96	462			
6	3.513	1.327	18.31	3.566	1.335	18.21	3.618	1.339	18.26	
7	3.671	1.337	18.61	3.723	1.327	19.32	3.775	1.301	20.32	
8	3.828	1.259	21.57	3.880	1.200	23.12	3.933	1.127	24.53	
9	3.985	1.046	25.69	4.038	.971	25.86	4.090	.910	24.78	
10	4.142	.863	22.33	4.195	.833	20.36	4.247	.823	19.09	
11	4.300	.832	17.12	4.352	.851	14.28	4.405	.869	10.60	
12	4.457	.875	6.28	4.510	.858	1.70	4.562	.810	-3.16	
13	4.614	.725	-8.30	4.667	.611	-16.16	4.719	.476	-26.96	
14	4.772	.352	-46.15	4.824	.284	-78.23	4.877	.313	-113.11	
15	4.929	.404	-137.13	4.981	.515	-152.37	5.034	.630	-164.41	
16	5.086	.740	-173.61	5.139	.842	178.79	5.191	.940	172.51	
17	5.244	1.045	167.18	5.296	1.163	161.99	5.348	1.294	156.86	
18	5.401	1.431	151.59	5.453	1.561	148.12	5.506	1.675	140.50	
19	5.558	1.764	134.79	5.611	1.829	128.98	5.663	1.869	123.00	
20	5.716	1.884	116.38	5.768	1.875	110.62	5.820	1.845	104.31	
21	5.873	1.300	98.03	5.925	1.747	91.92	5.973	1.692	85.23	
22	6.030	1.636	81.26	6.083	1.577	77.25	6.115	1.518	74.63	
23	6.187	1.457	73.06	6.240	1.401	72.32	6.232	1.349	71.79	
24	6.345	1.200	71.09	6.397	1.156	63.31	6.450	1.212	57.35	
25	6.502	1.192	65.07	6.555	1.175	61.75	6.607	1.166	56.99	
.
135	64.601	.557	29.77	65.021	.558	30.77	65.440	.576	30.16	
136	65.260	.626	30.55	66.279	.647	23.12	66.639	.620	28.53	
137	67.118	.627	30.85	67.538	.648	22.91	67.257	.638	32.26	
138	68.377	.690	30.31	68.796	.674	30.16	69.216	.696	10.10	
139	69.635	.718	28.74	70.055	.727	24.59	70.474	.703	23.83	
140	70.894	.693	25.18	71.313	.688	26.94	71.733	.632	23.19	
141	72.152	.687	27.35	72.572	.709	29.52	72.991	.694	23.00	
142	73.411	.687	27.68	73.830	.680	28.47	74.250	.667	22.10	
143	74.669	.696	27.39	75.089	.648	26.91	75.508	.673	26.64	
144	75.923	.685	25.09	76.347	.692	20.15	76.767	.719	19.21	
145	77.136	.711	18.50	77.606	.716	15.90	78.025	.744	15.11	
146	78.445	.752	13.83	78.864	.749	12.77	79.284	.748	14.62	
147	79.703	.726	17.39	80.123	.719	16.37	80.542	.707	17.37	
148	80.962	.706	20.77	81.381	.671	23.10	81.601	.689	26.53	
149	82.220	.653	24.78	82.640	.664	28.65	83.059	.665	27.92	
150	83.479	.679	25.31	83.898	.652	25.41	84.317	.658	25.32	
151	84.737	.697	24.24	85.156	.683	23.18	85.576	.698	22.42	
152	85.995	.714	20.68	86.415	.703	20.94	86.834	.703	17.51	
153	87.254	.709	20.39	87.673	.735	20.48	88.093	.728	19.18	
154	88.512	.731	19.08	89.932	.746	14.39	89.351	.744	16.30	
155	89.771	.752	14.92	90.190	.757	13.24	90.610	.745	12.87	
156	91.029	.733	11.80	91.449	.740	15.03	91.268	.756	13.76	
157	92.289	.746	14.38	92.707	.754	16.33	93.127	.713	15.57	
158	93.546	.707	19.31	93.966	.738	21.34	94.385	.757	21.37	
159	94.305	.770	22.10	95.224	.916	23.73	95.644	.860	28.16	

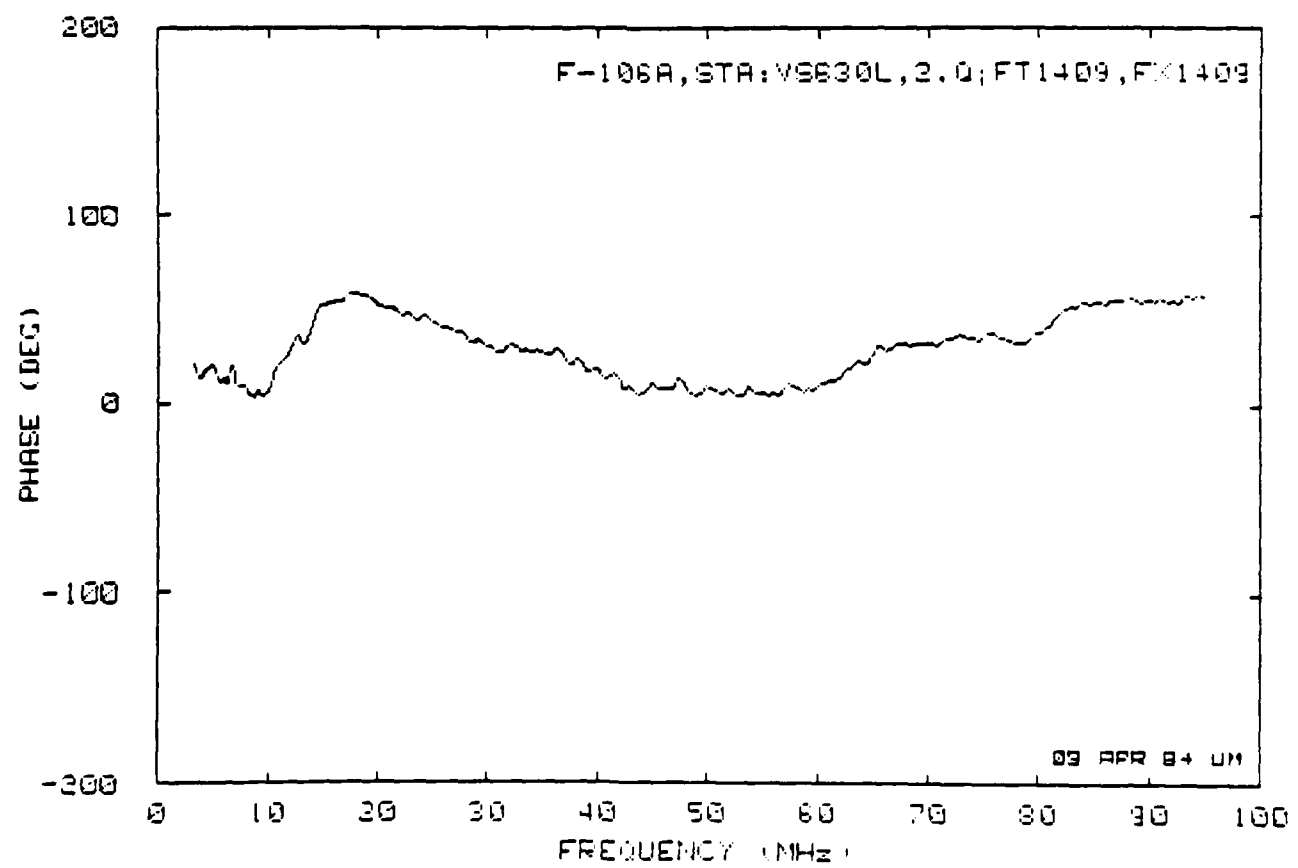
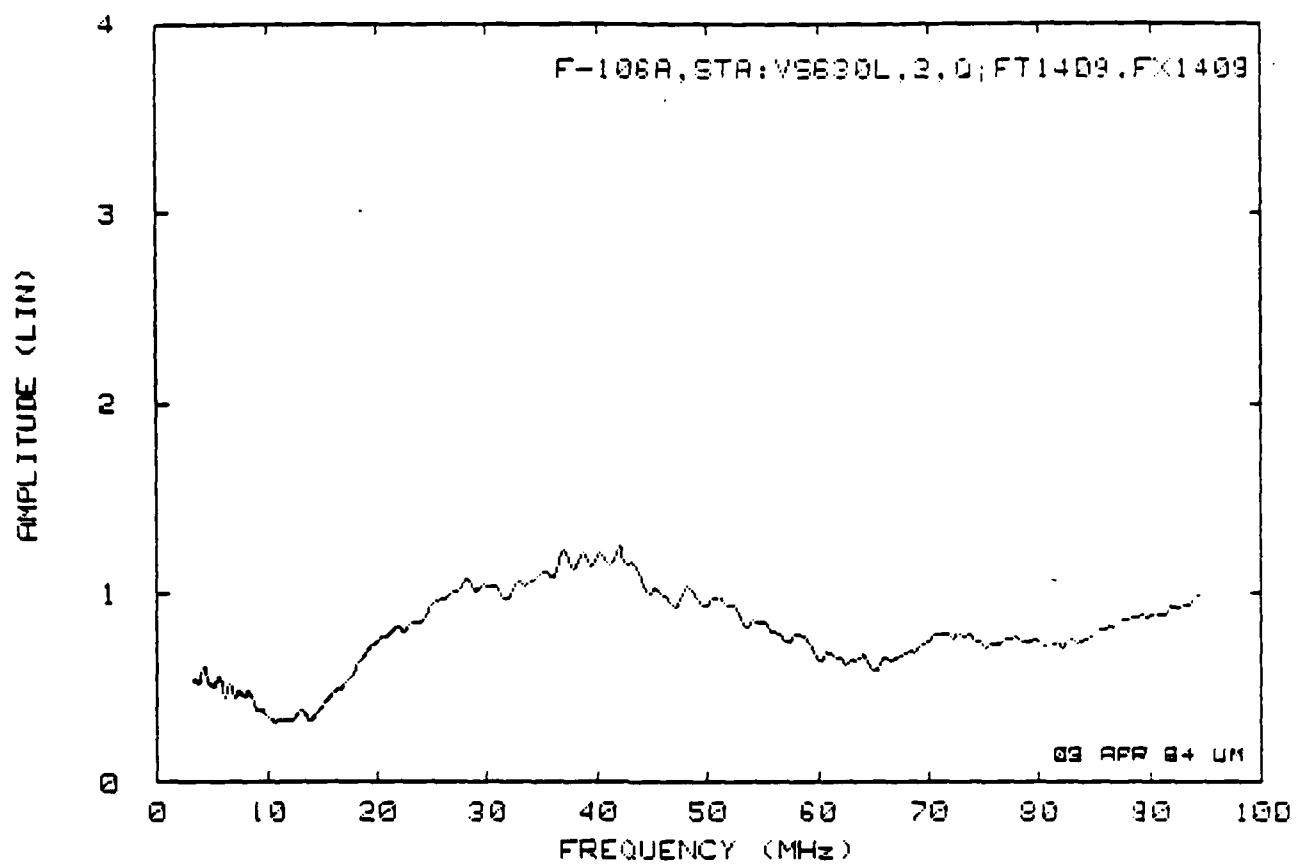
V. CONCLUSIONS AND RECOMMENDATIONS

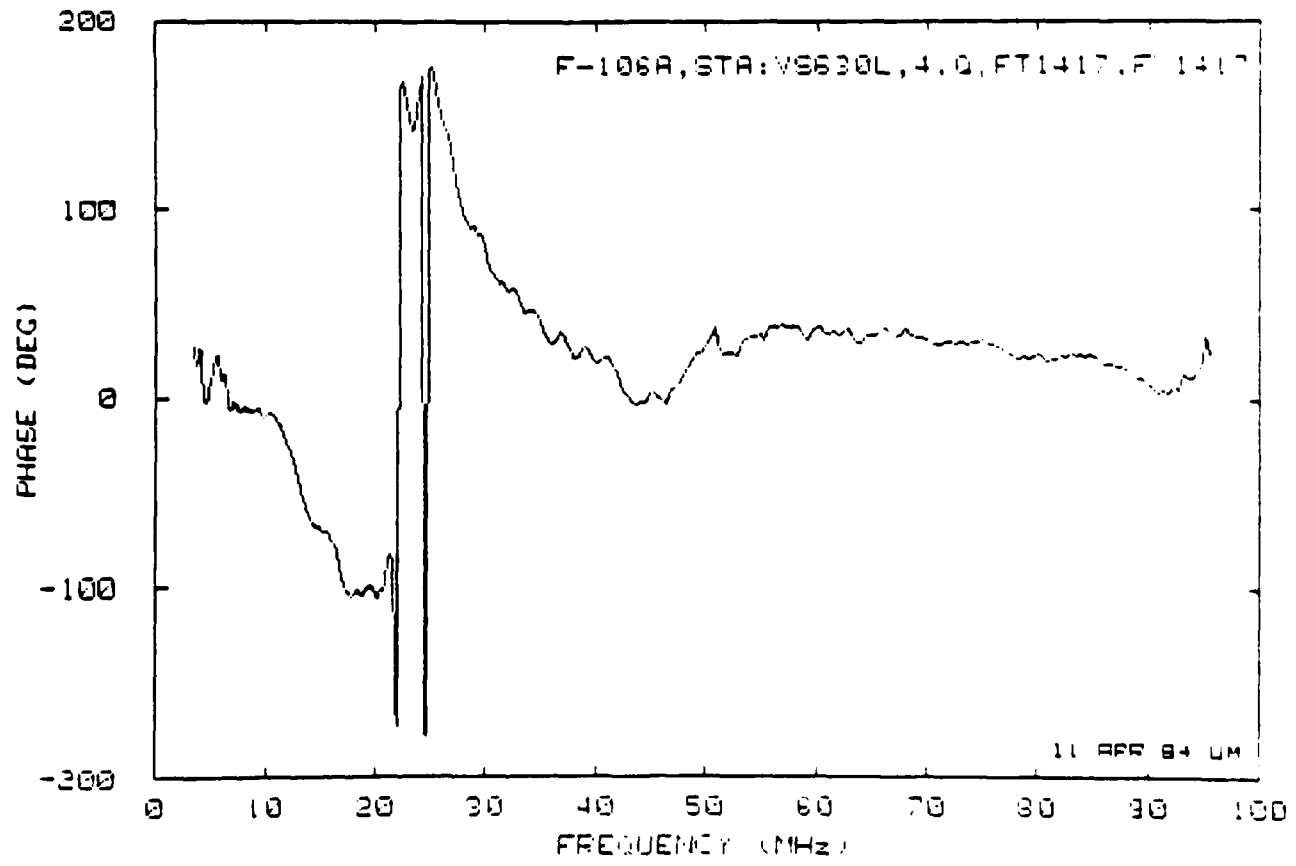
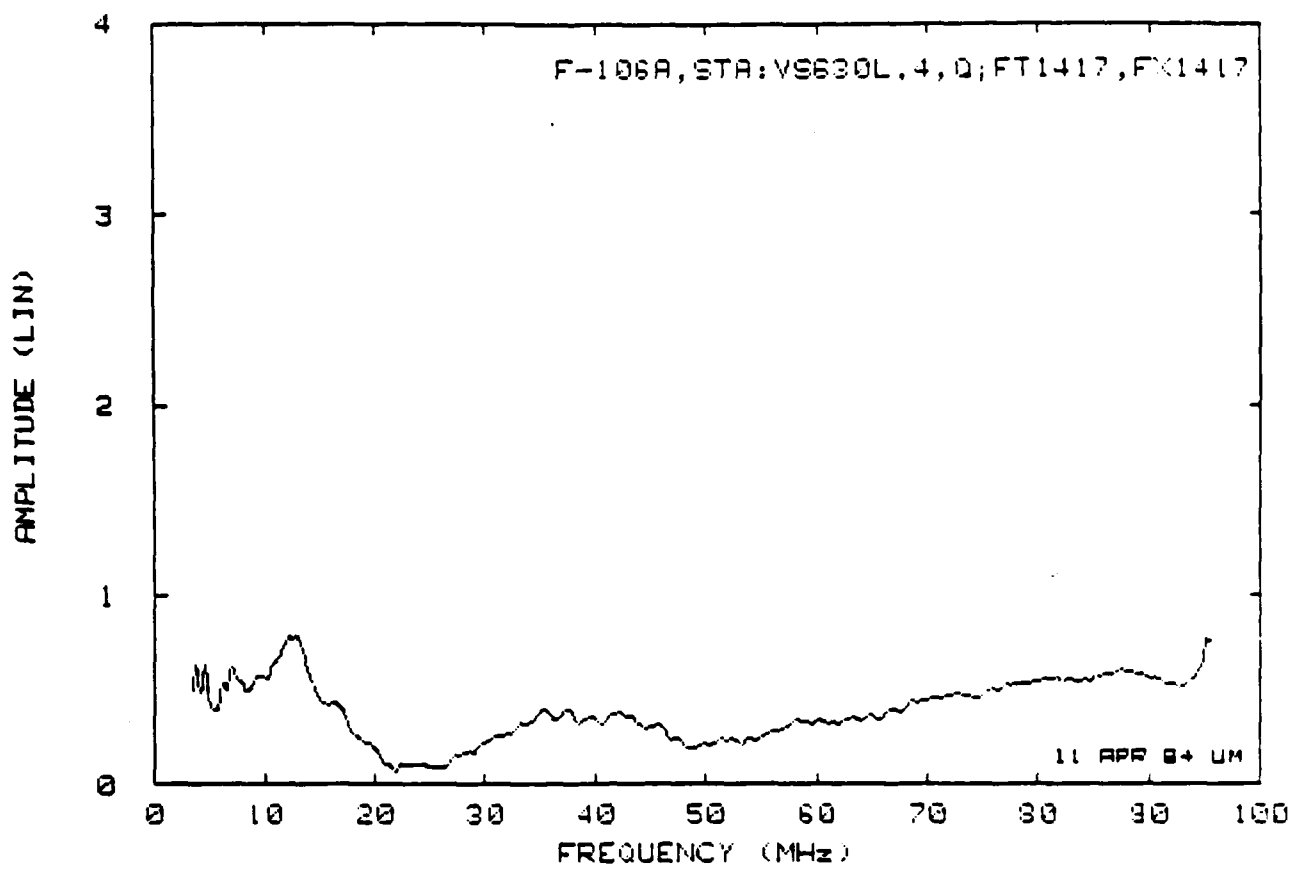
The measurements performed on a scale model aircraft have provided data for the exterior response of NASA F-106B at locations where lightning sensors are located on the aircraft. These data can now be used (after substantial data processing) to determine the effect of the aircraft interaction with the lightning generated signals. It is also conceivable that these data, in certain cases, can be used to deconvolute or remove the aircraft interactions from the measured data to give true lightning signal signature.

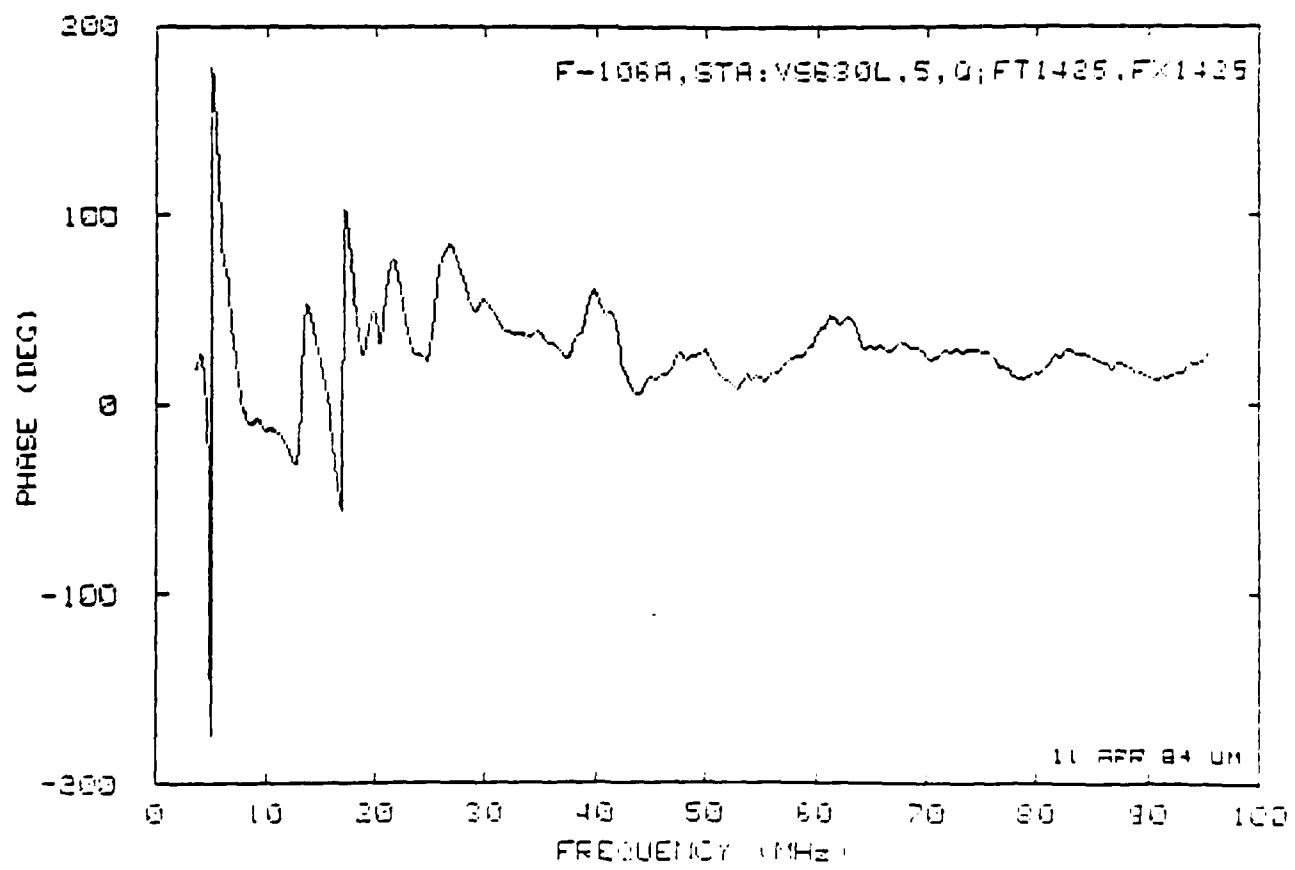
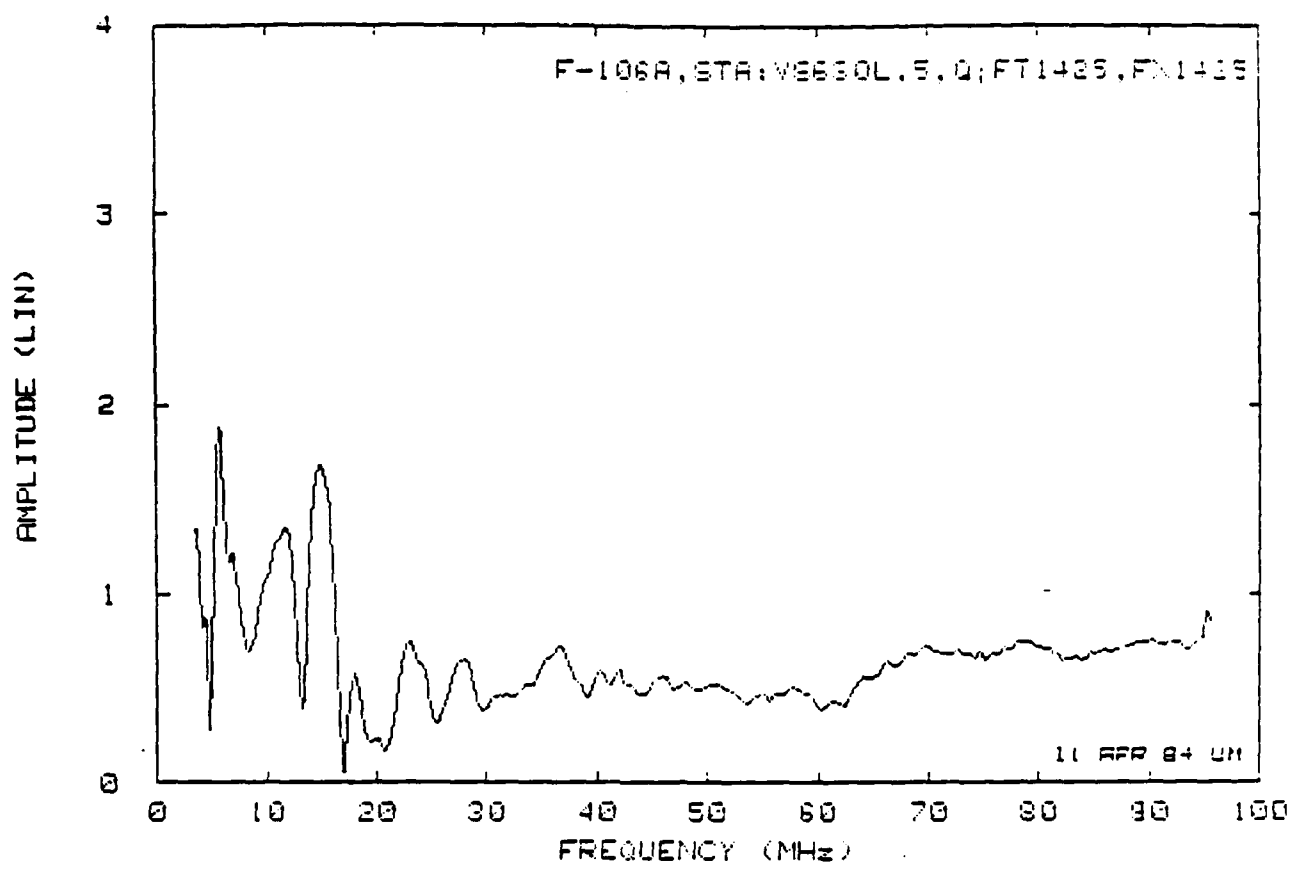
The data measured and provided herein cover about 2 to 95 MHz range. Since the lightning spectrum extends down to DC, it would also be appropriate to provide data at low frequencies. In the anechoic chamber this is not feasible, but currently a low frequency magnetostatic measurement facility is being developed to perform such measurements and it is expected to provide data in 60 to 500 kHz range.

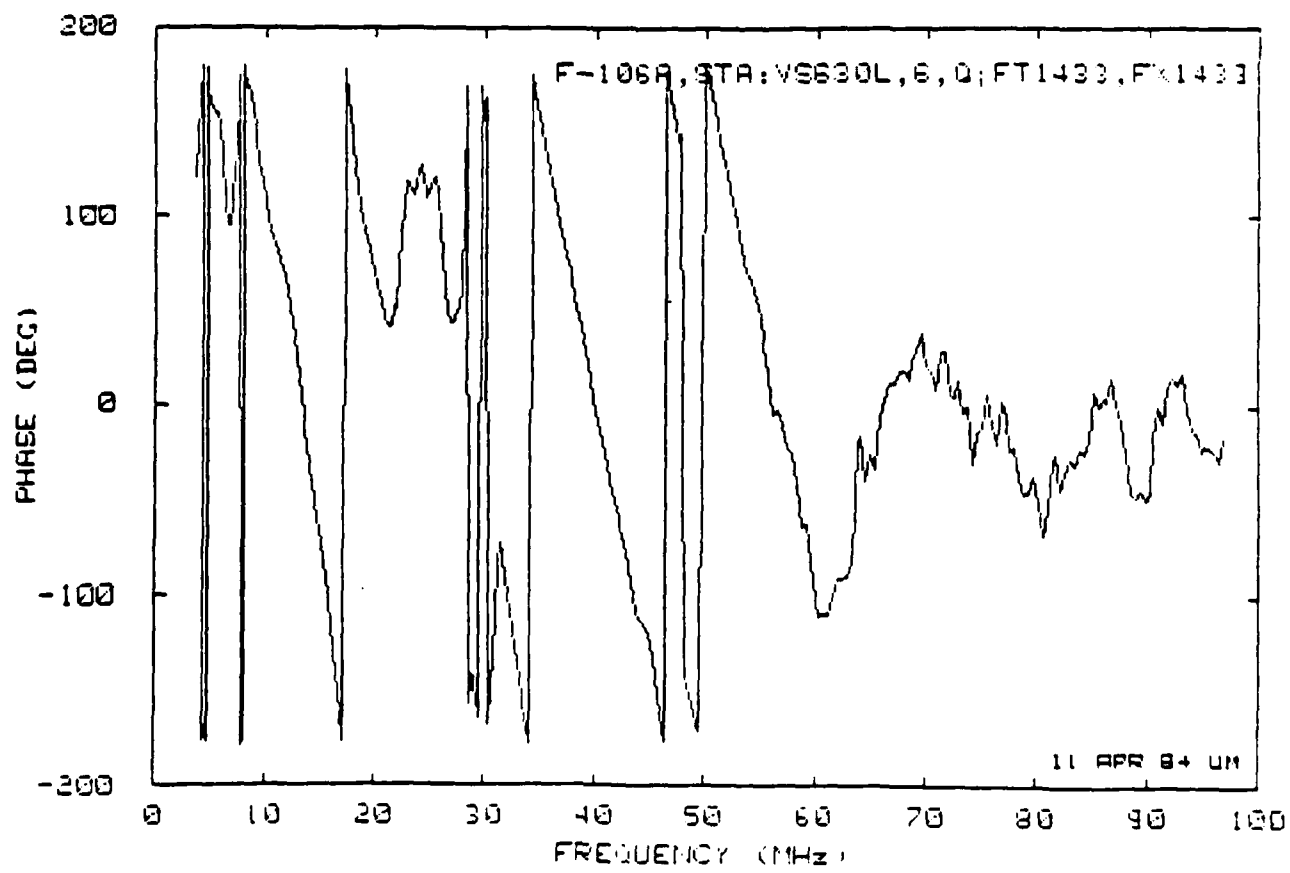
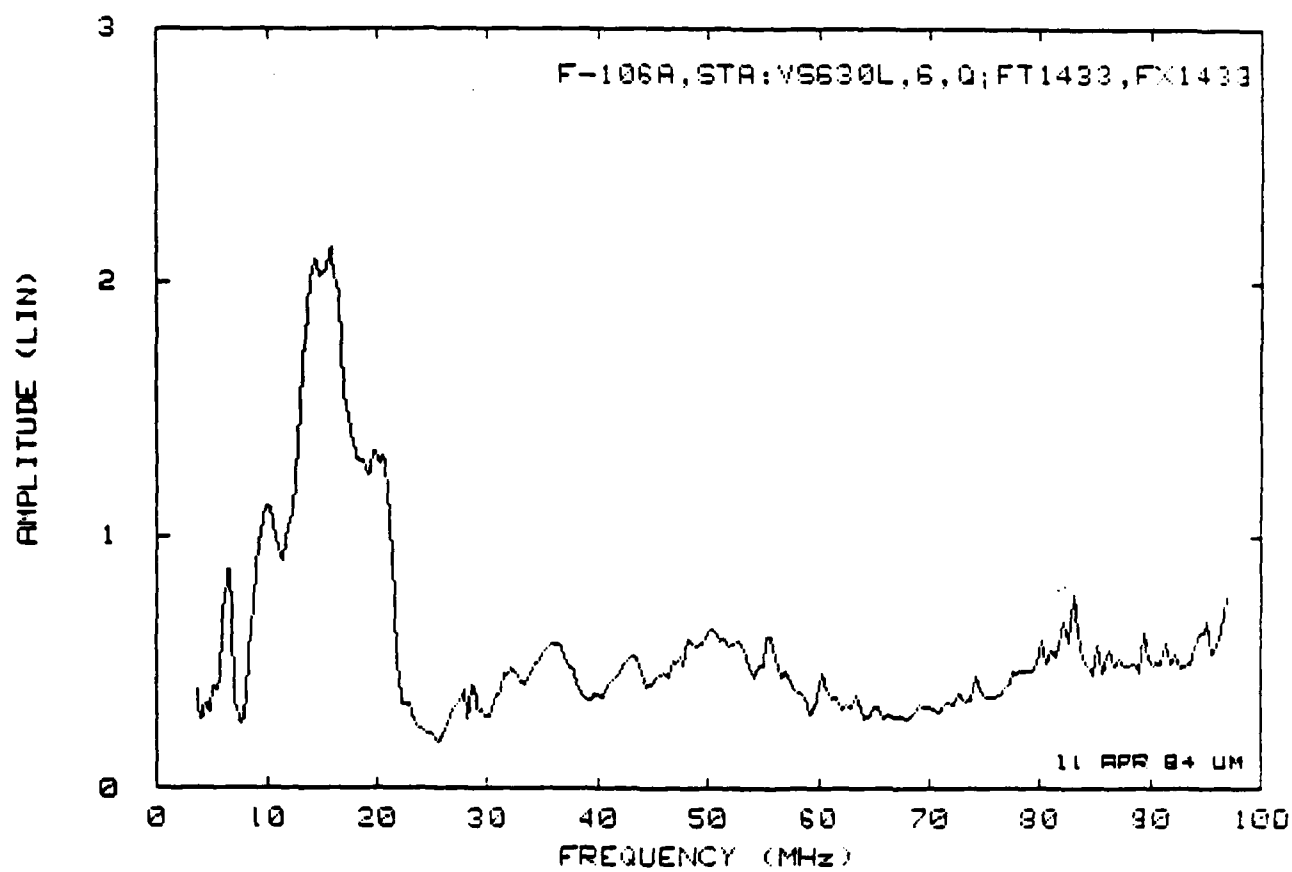
VI. DATA PLOTS

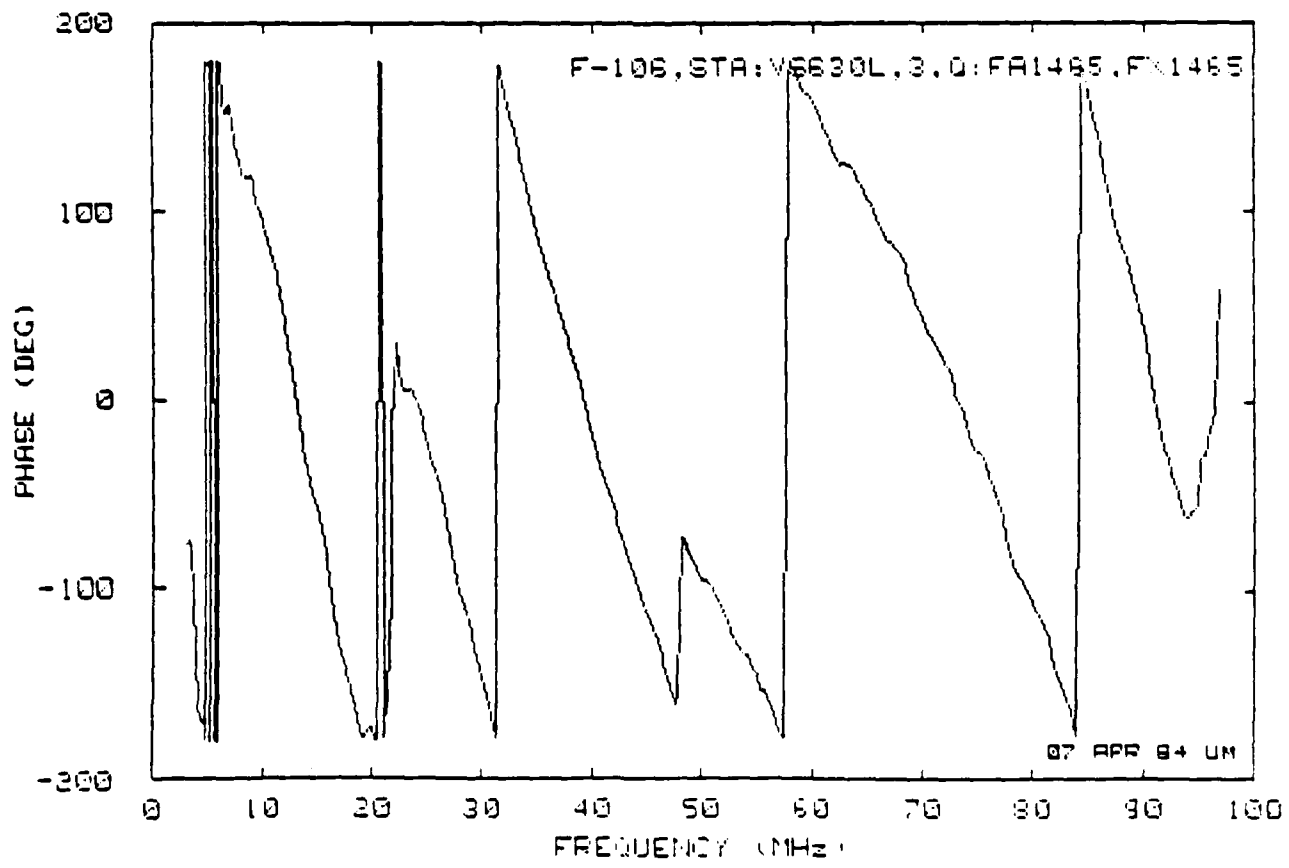
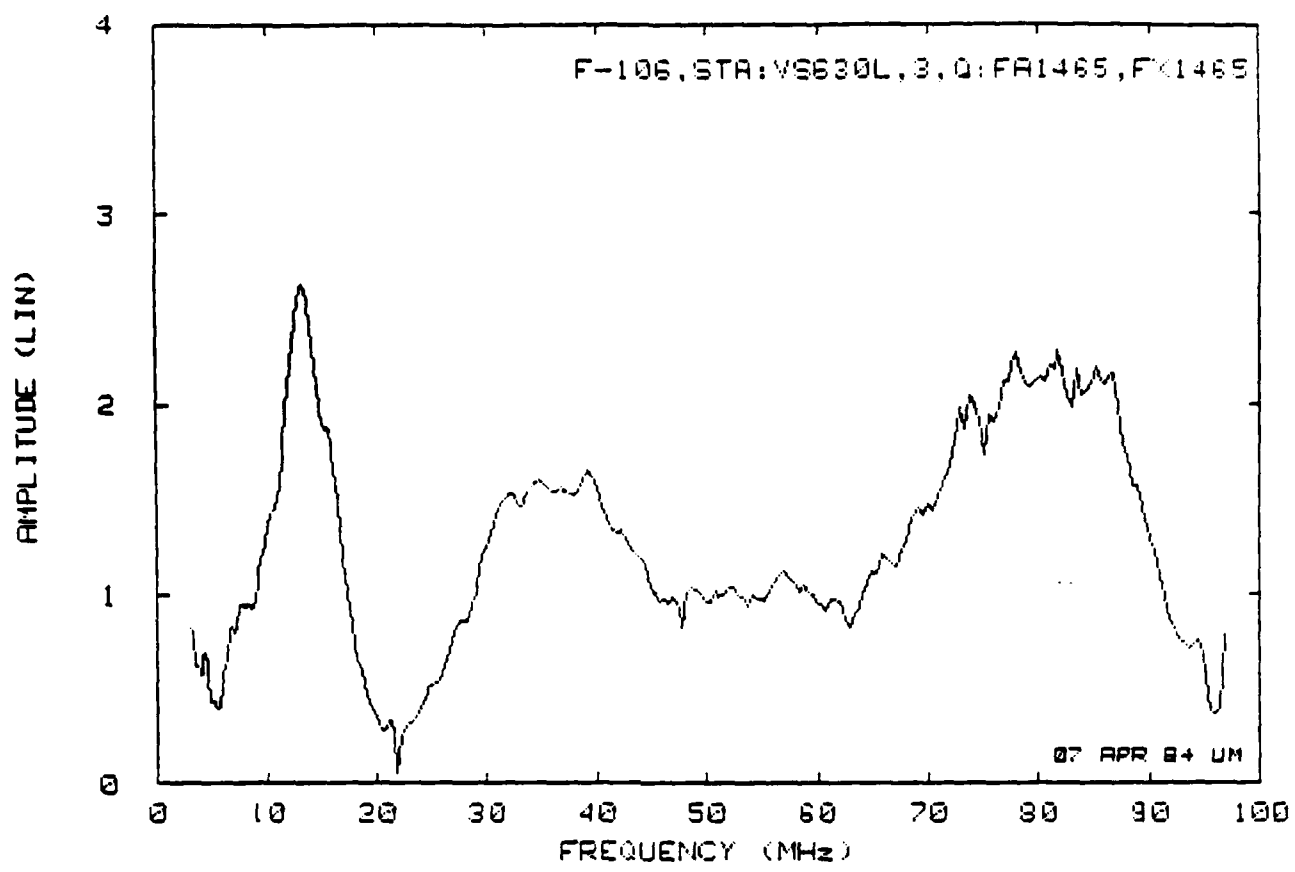


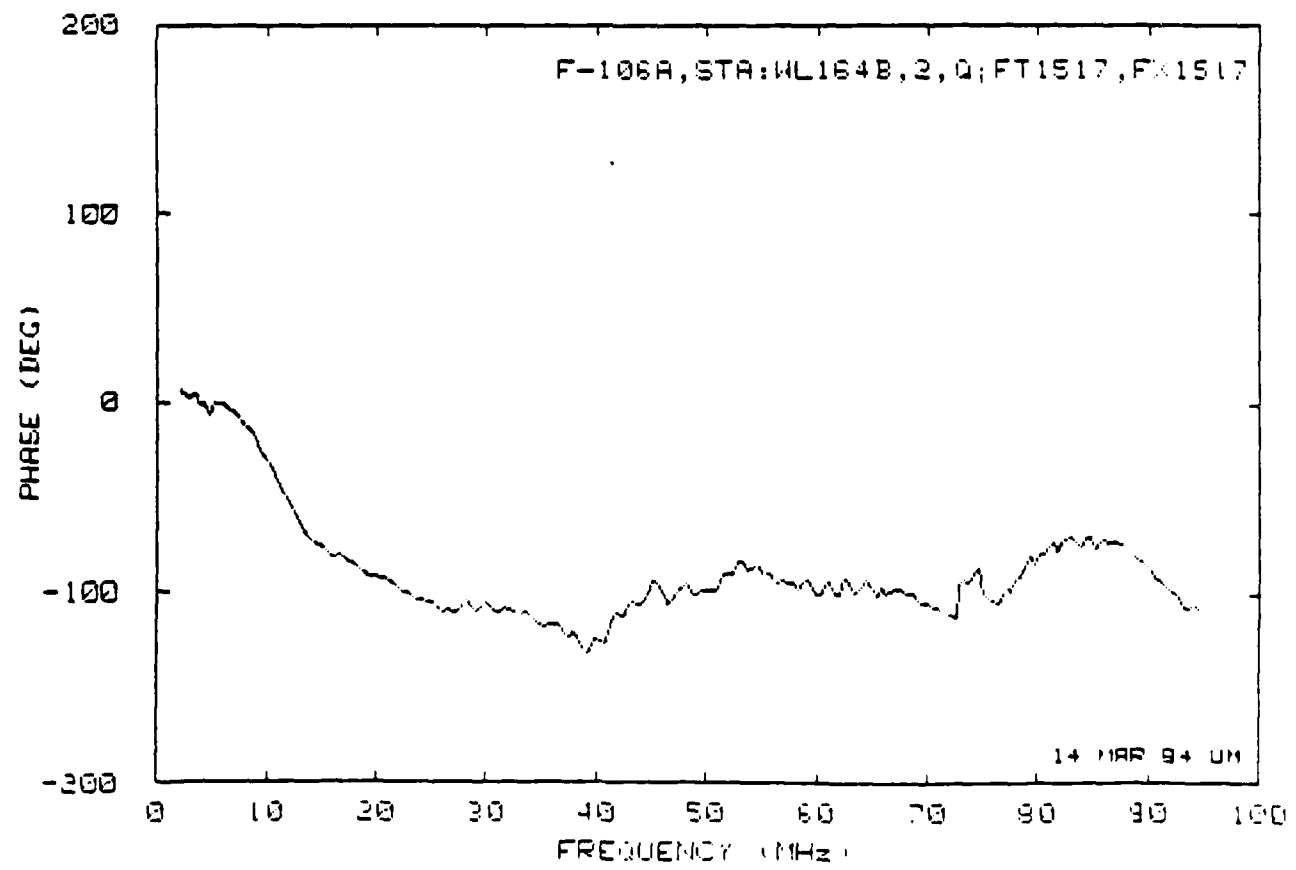
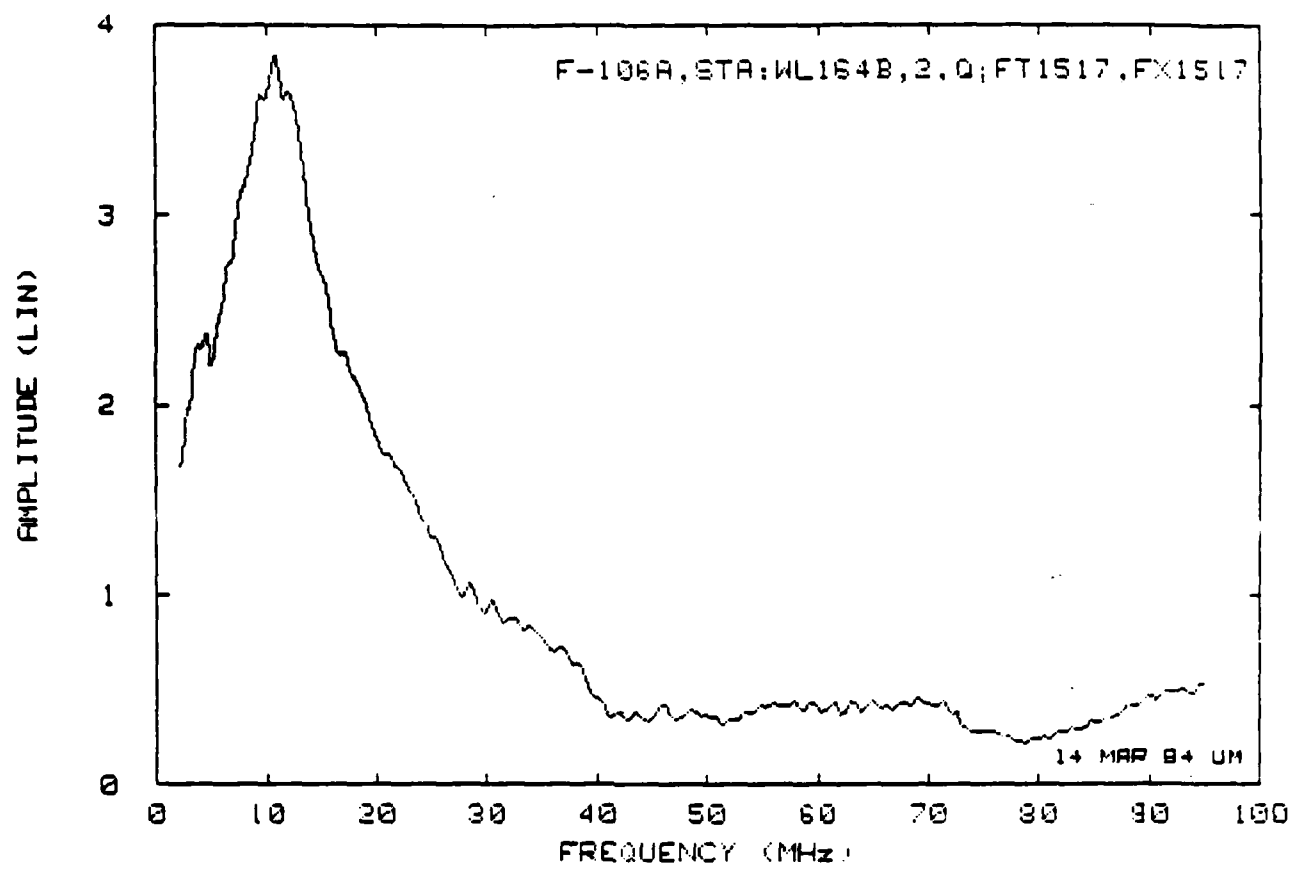


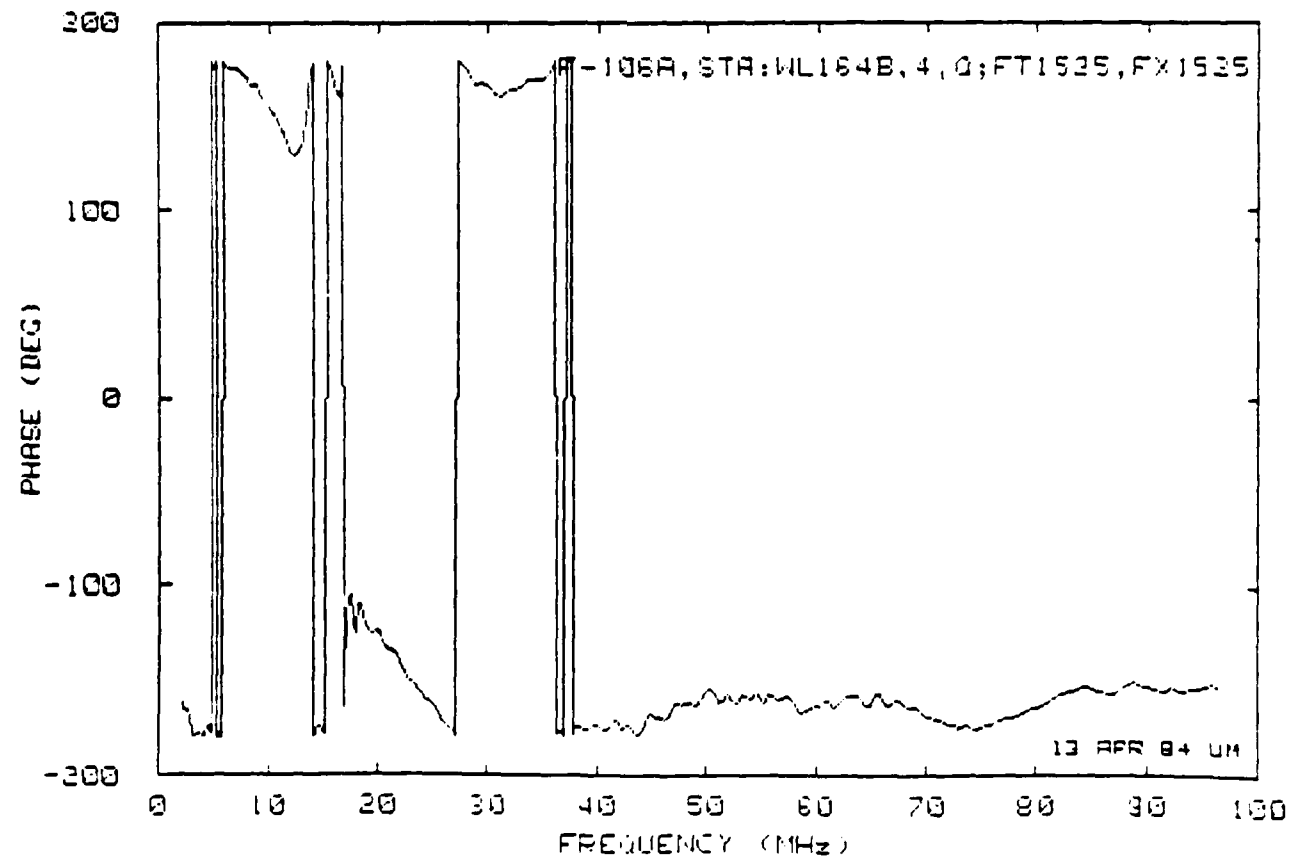
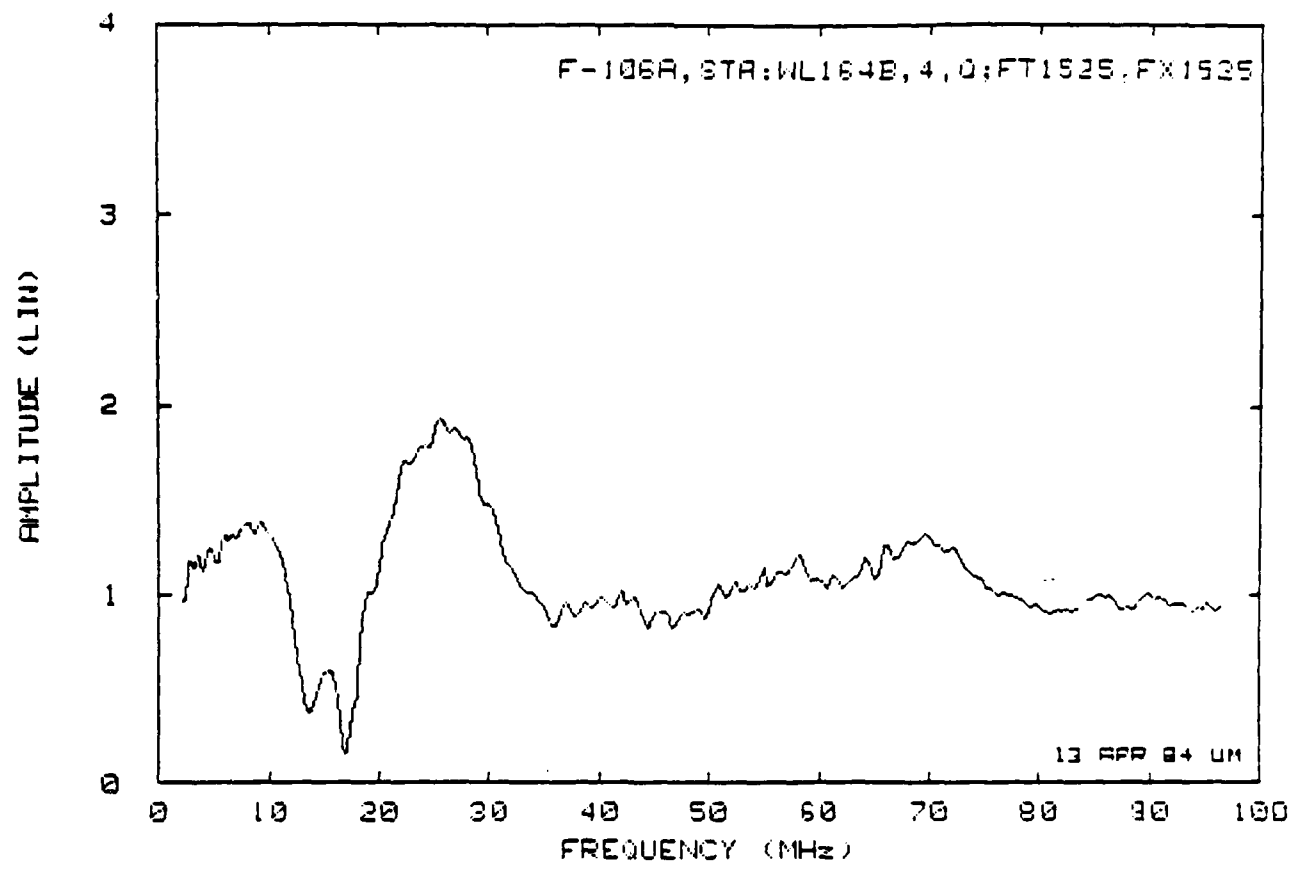


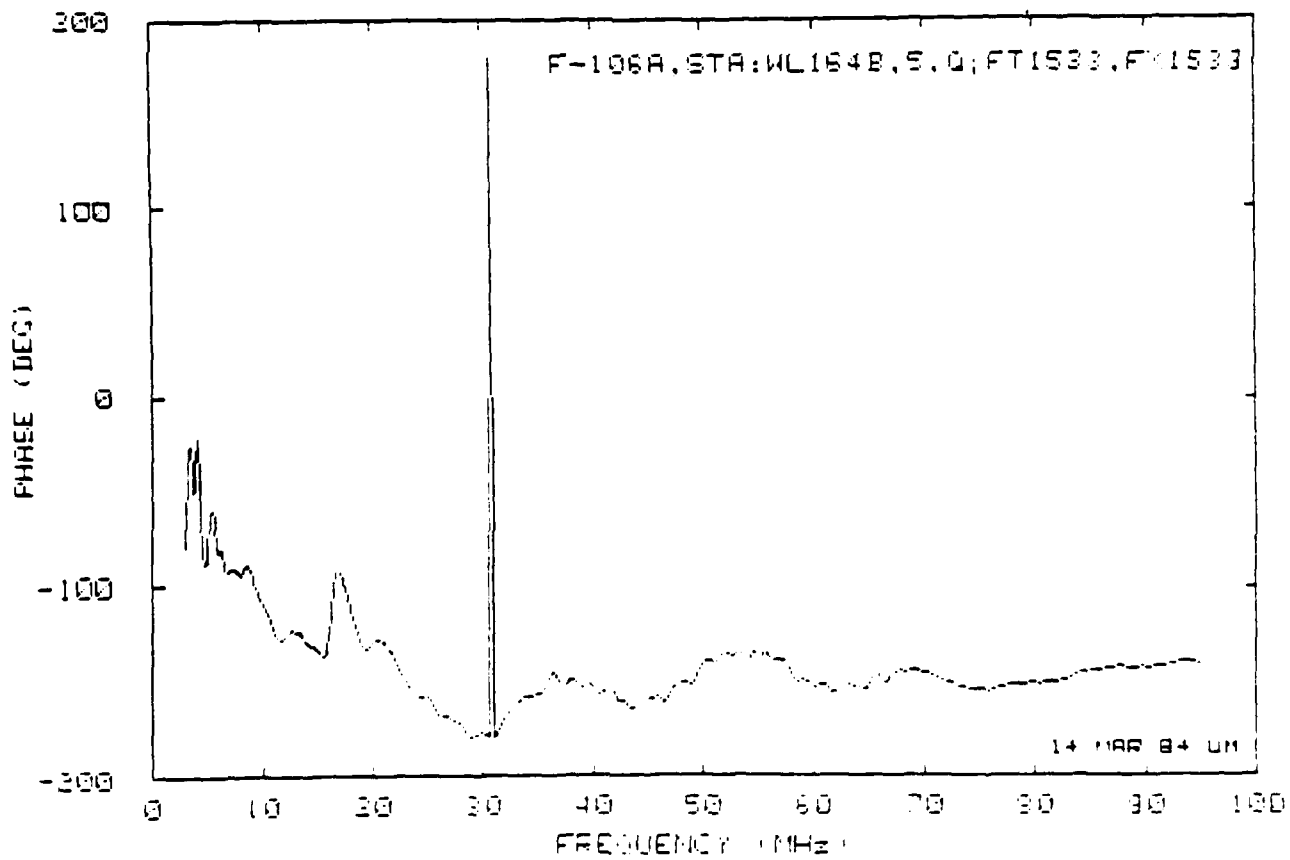
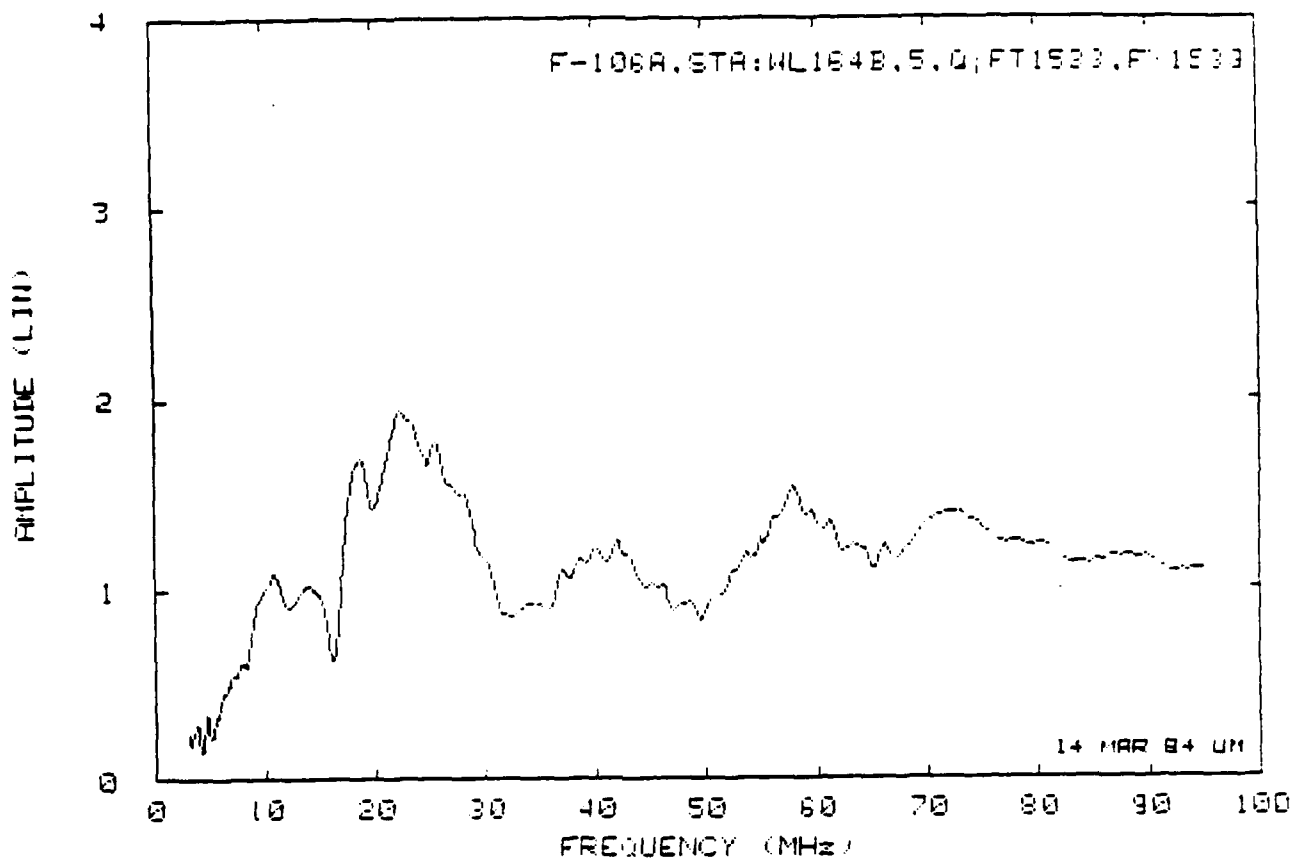


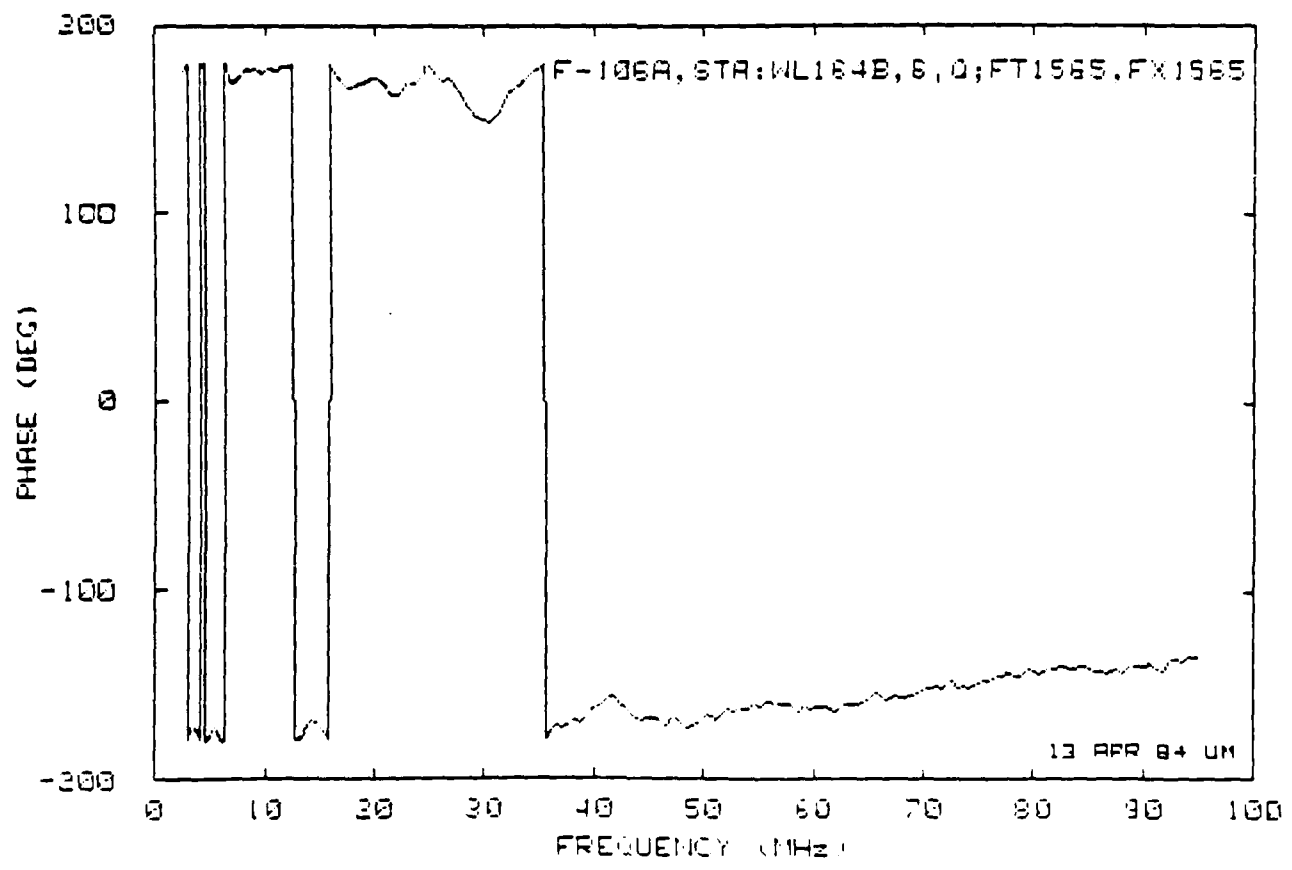
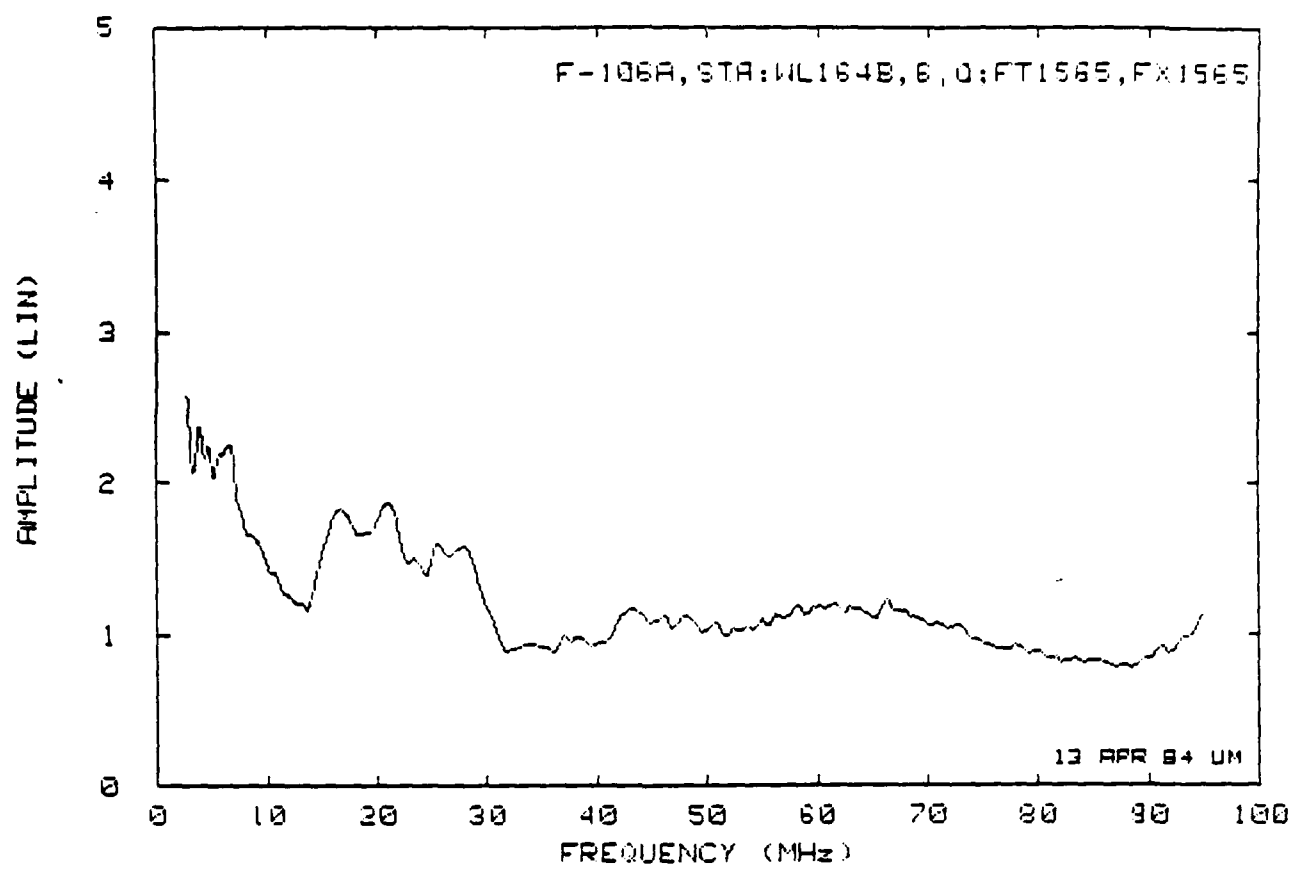


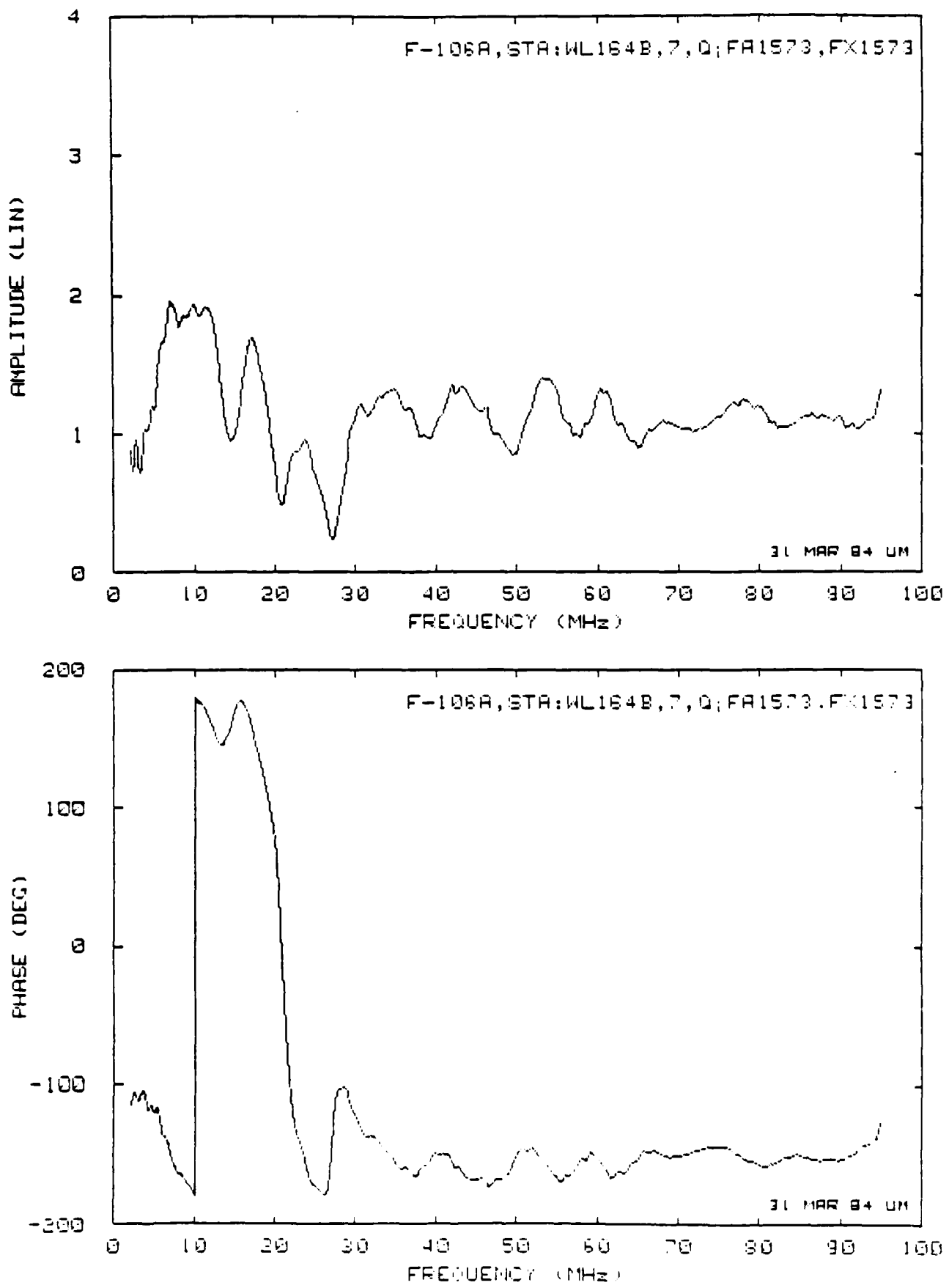


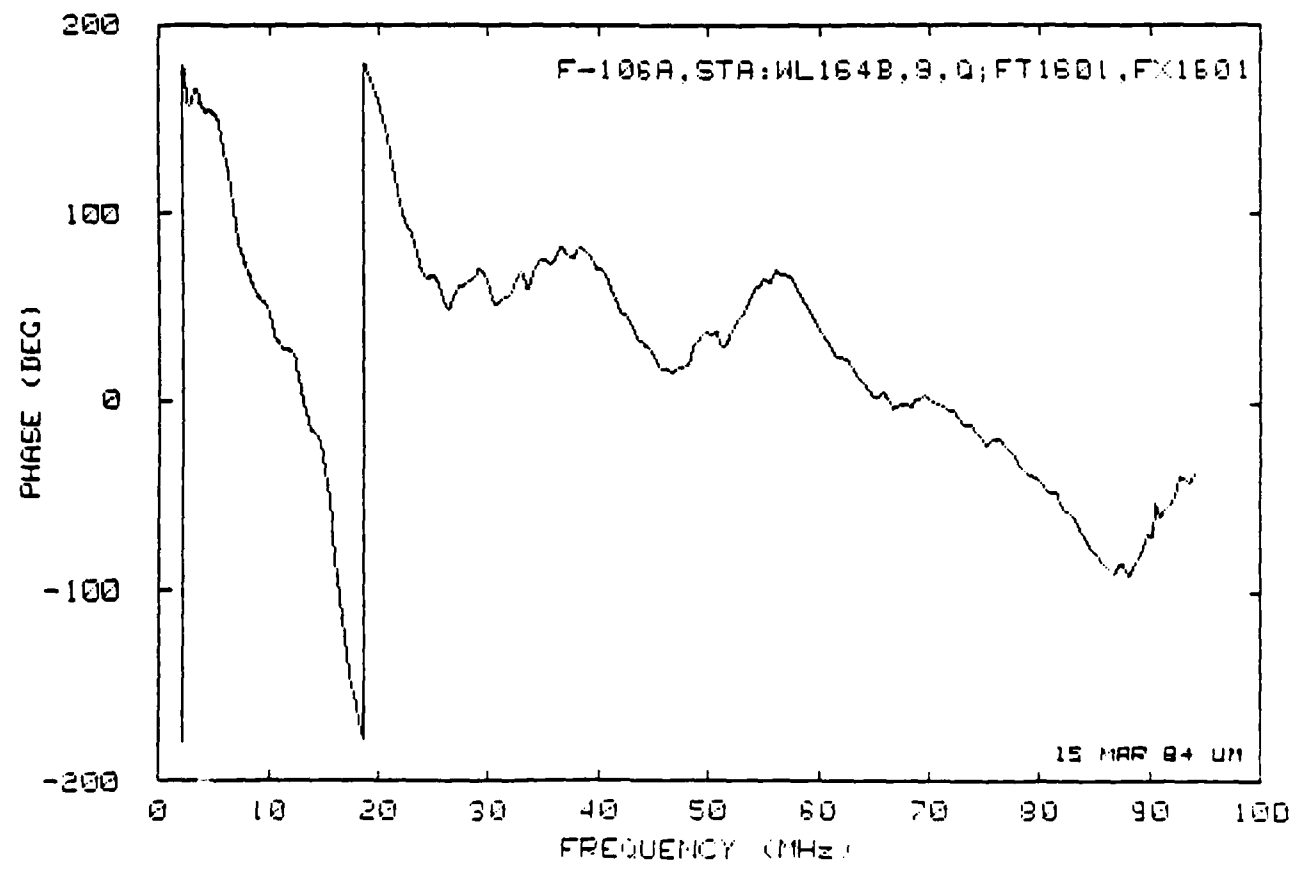
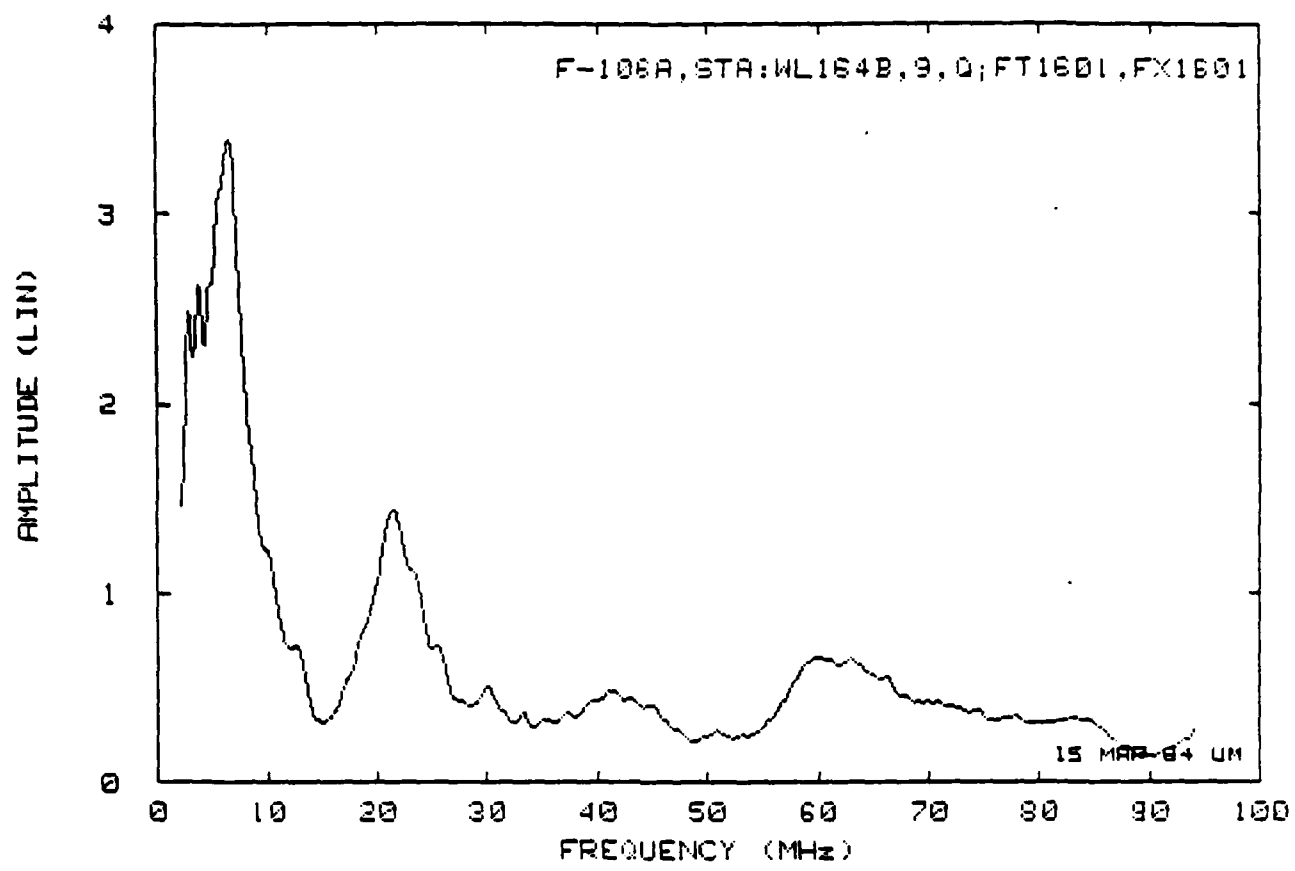


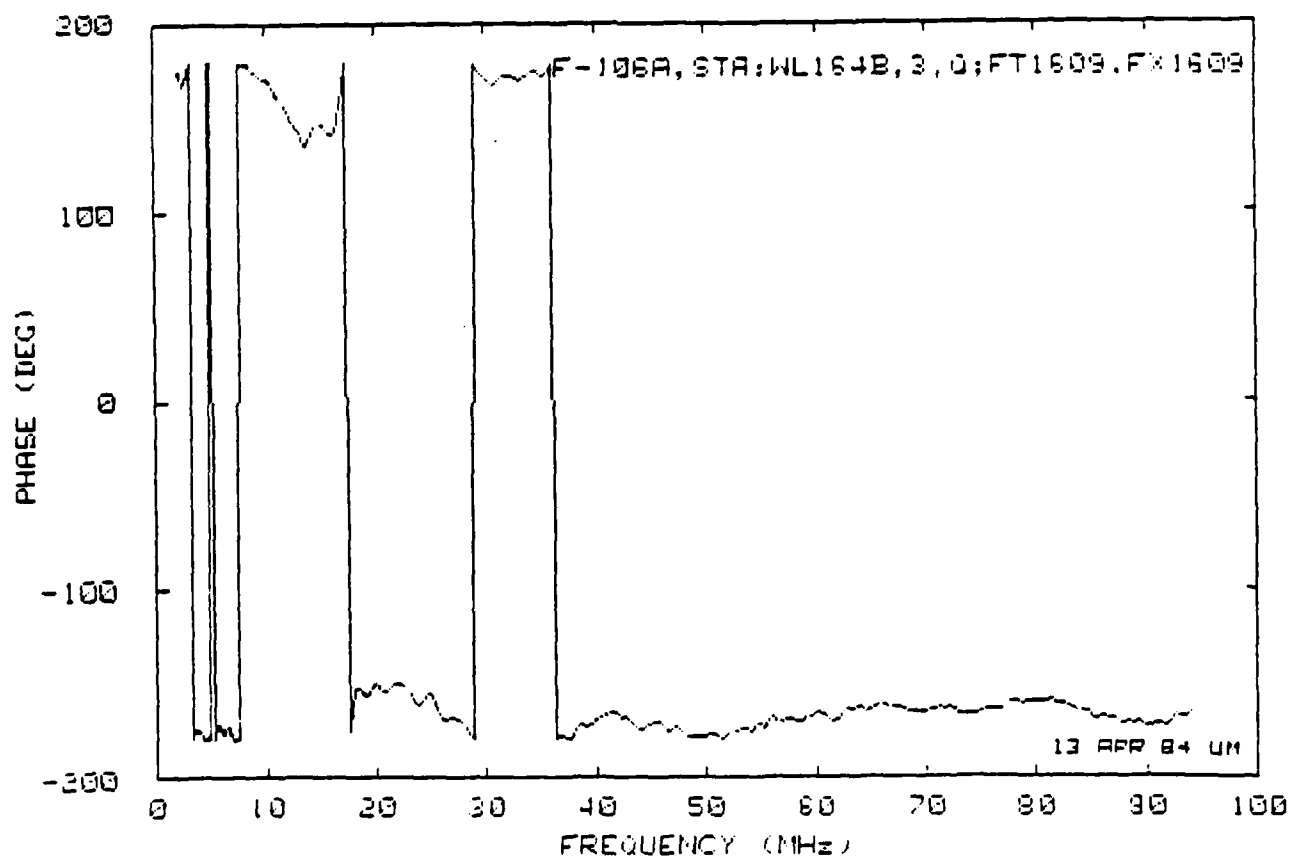
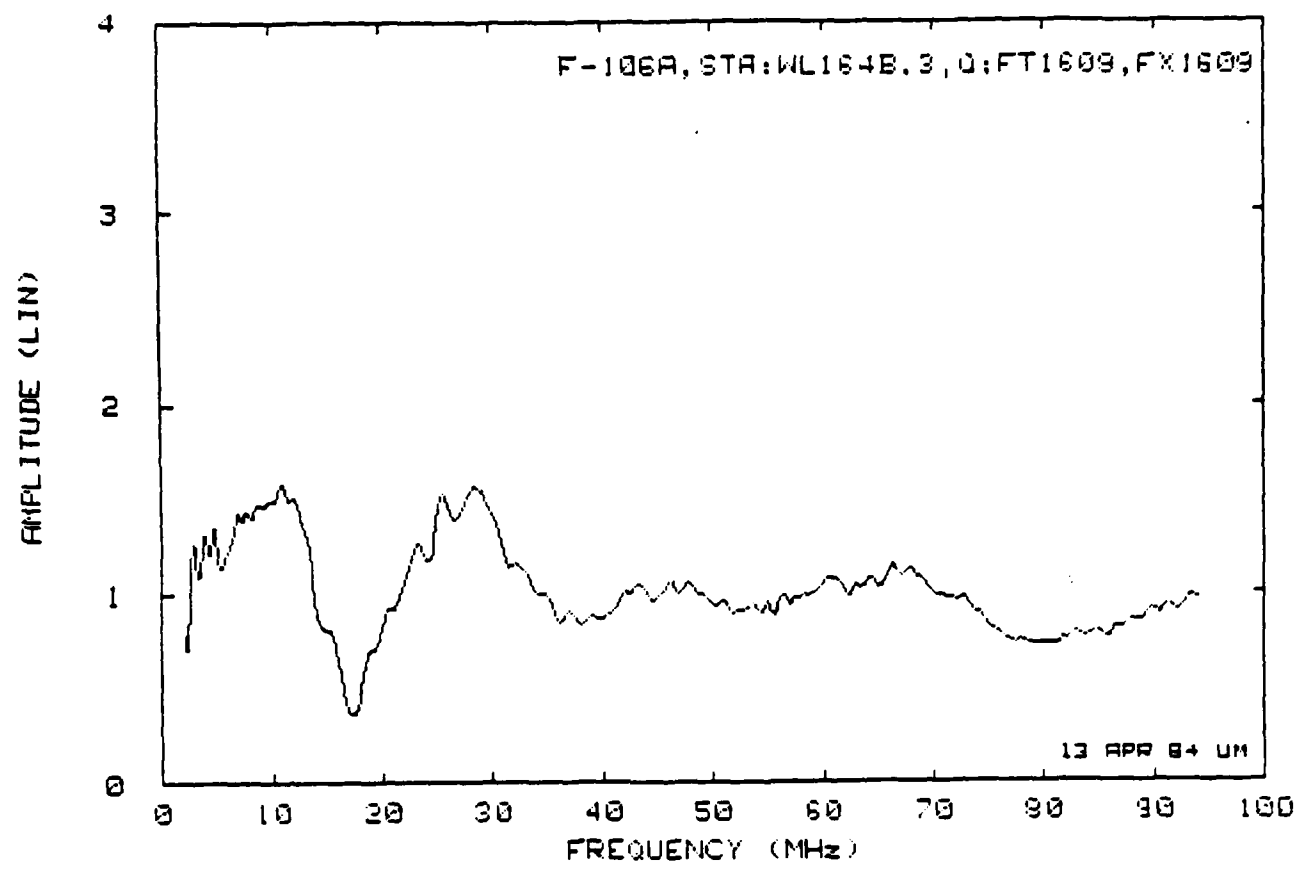


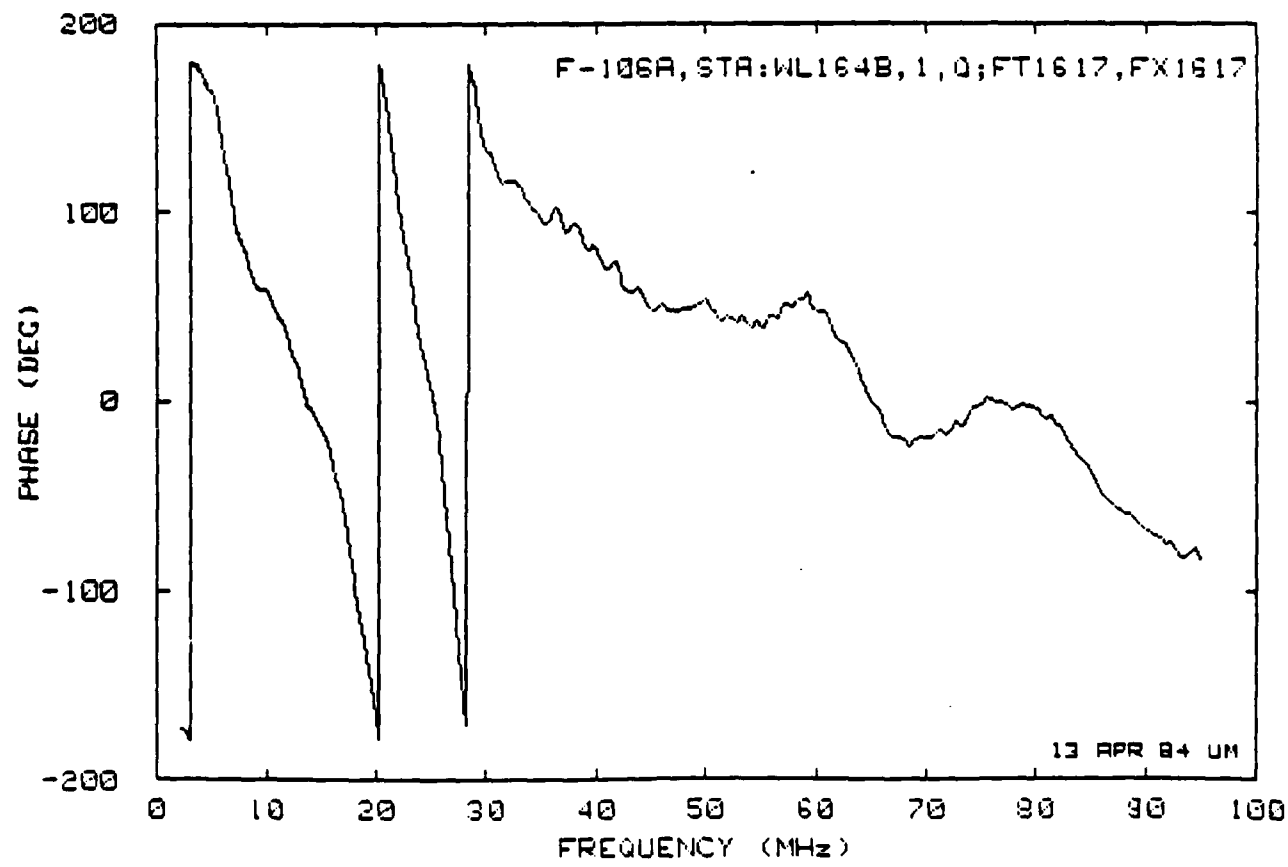
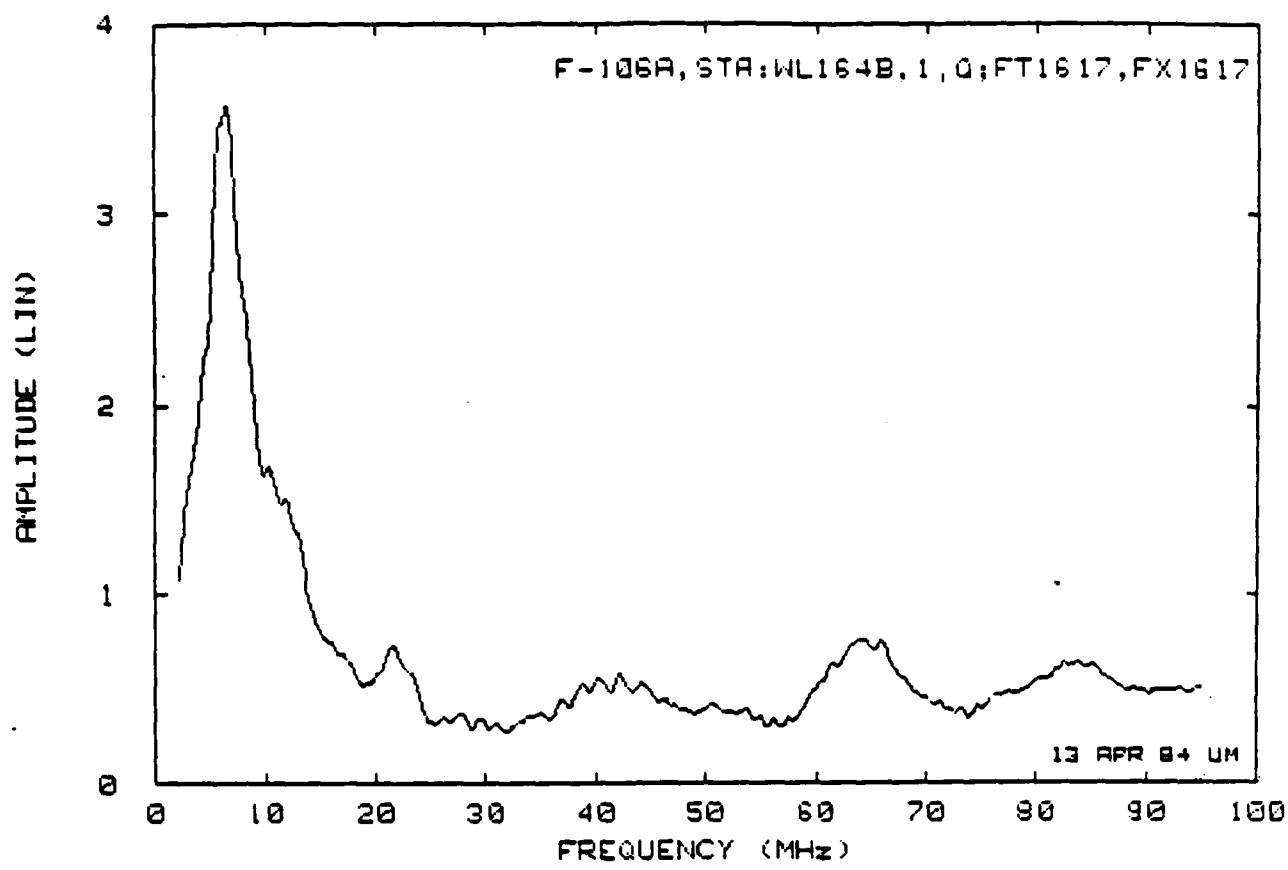


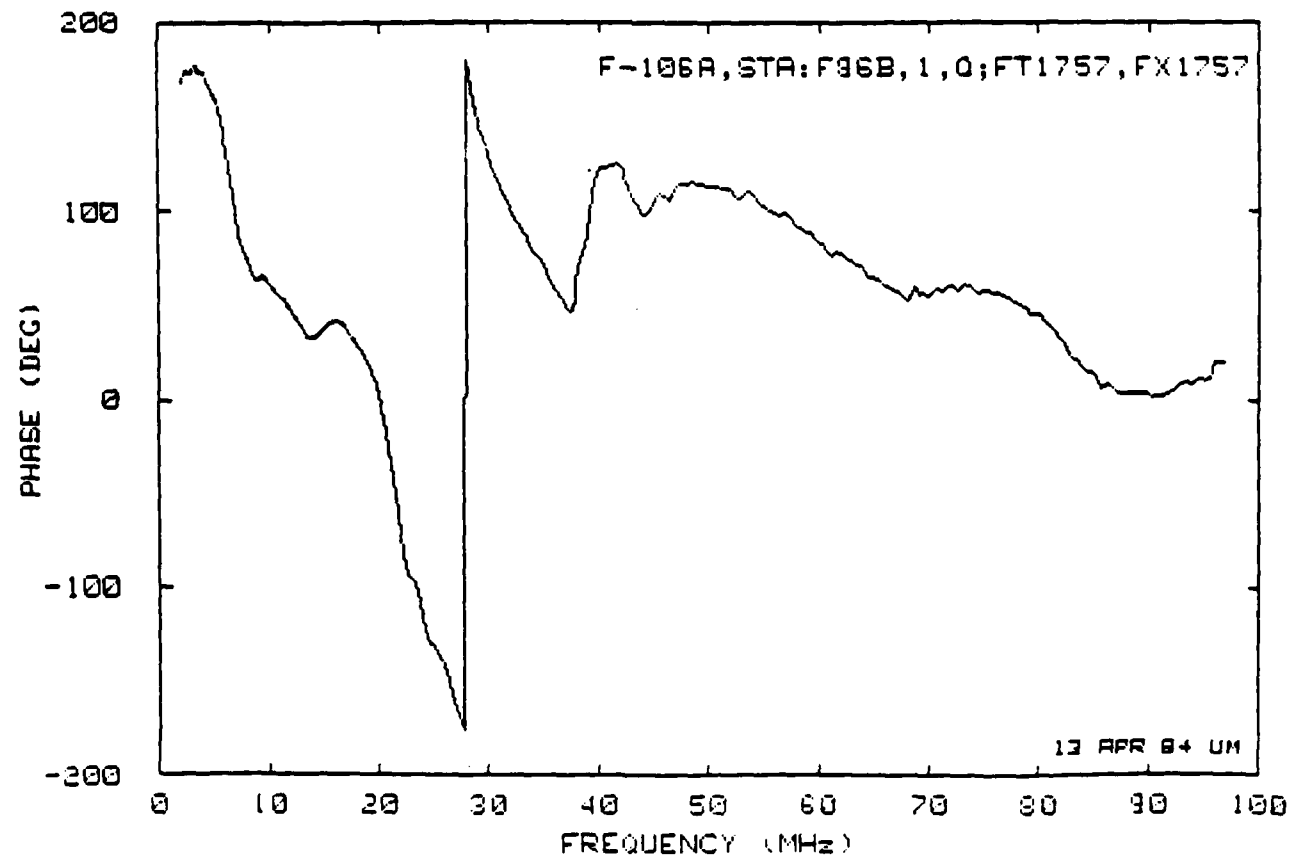
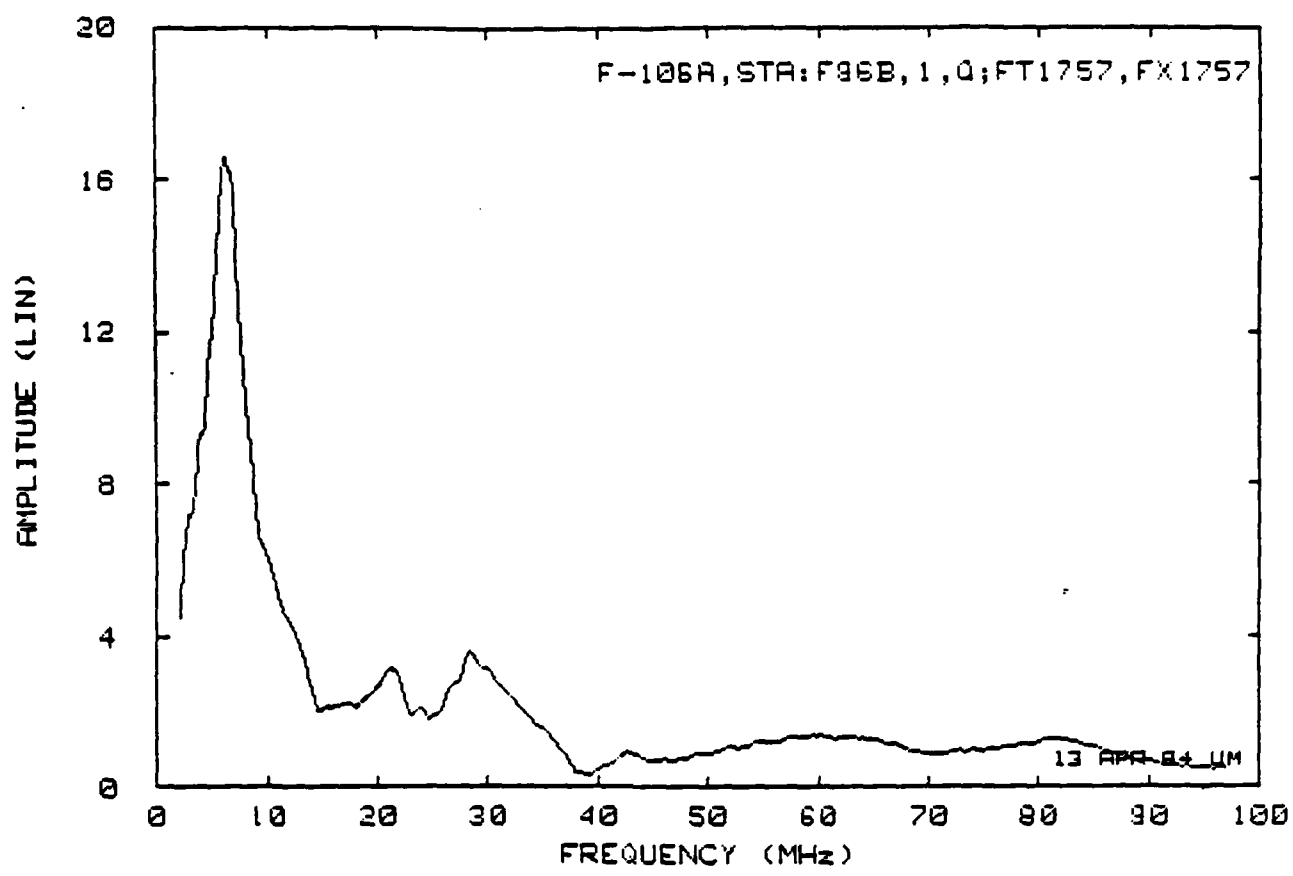


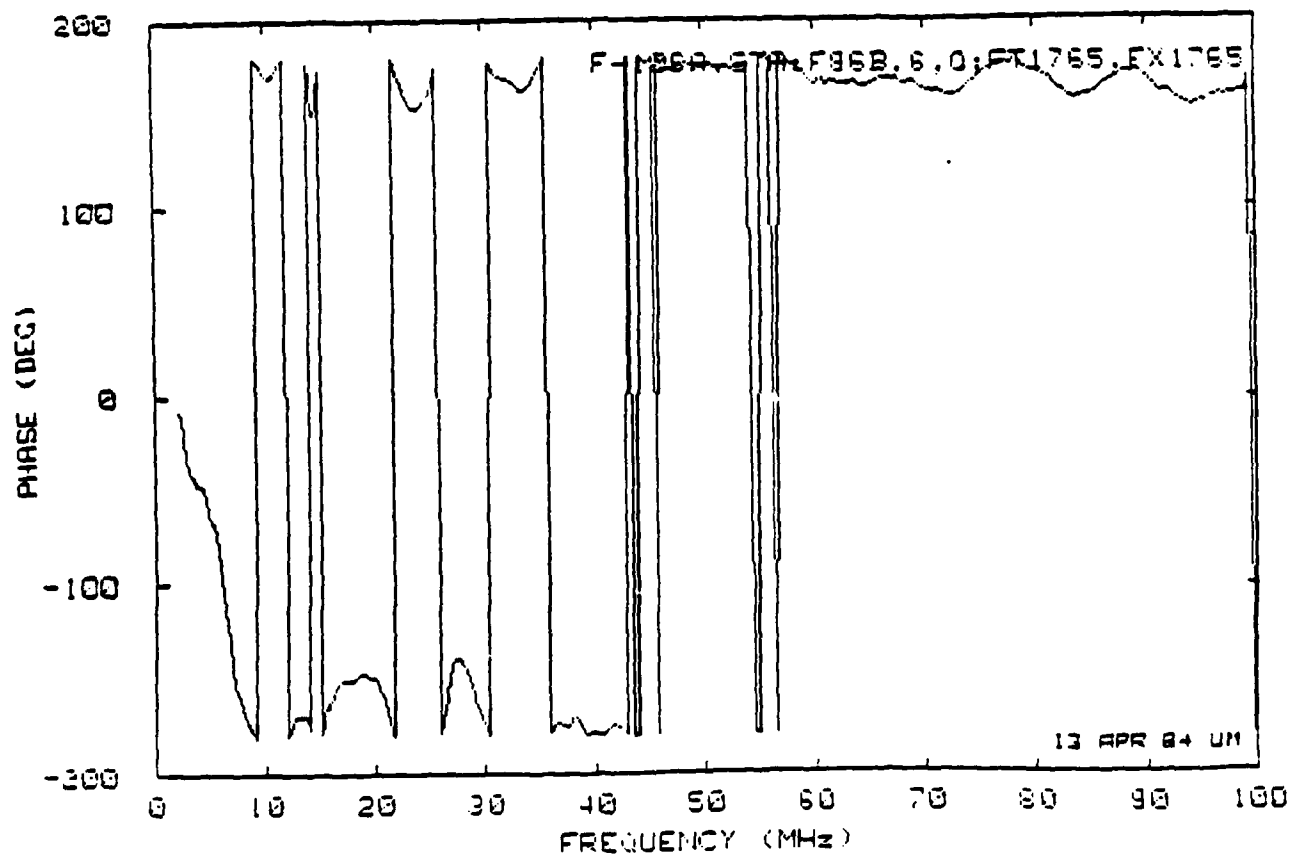
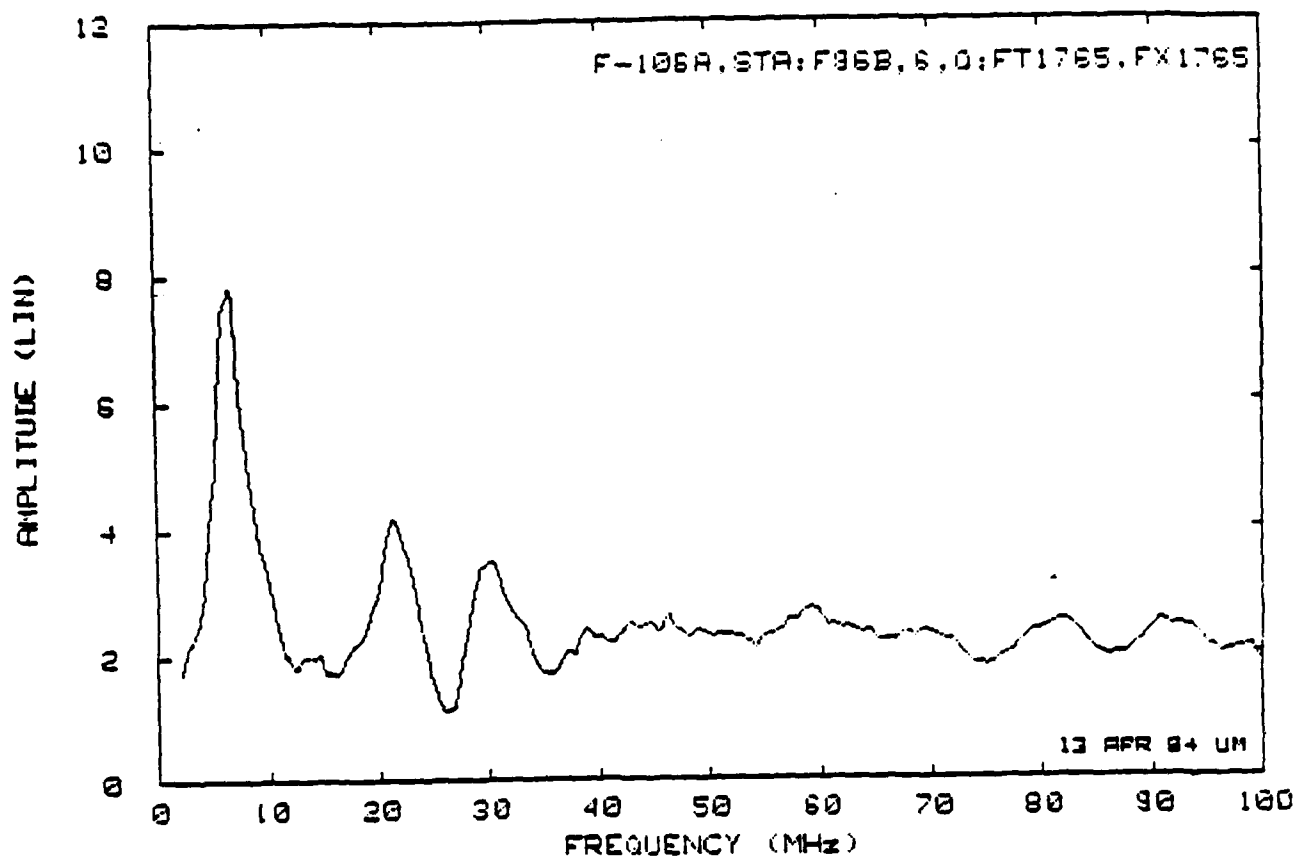


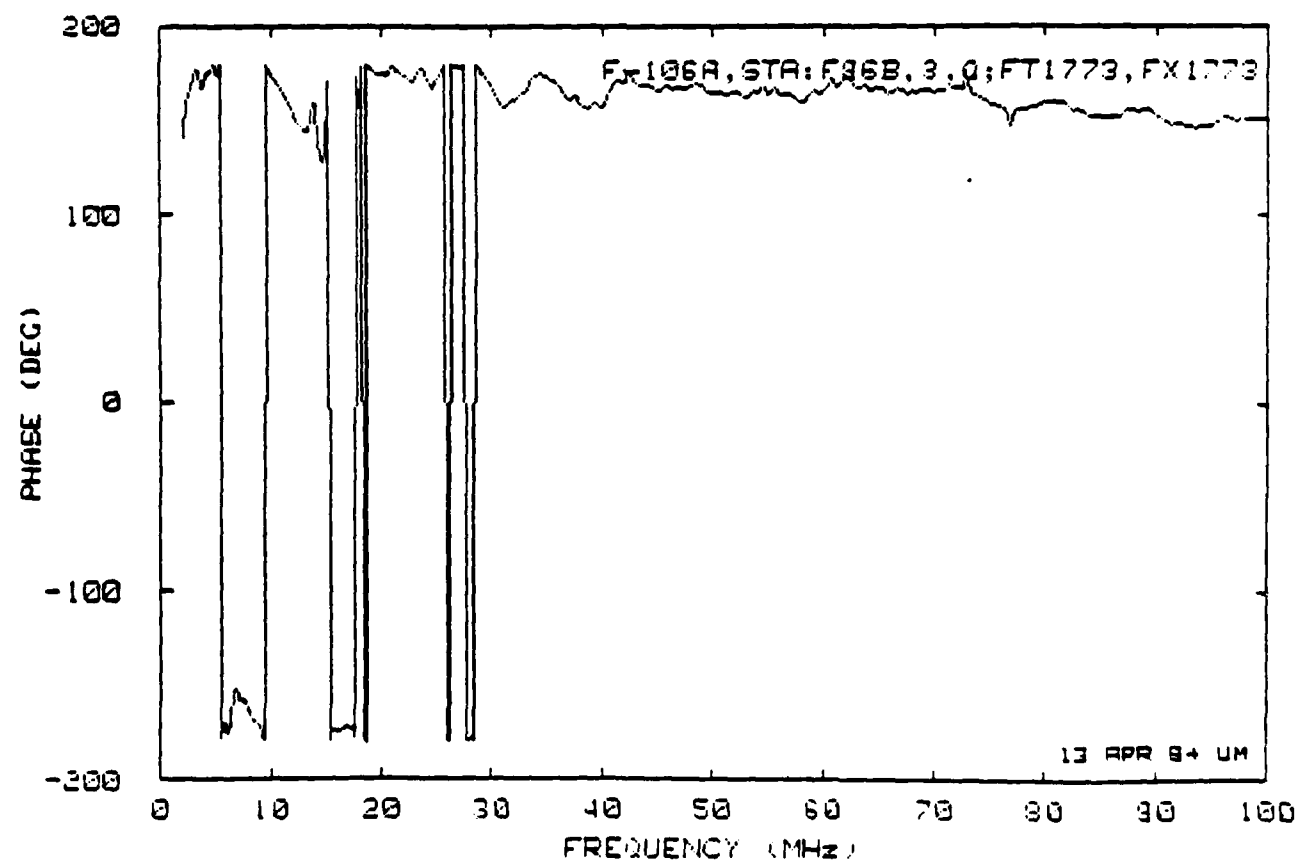
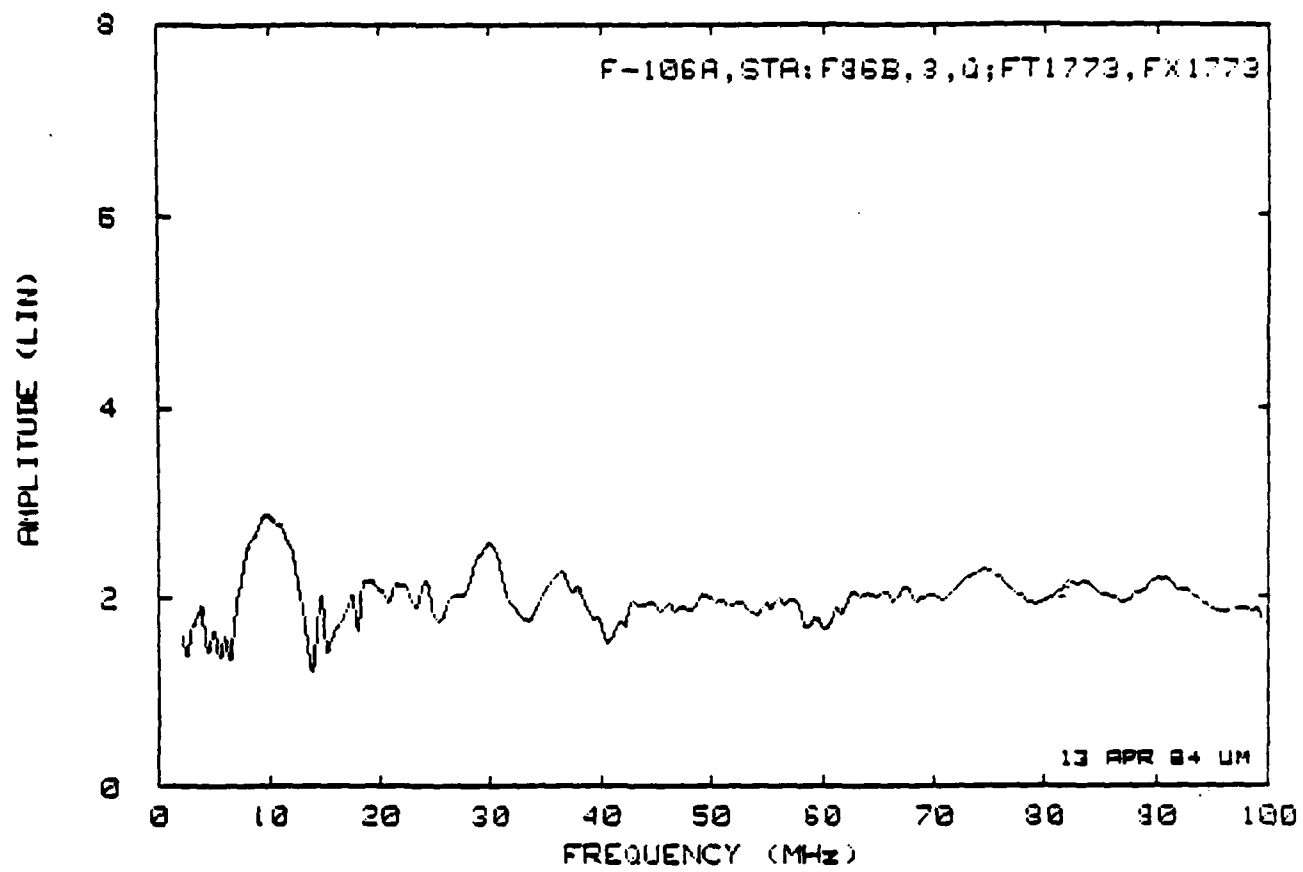


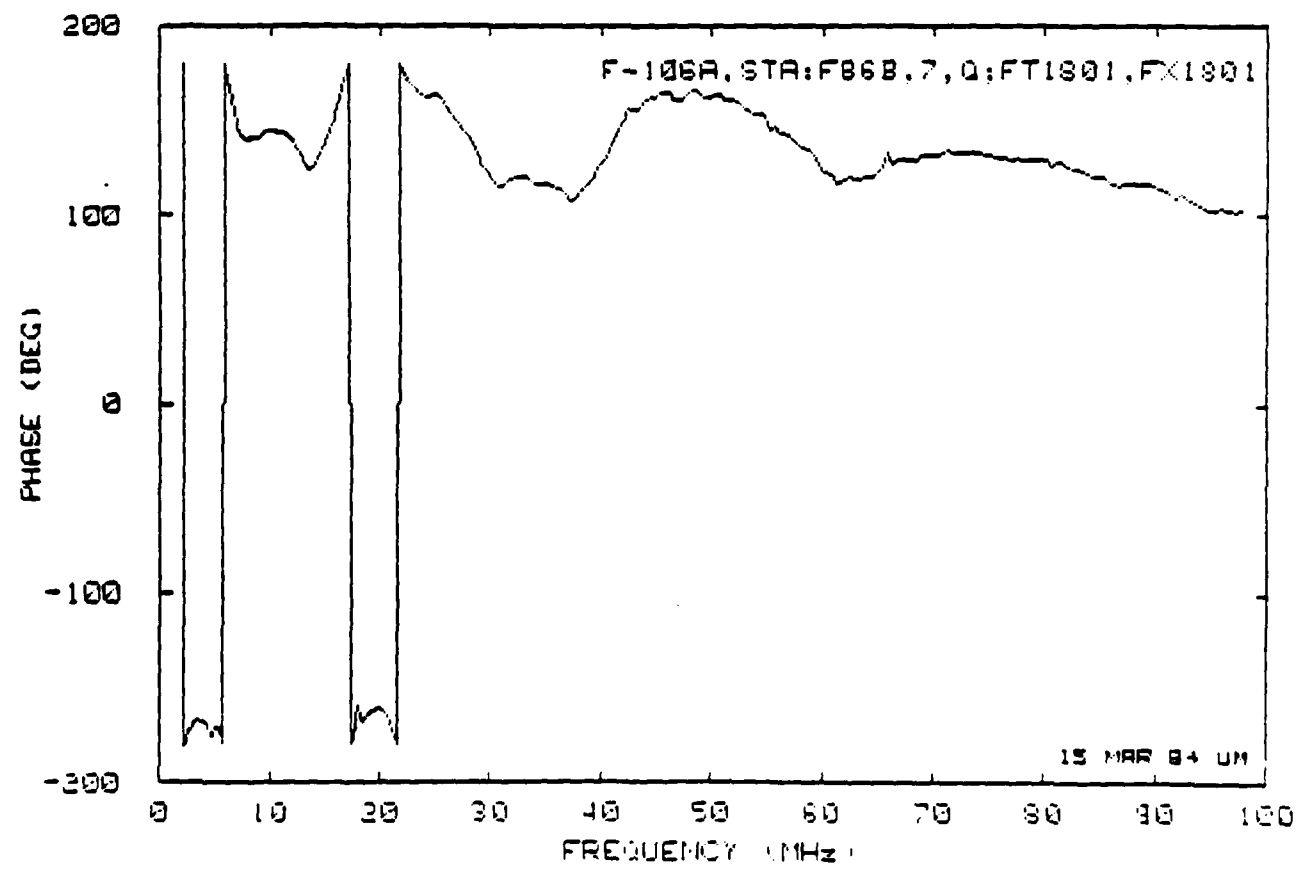
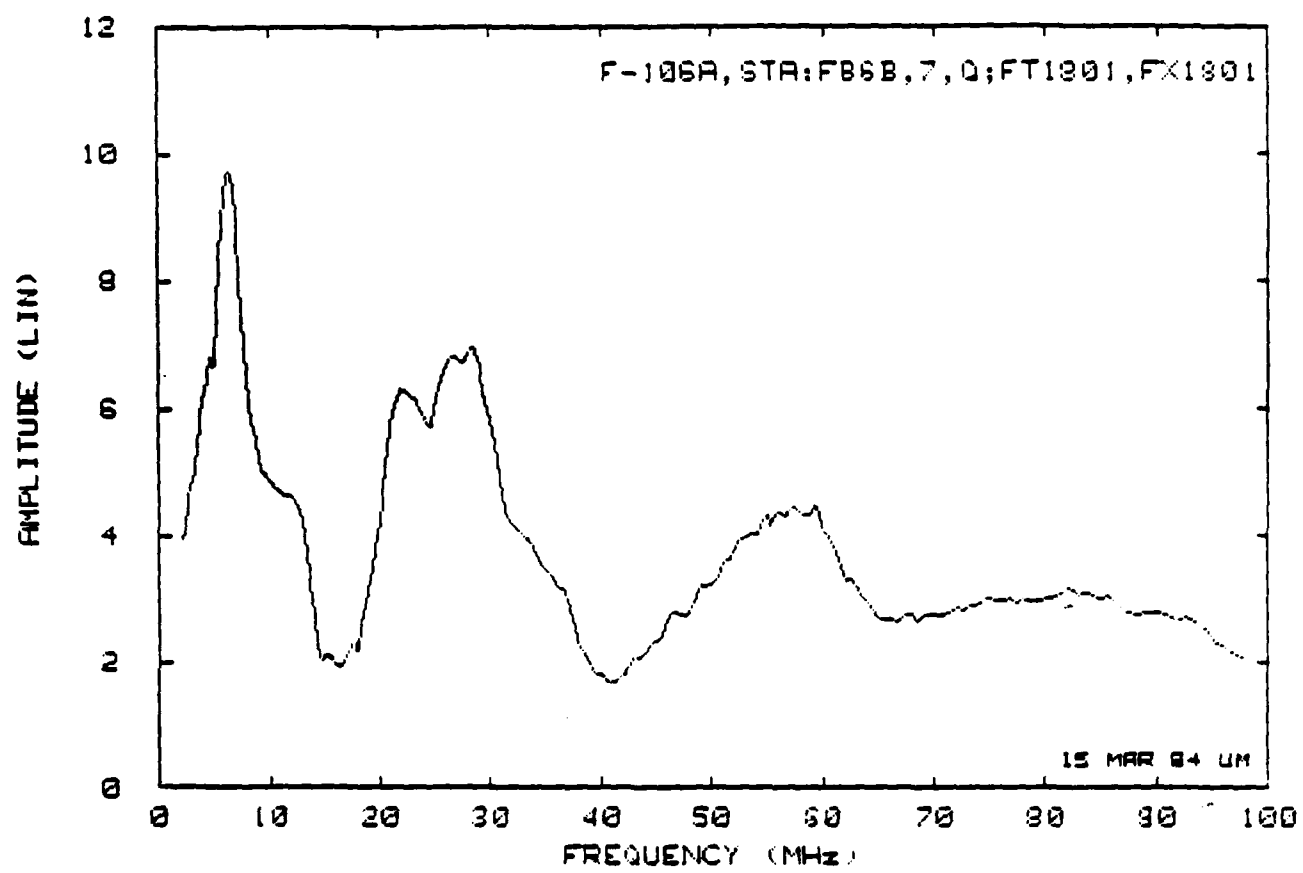


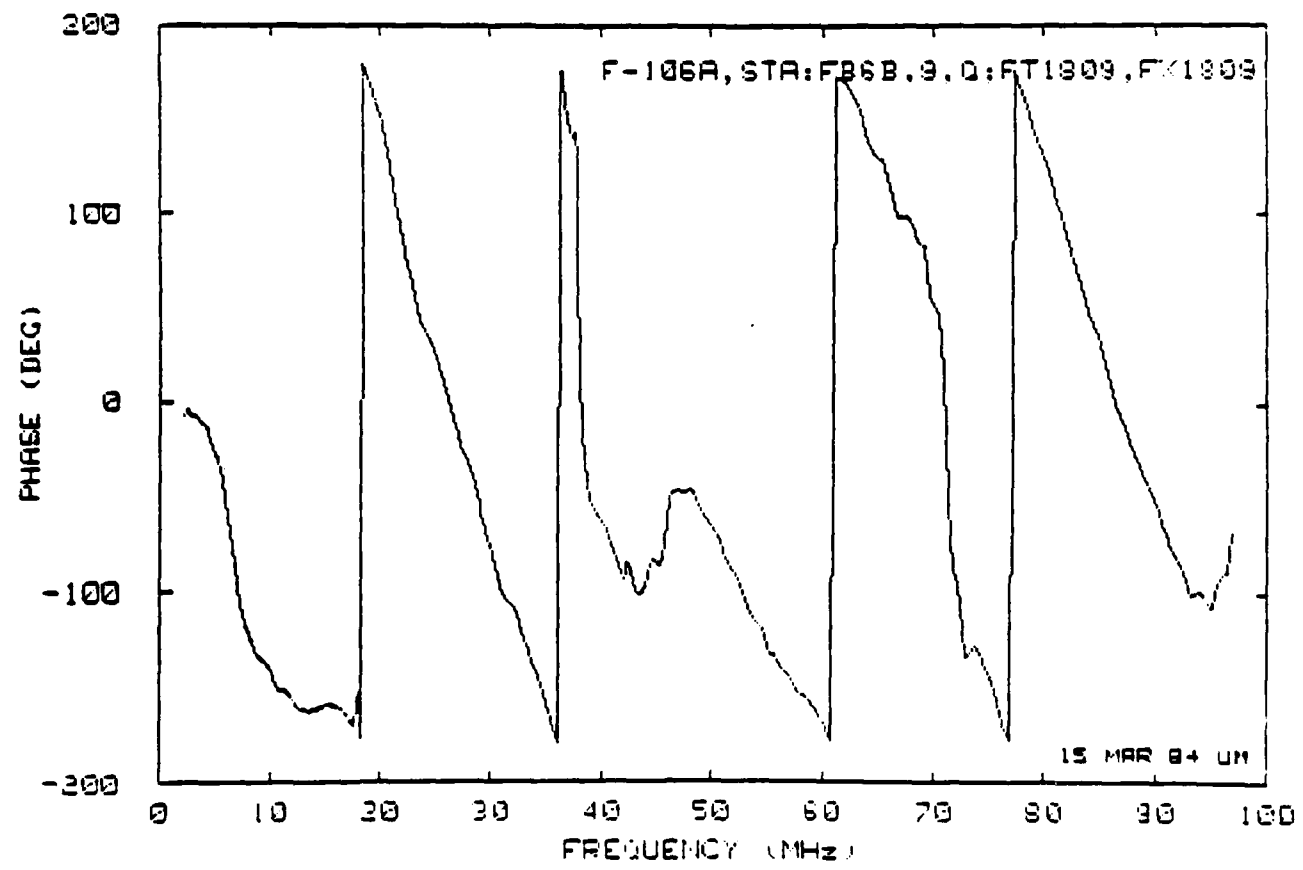
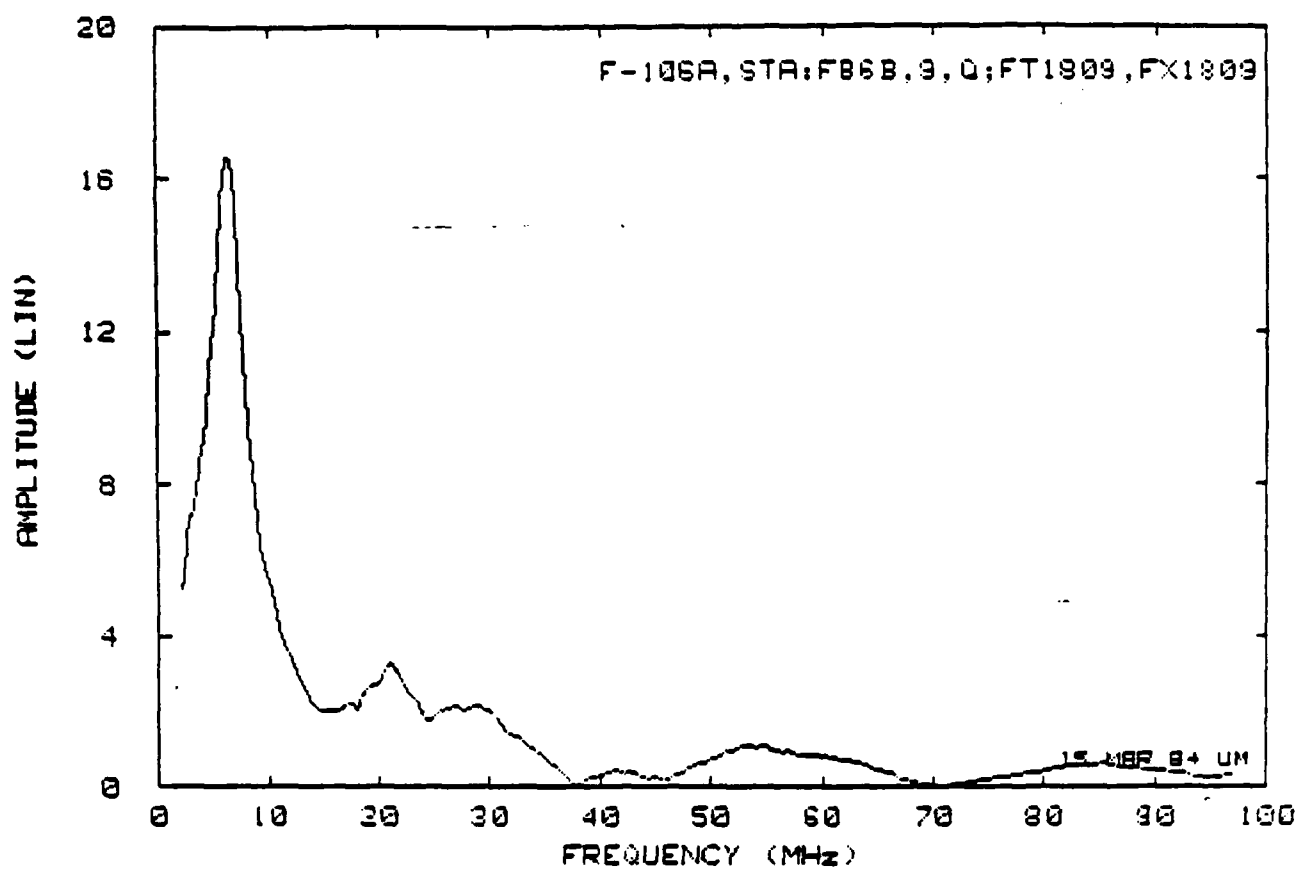


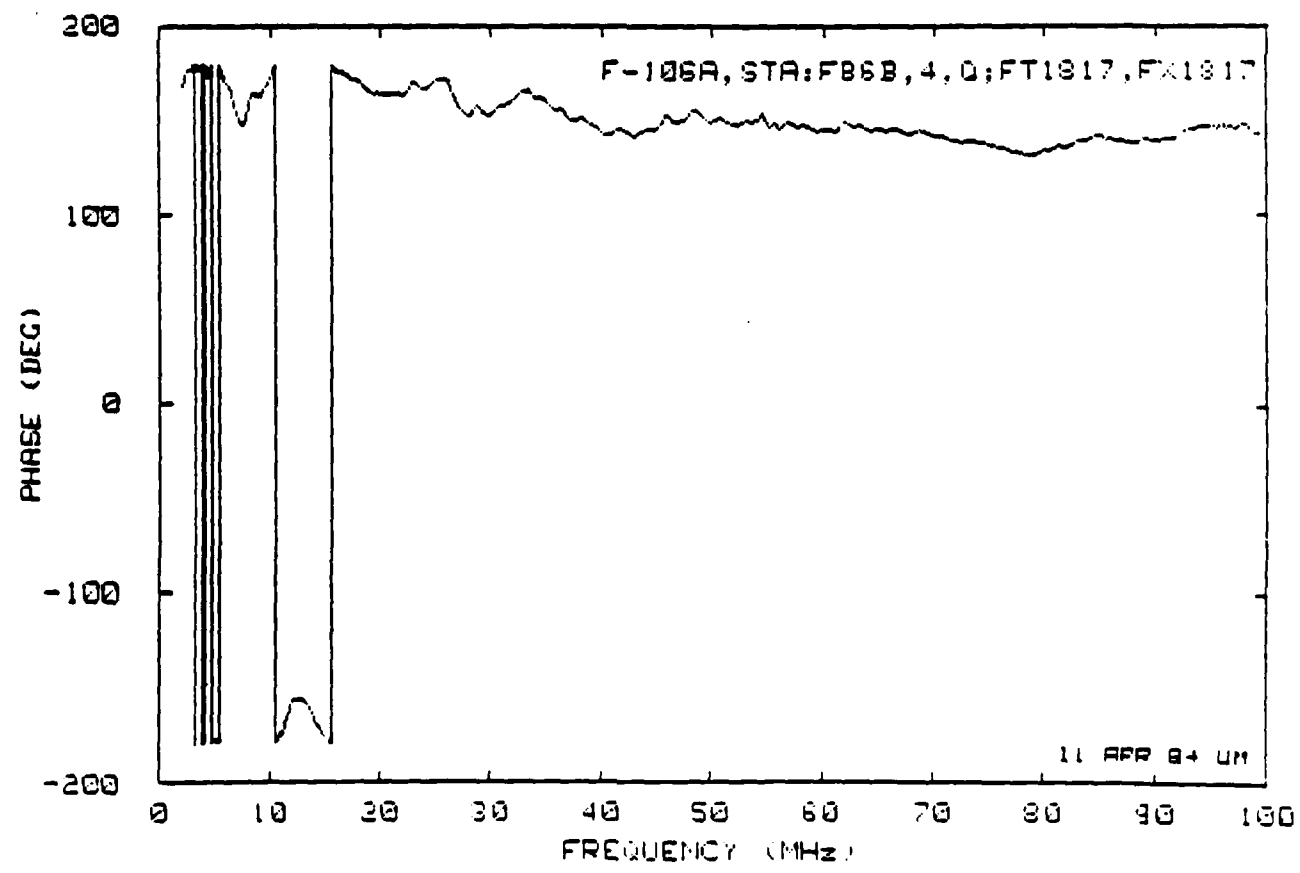
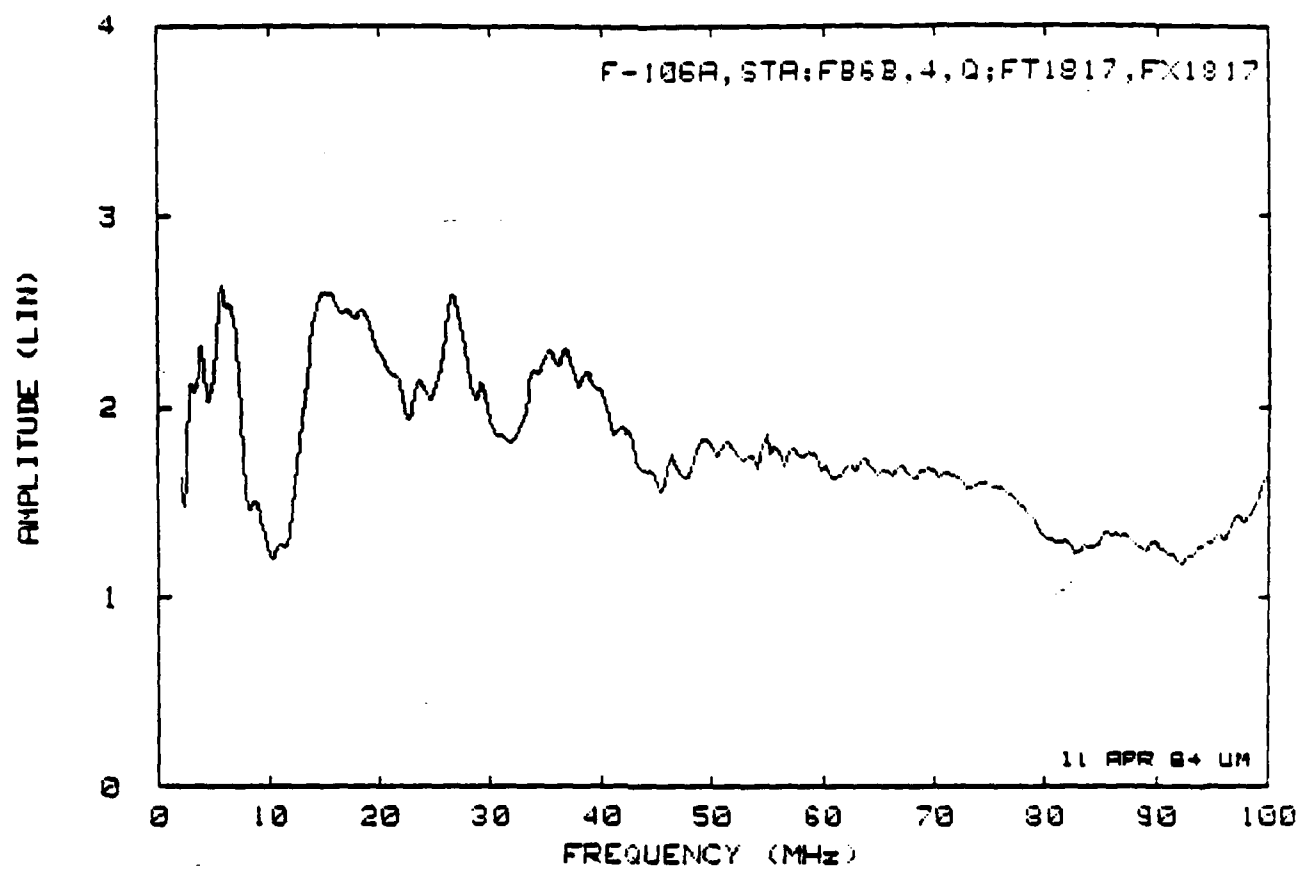


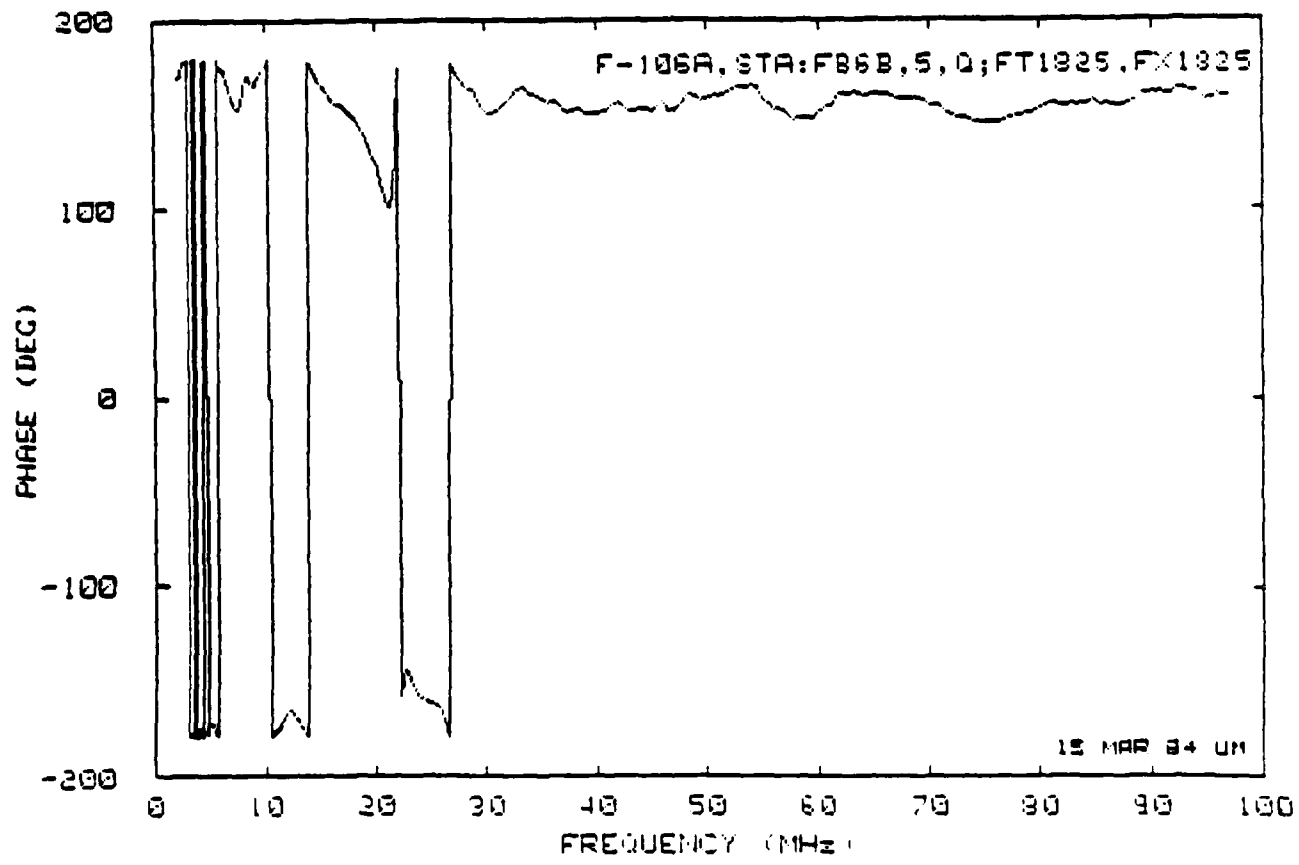
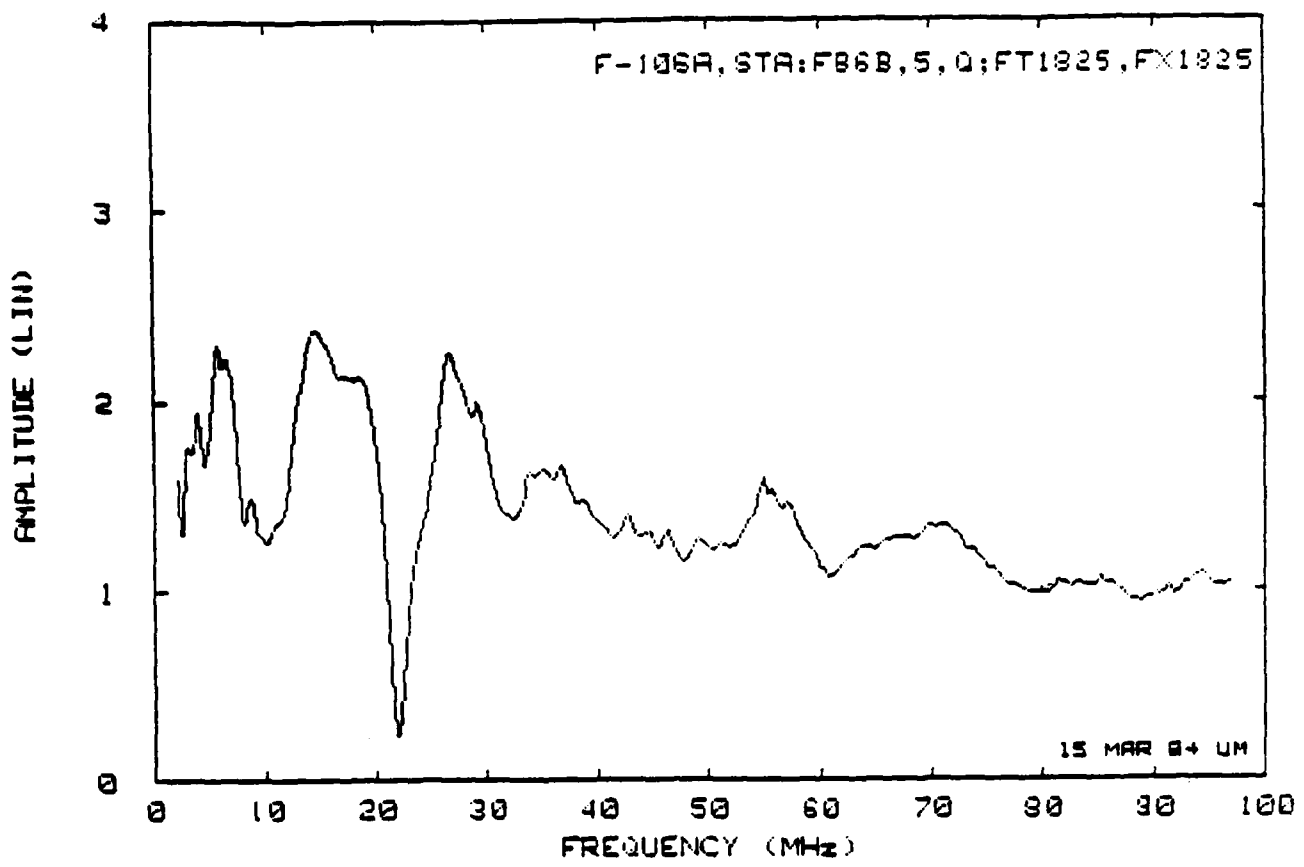


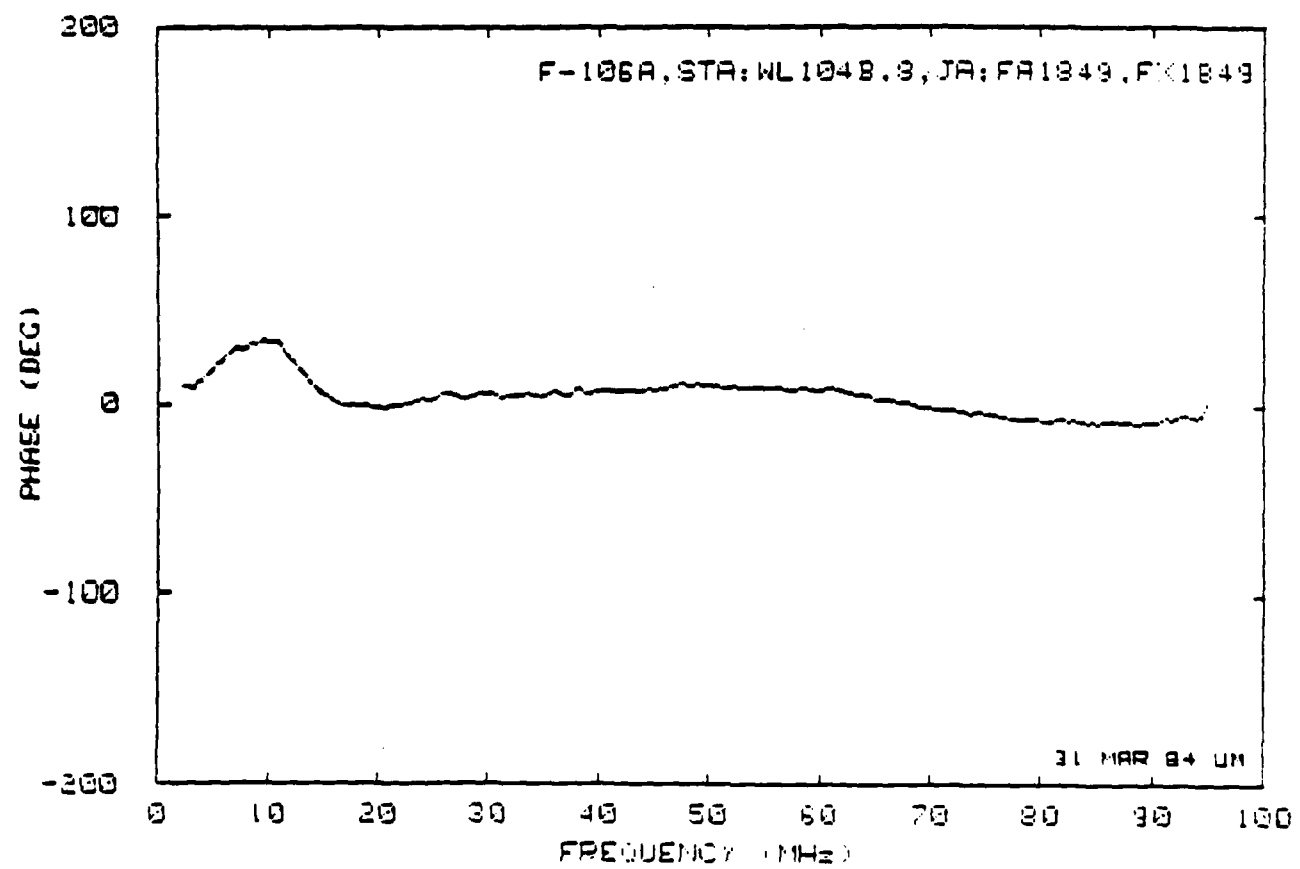
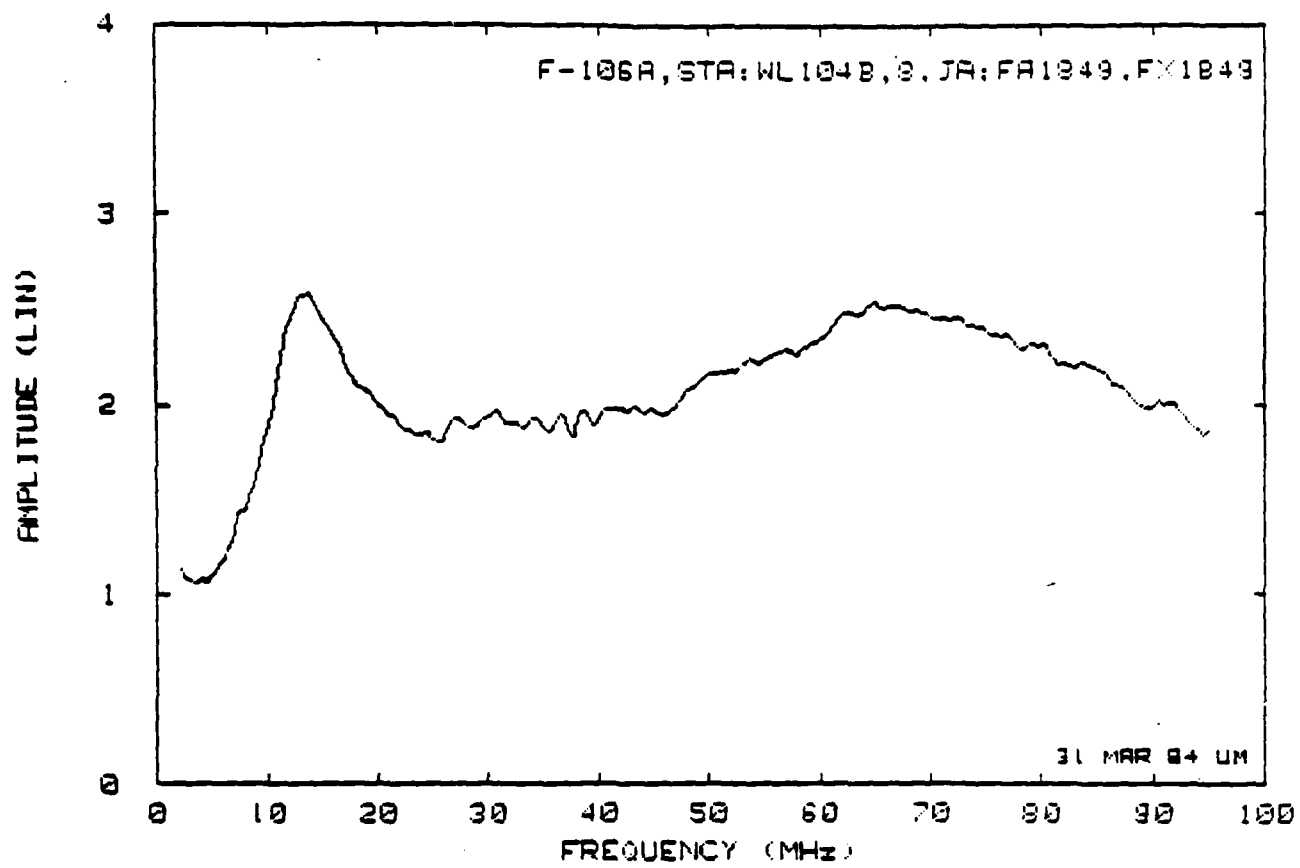


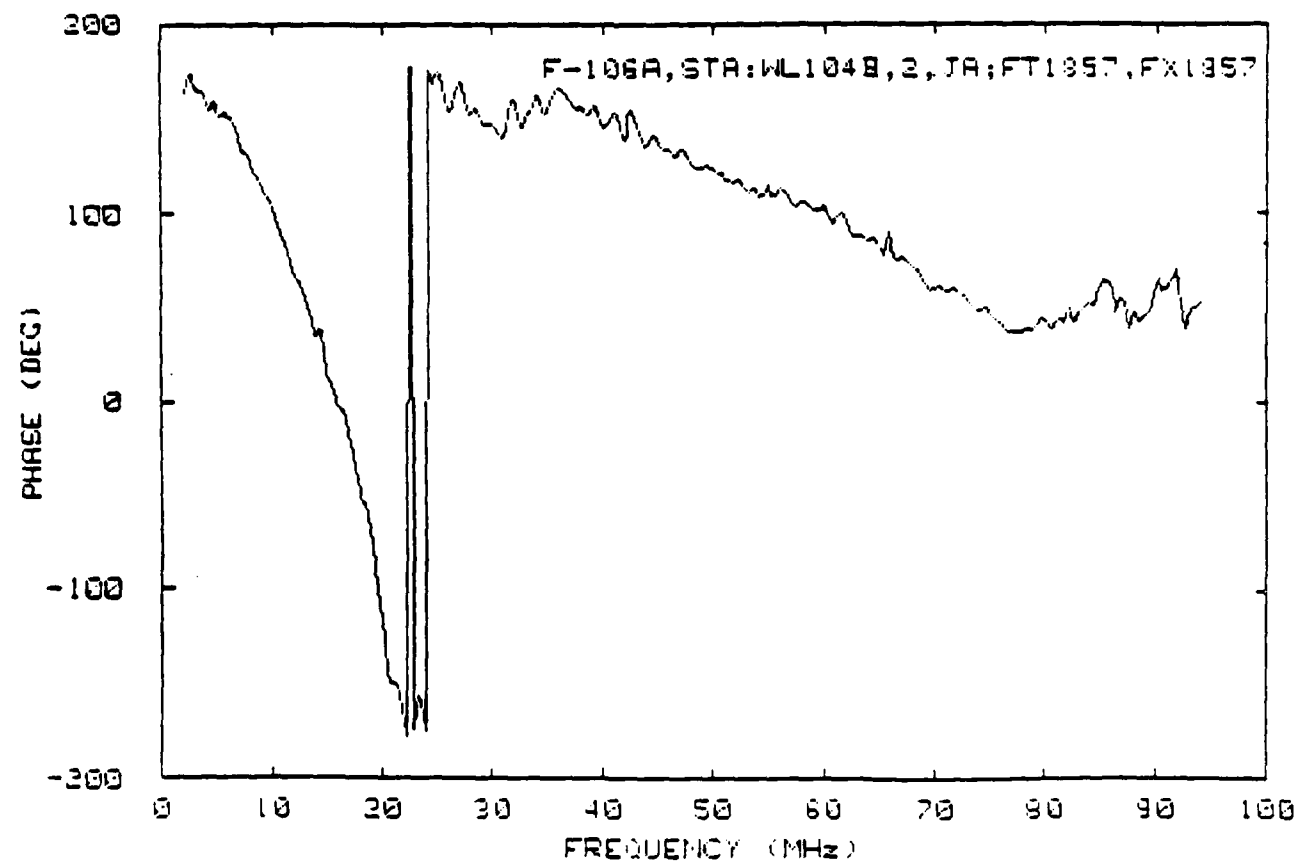
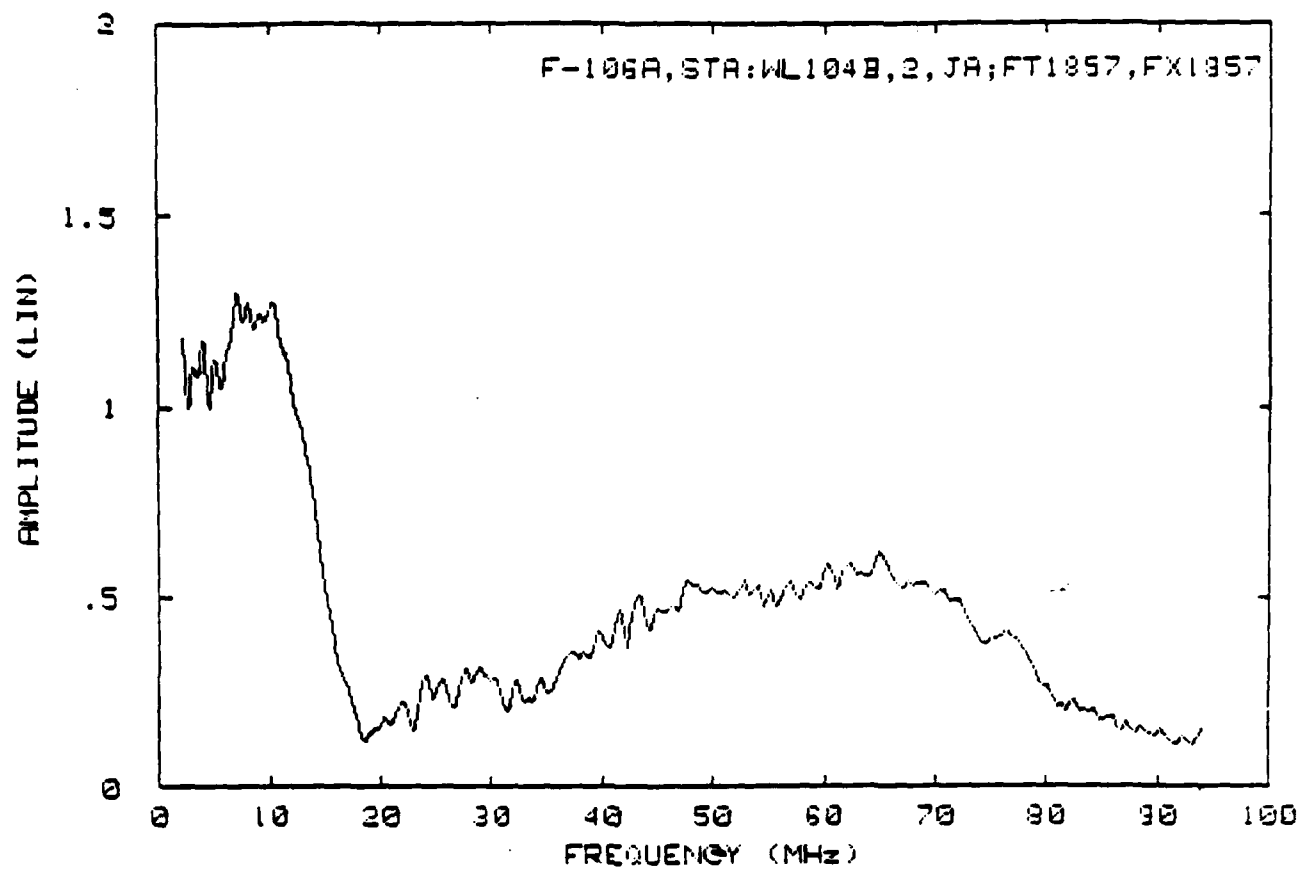


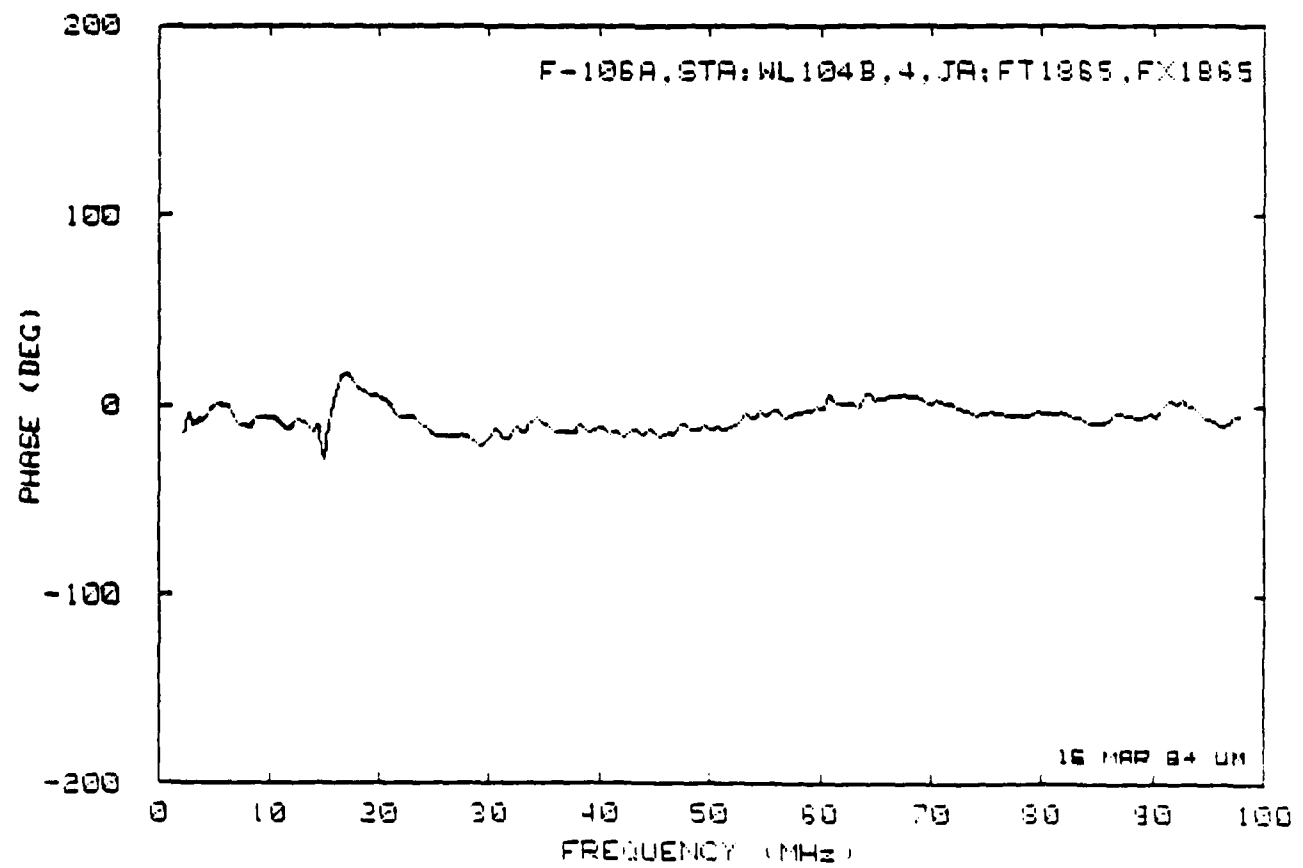
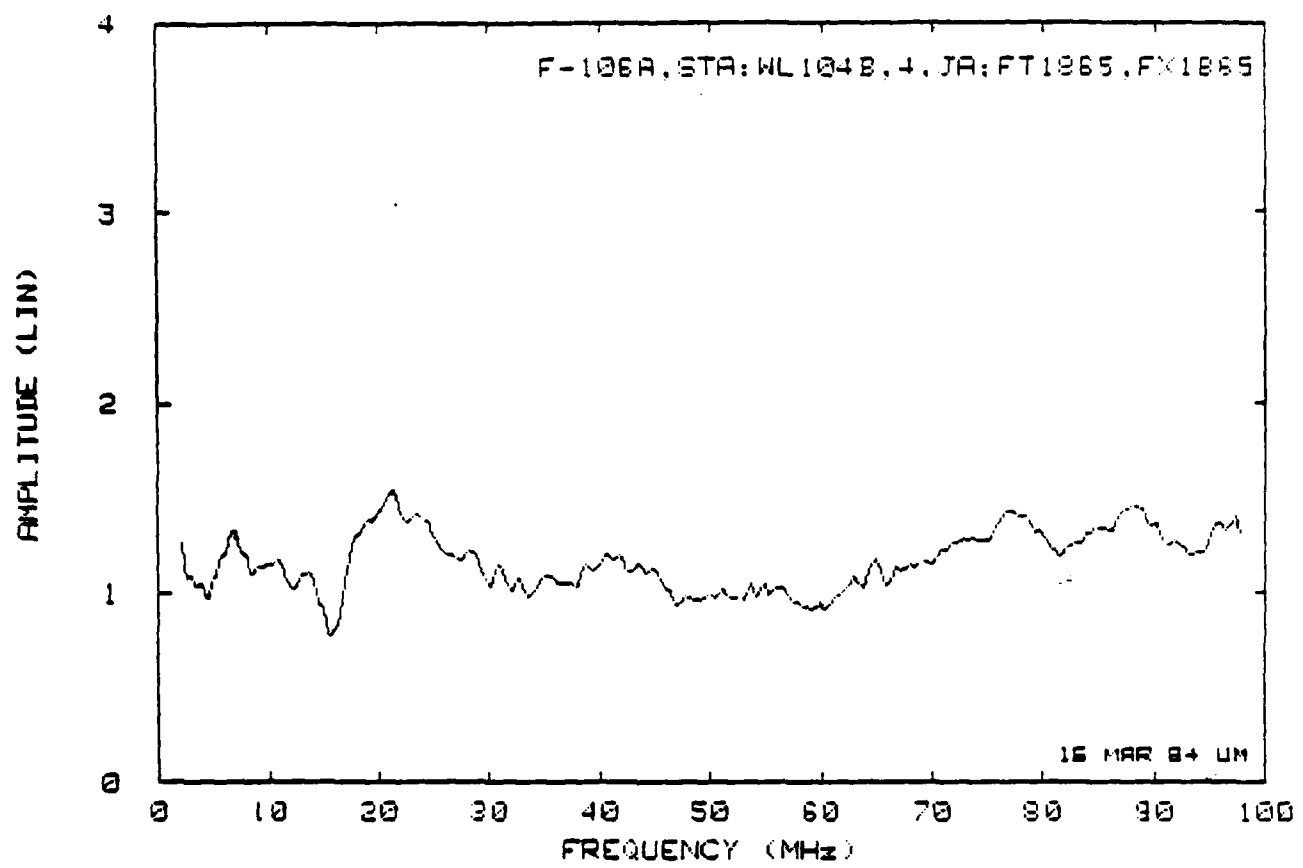


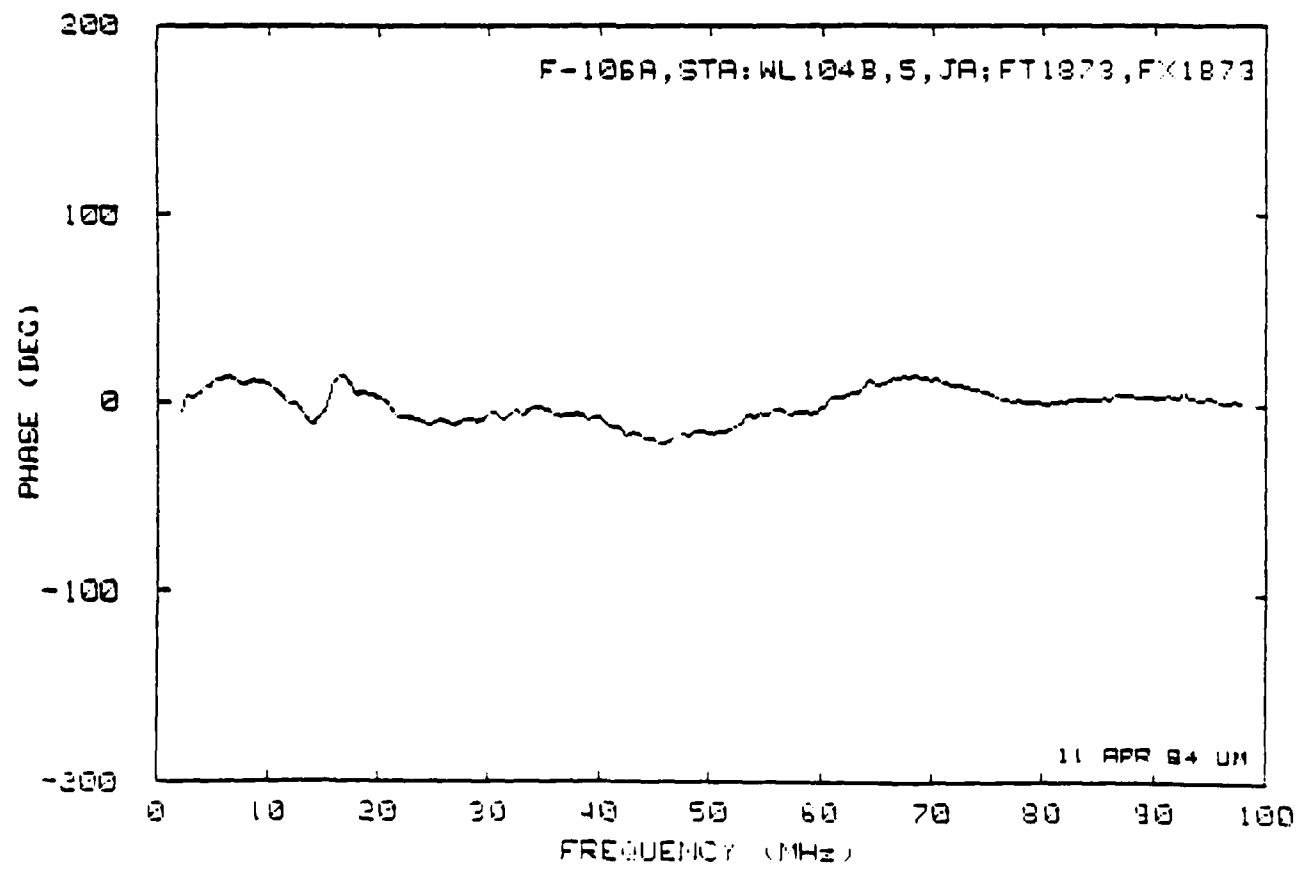
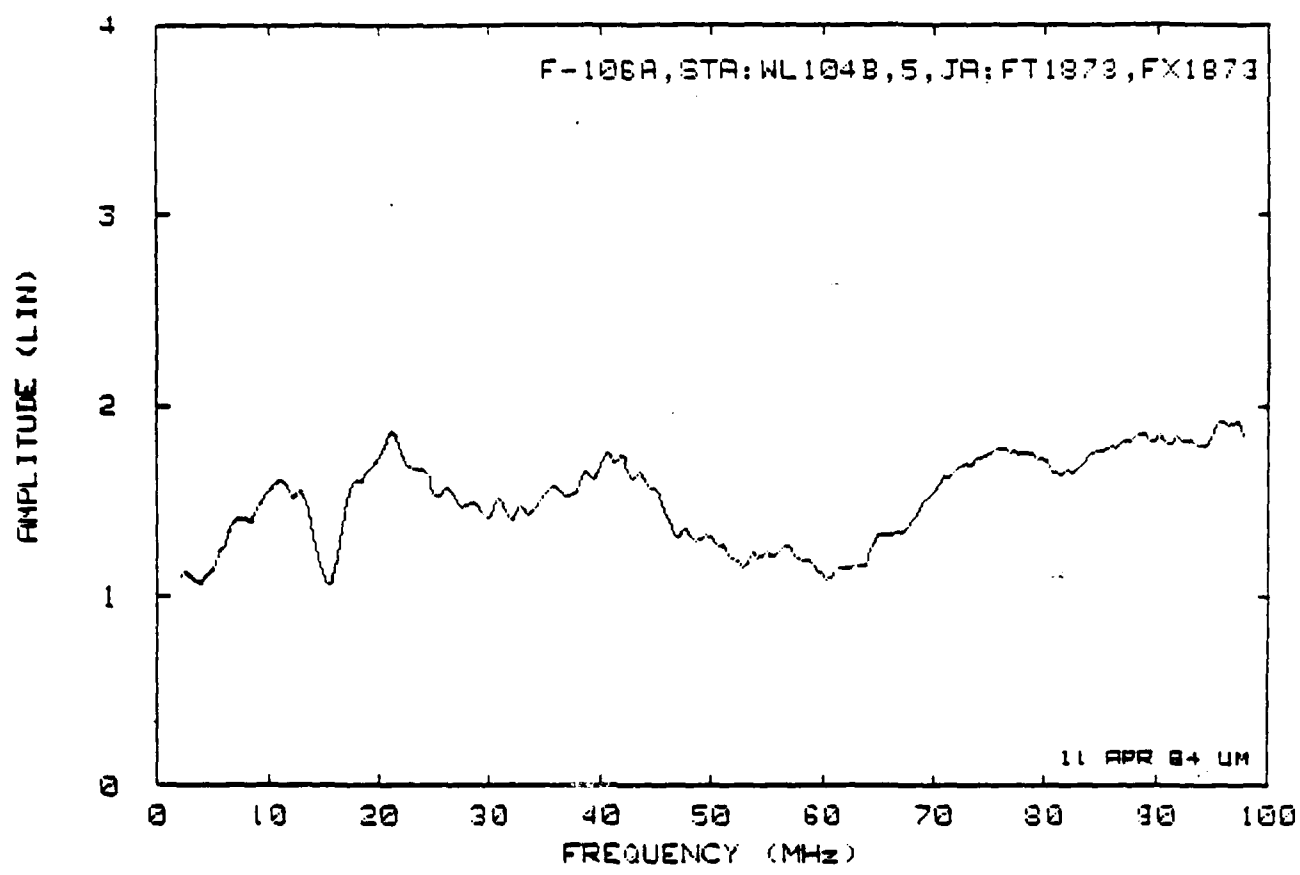


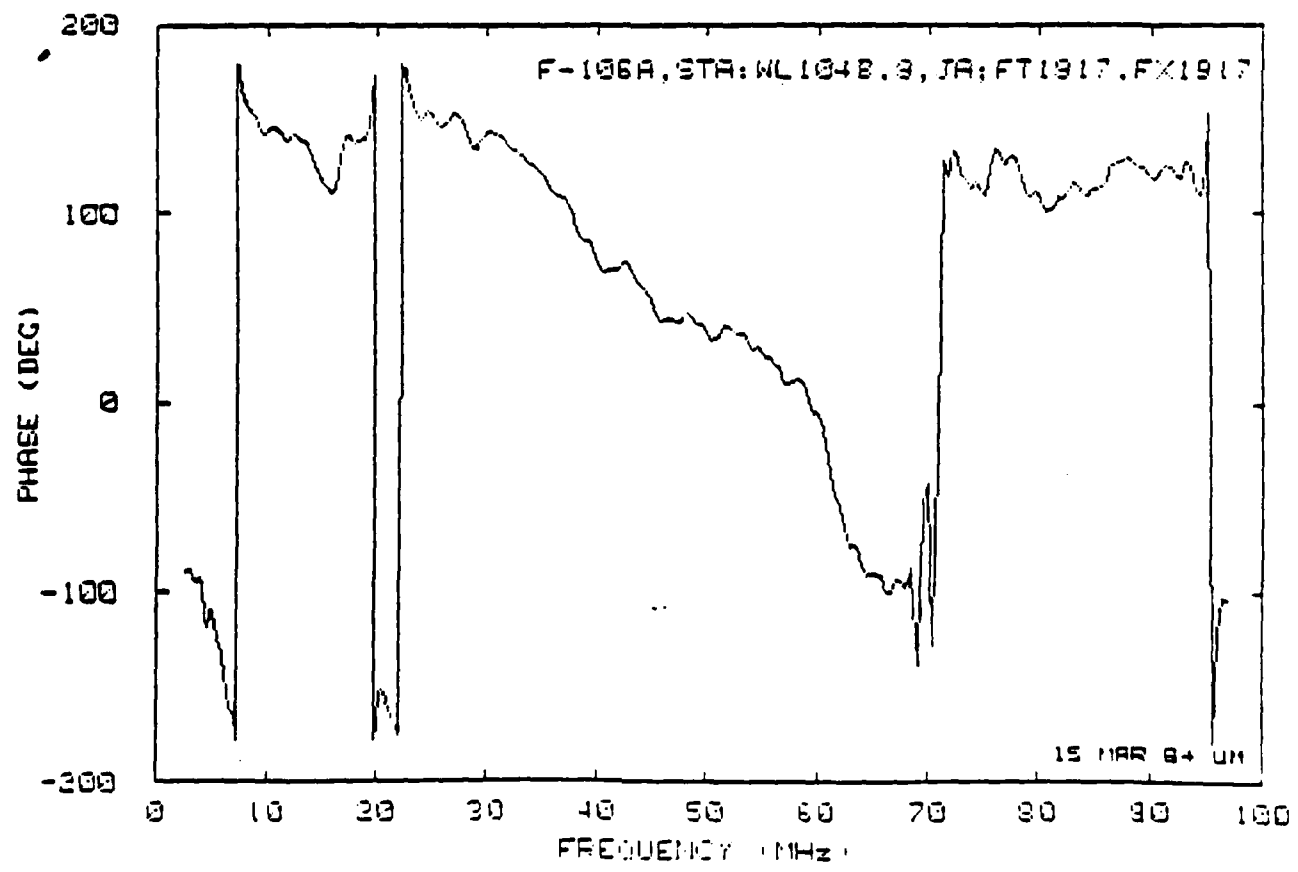
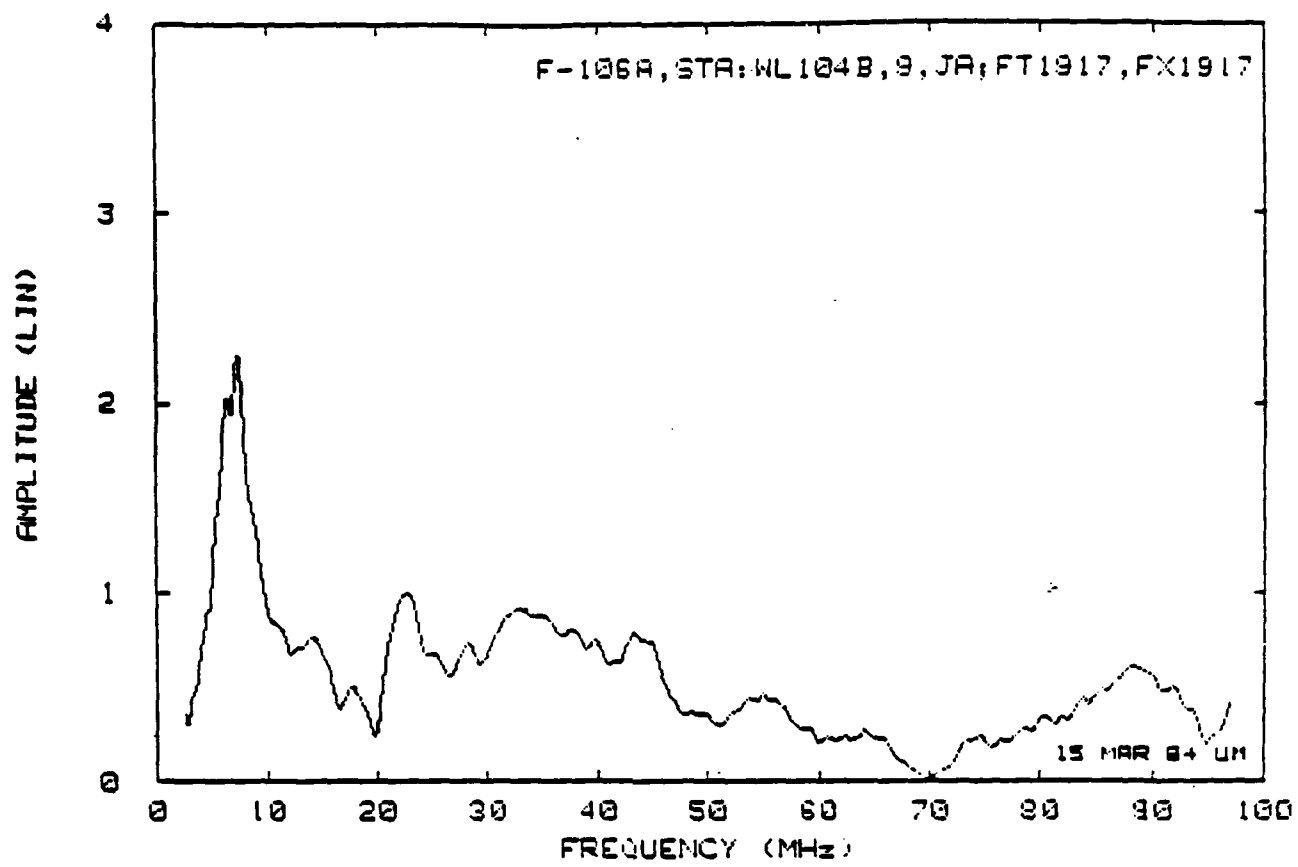


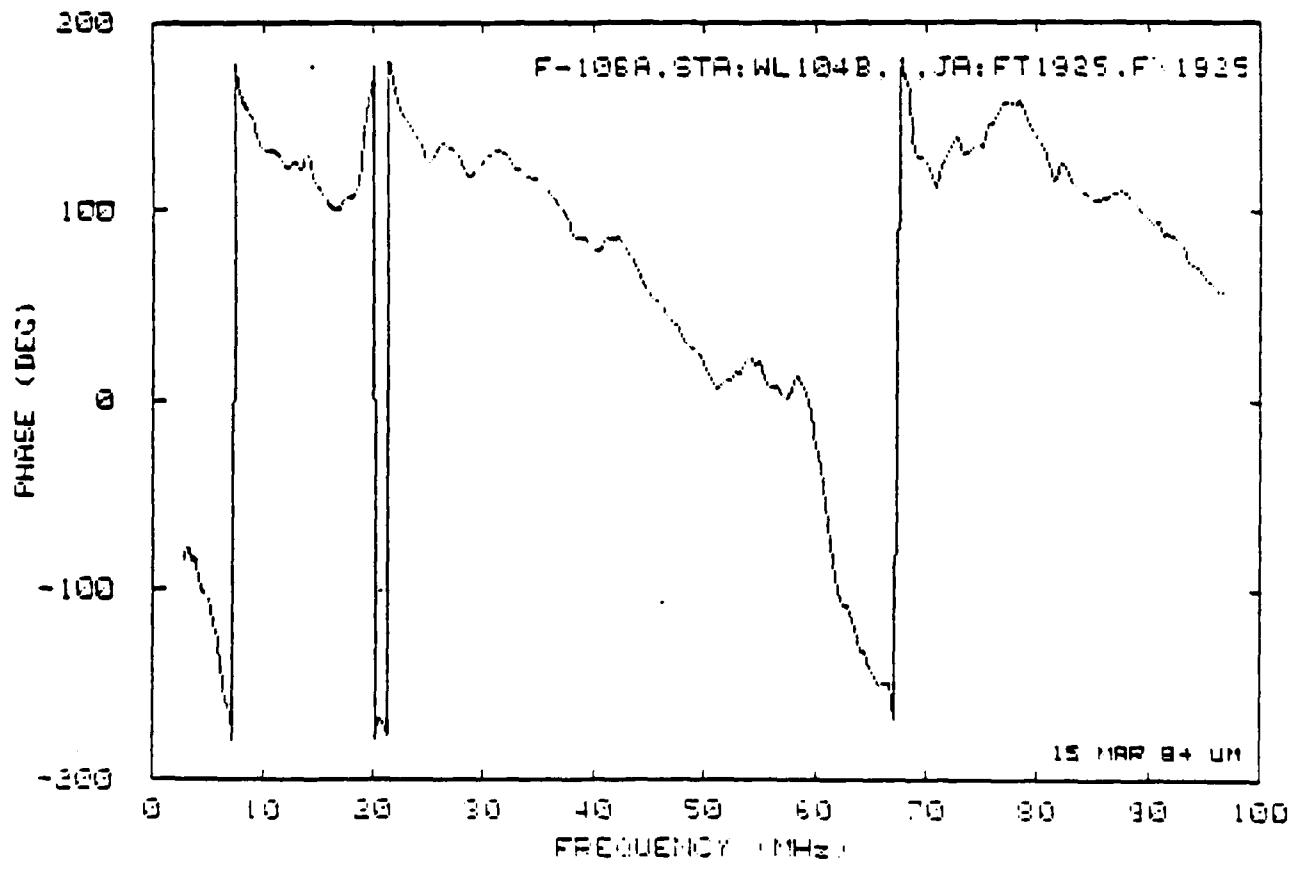
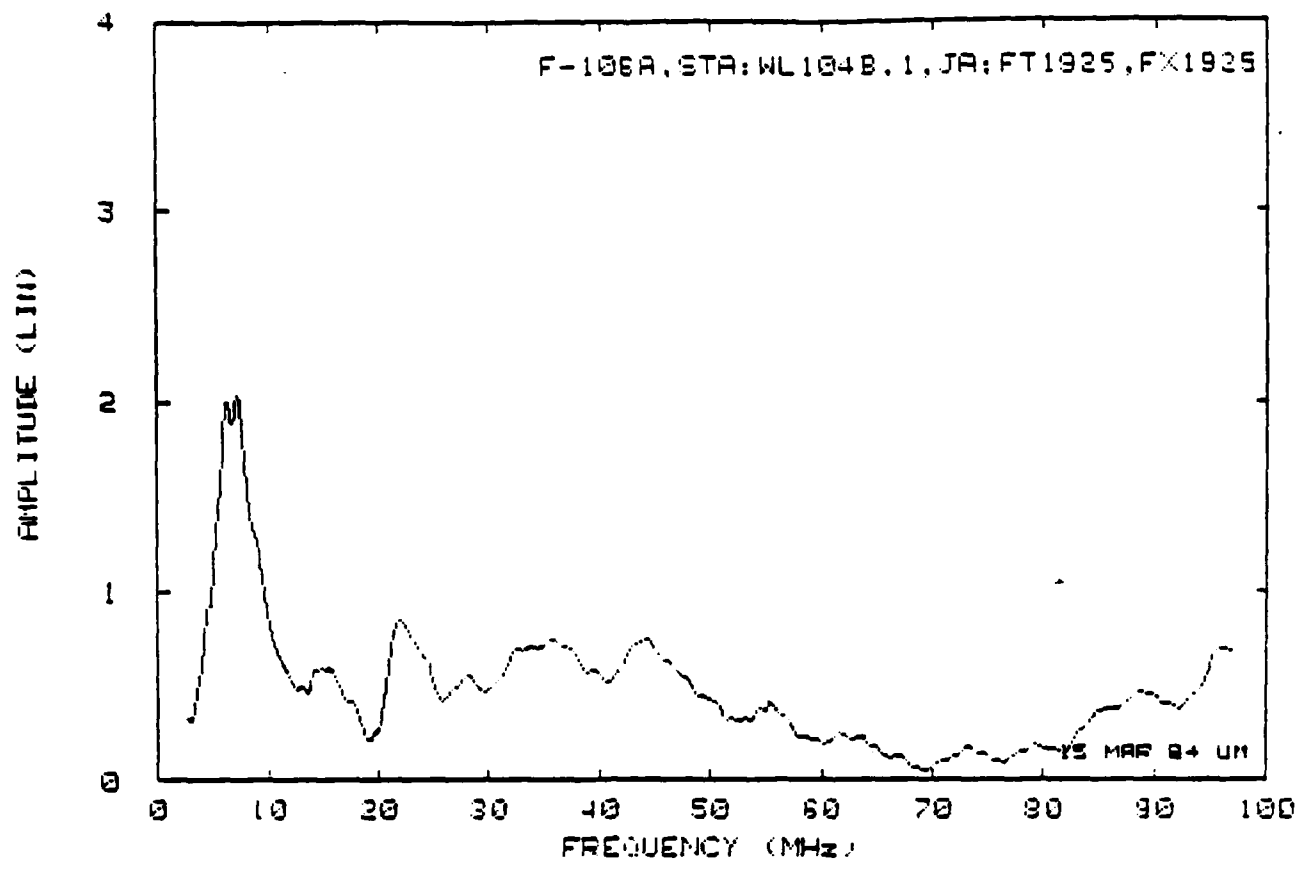


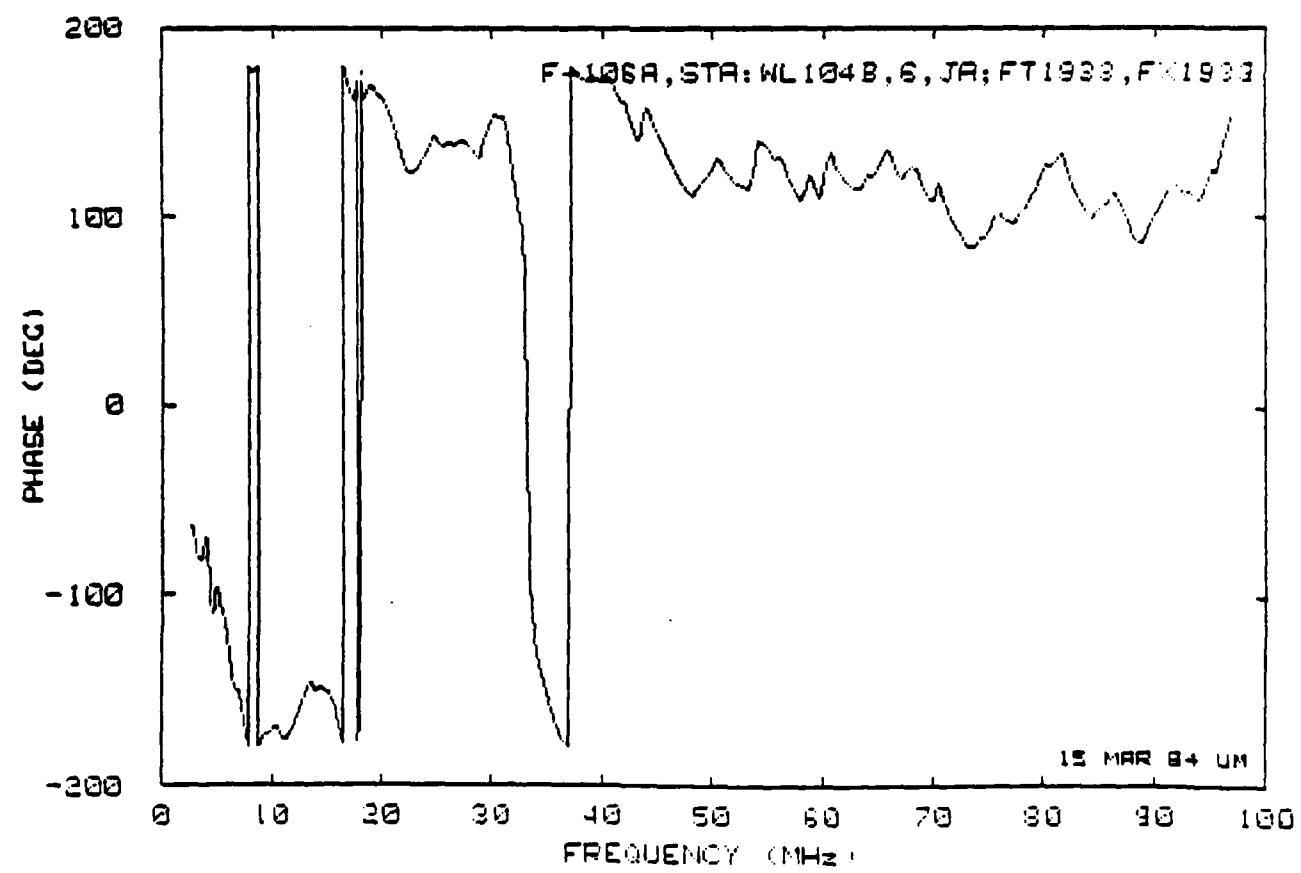
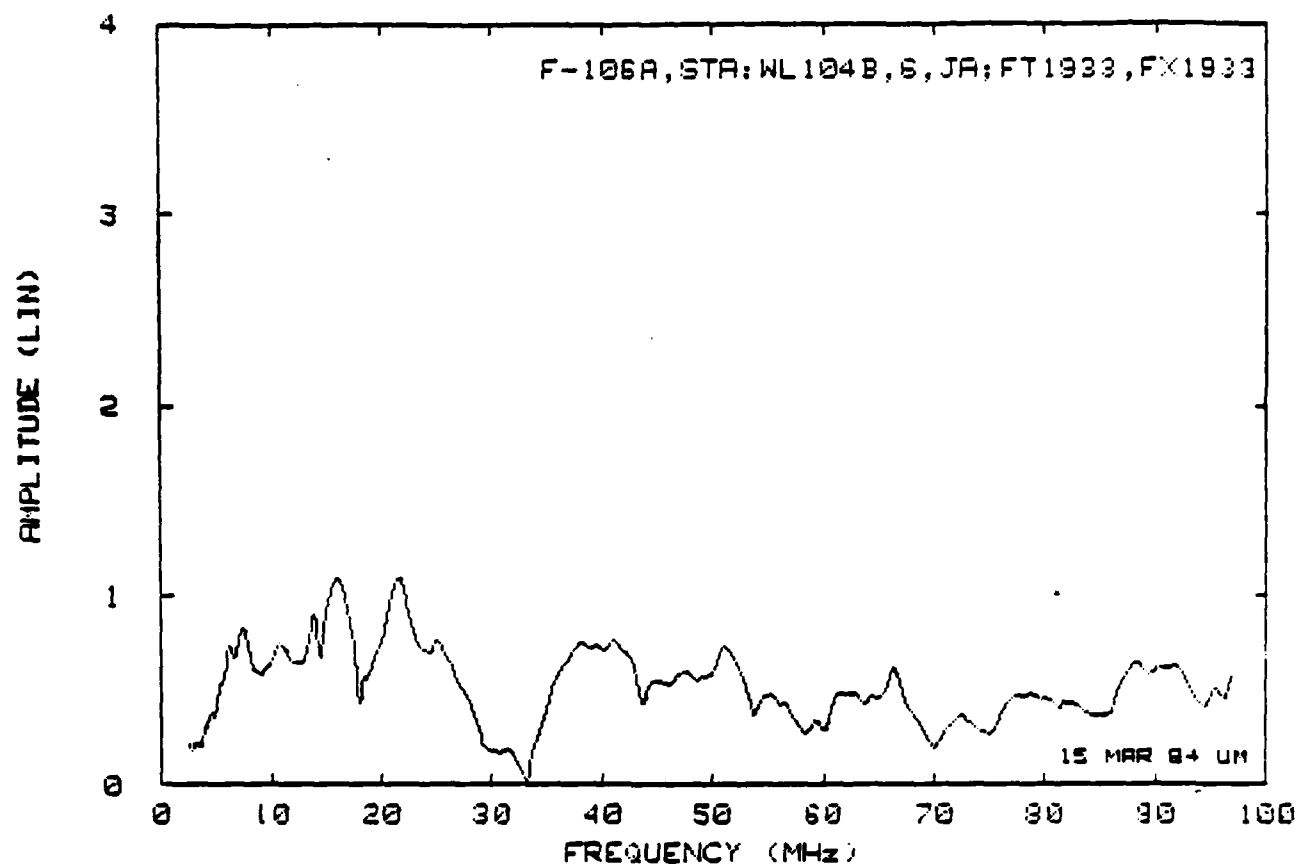


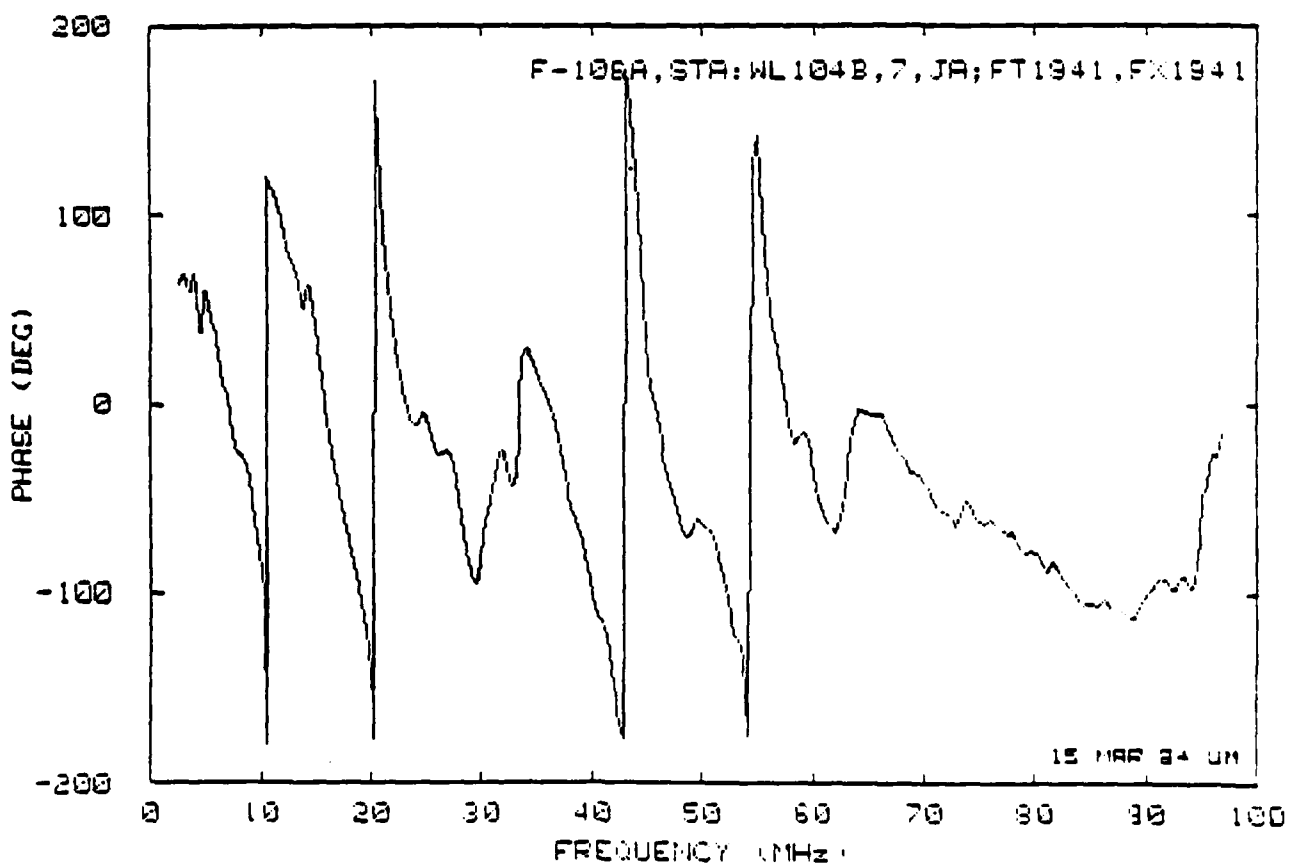
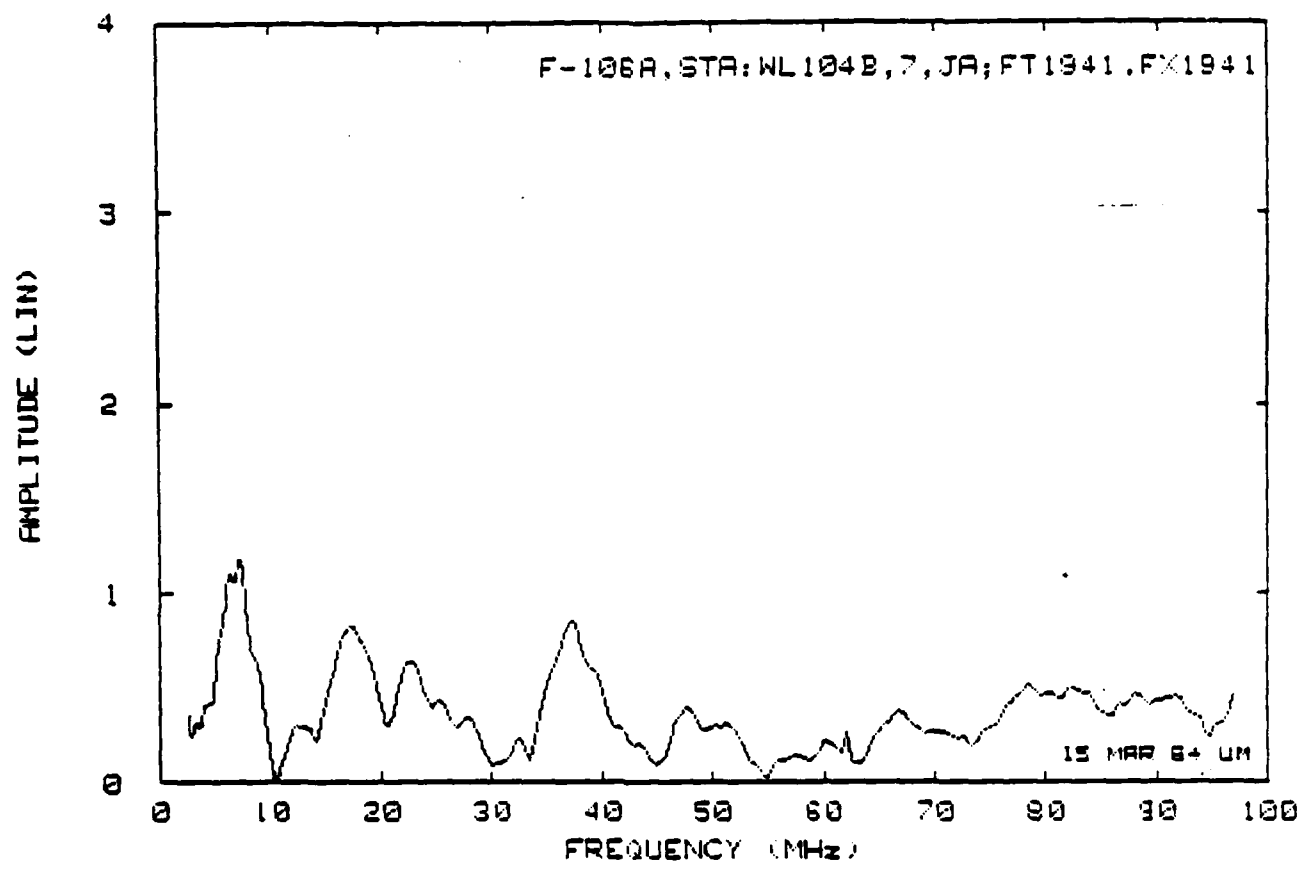


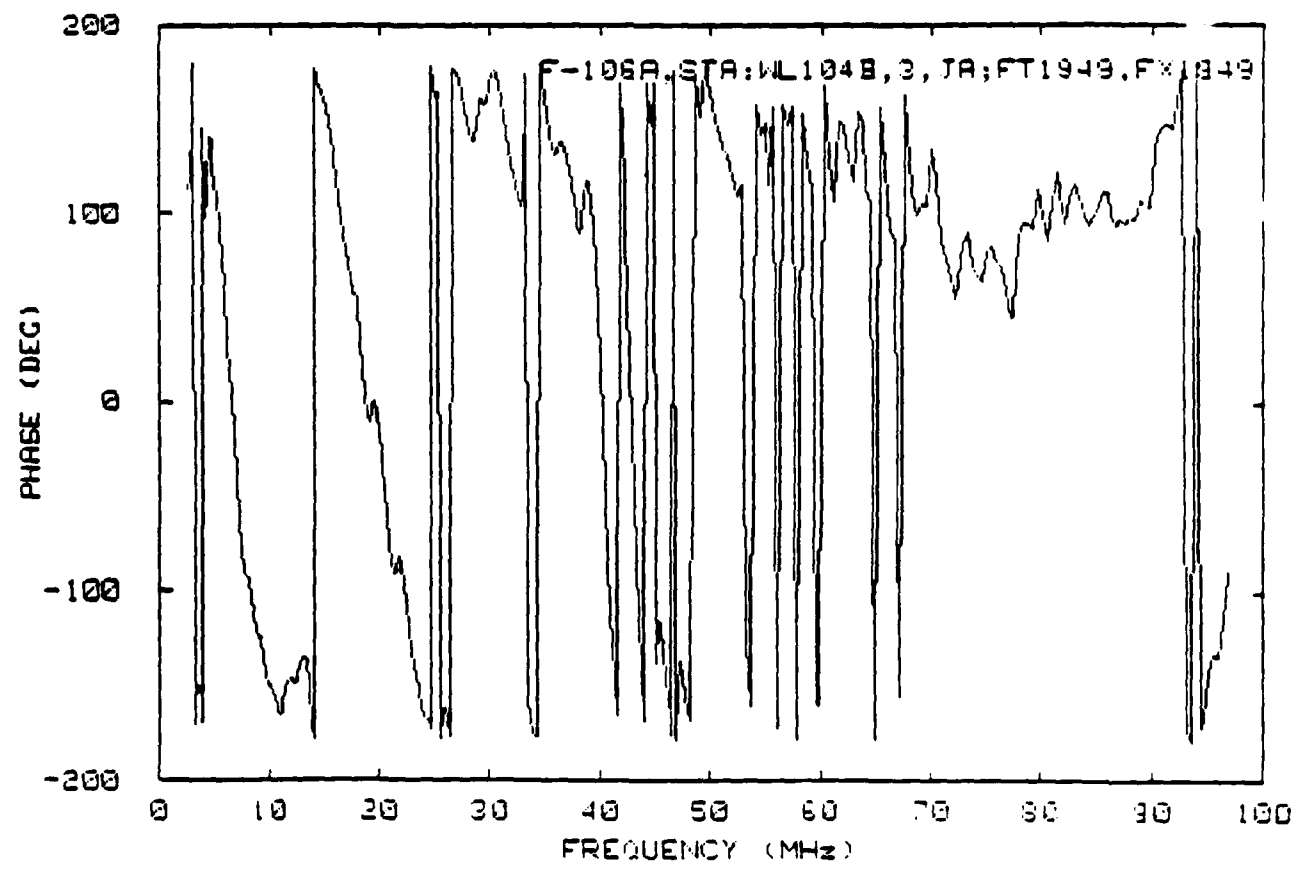
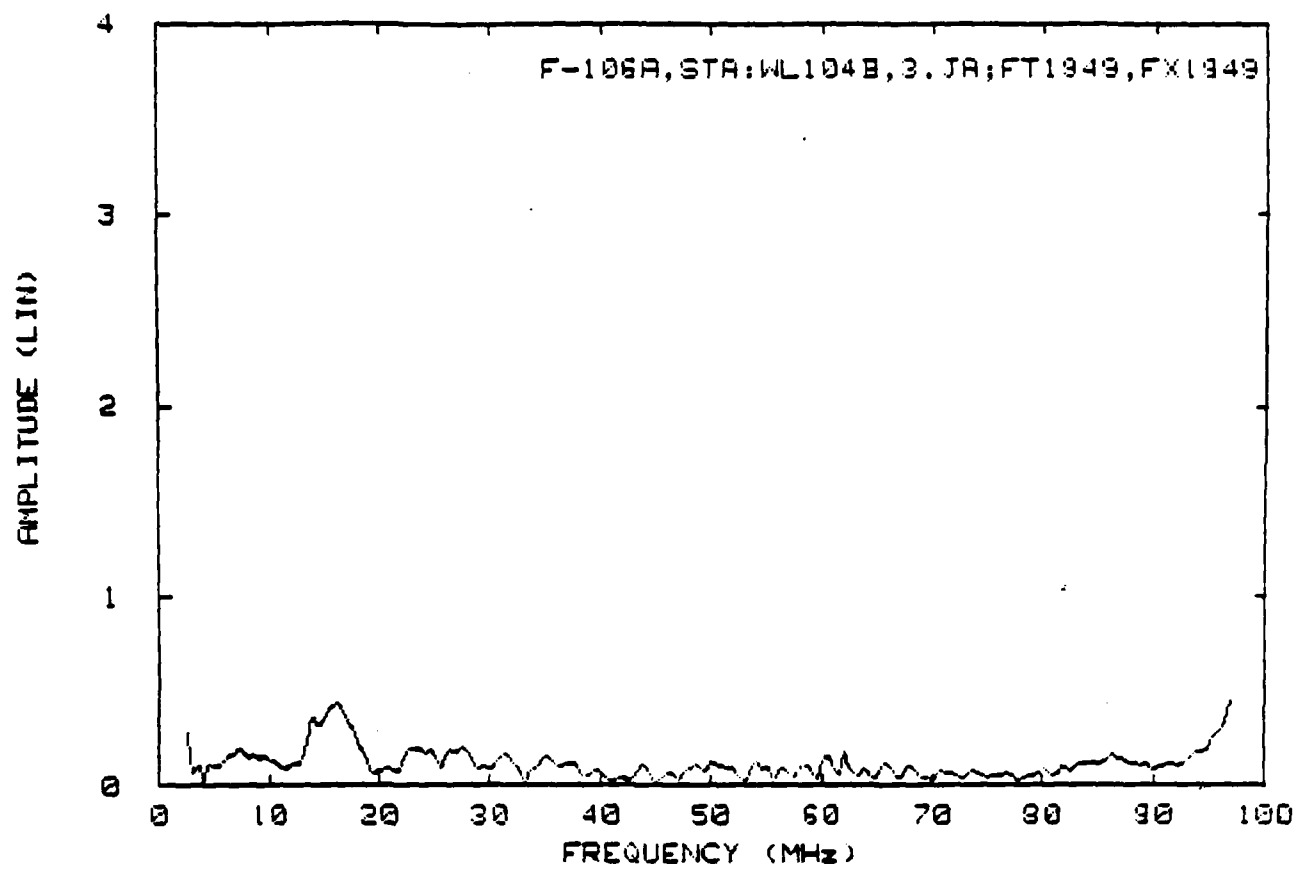


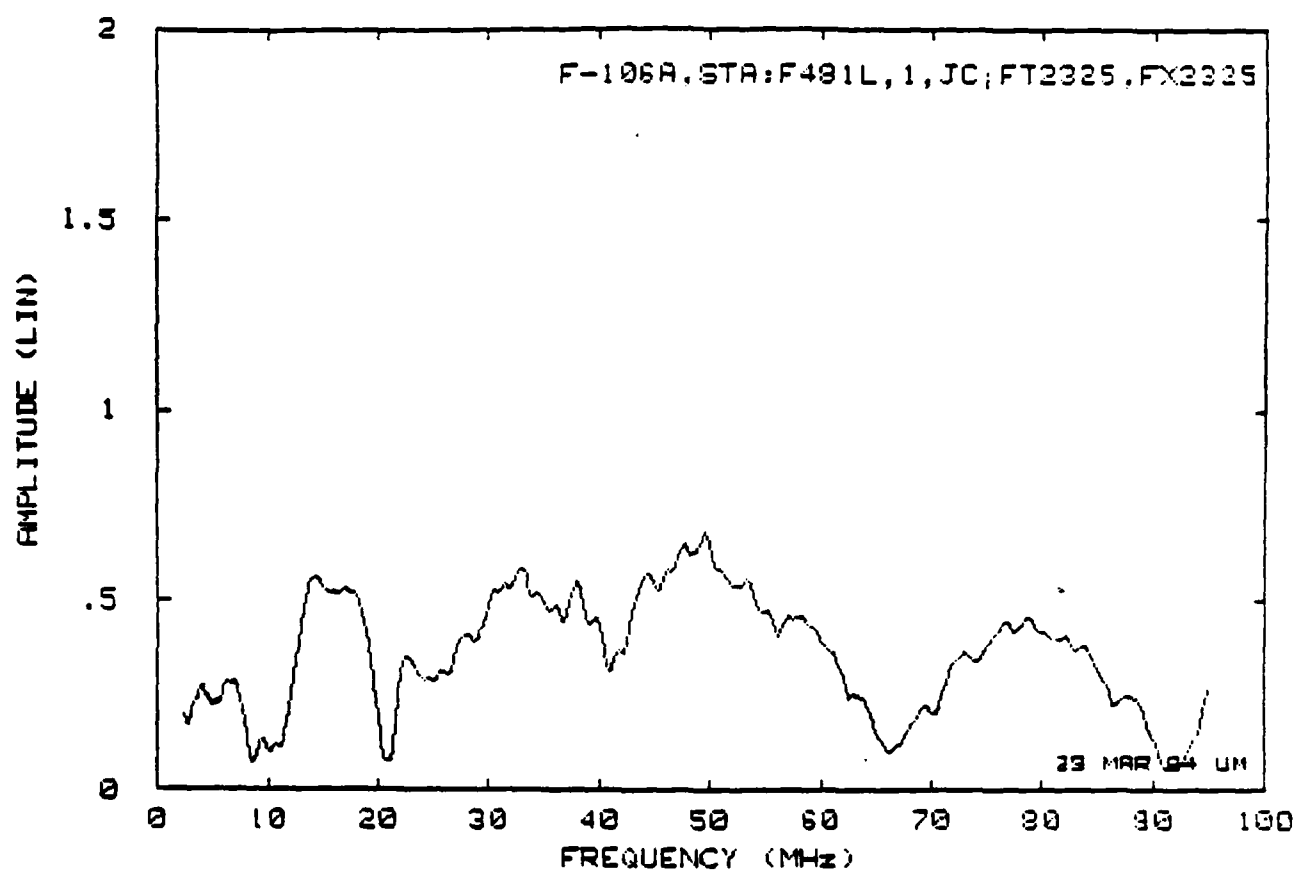


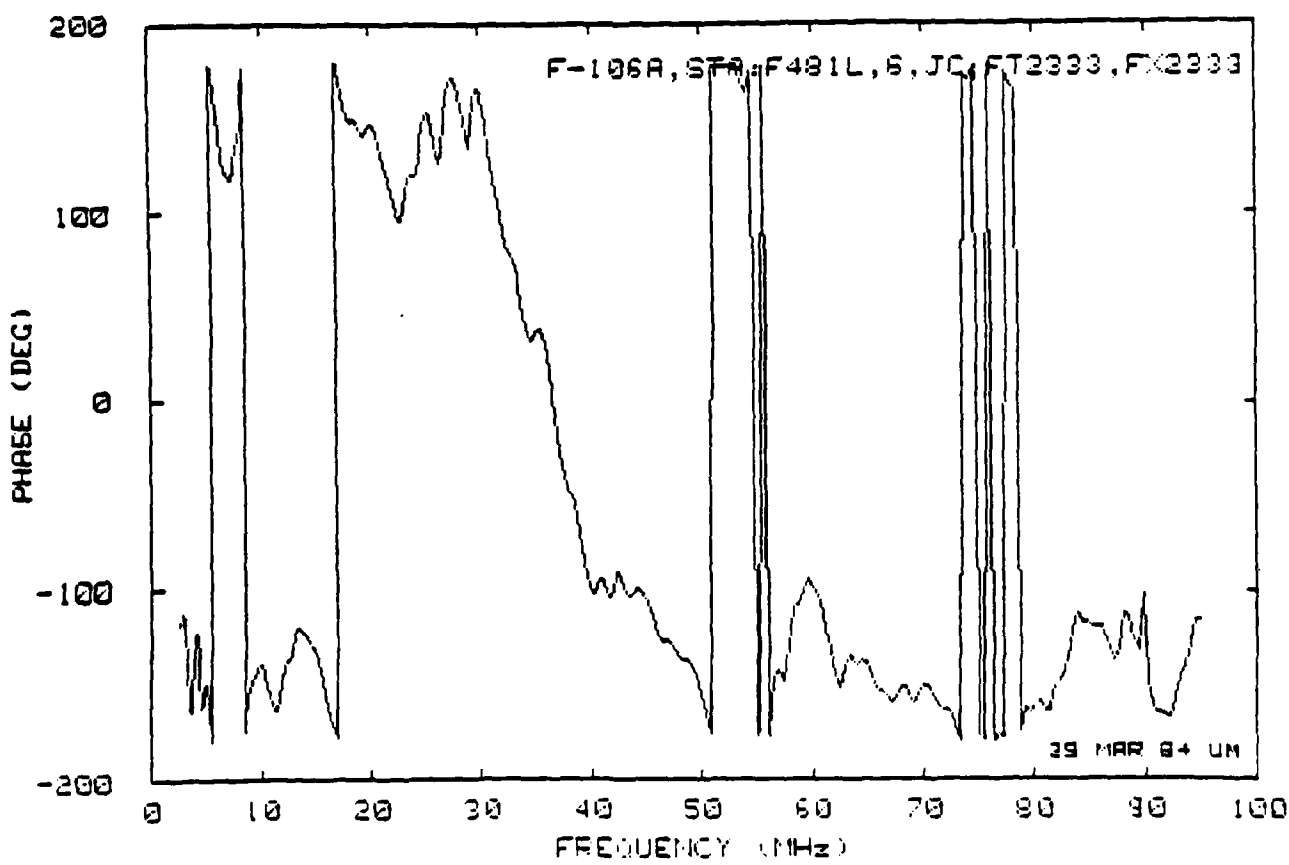
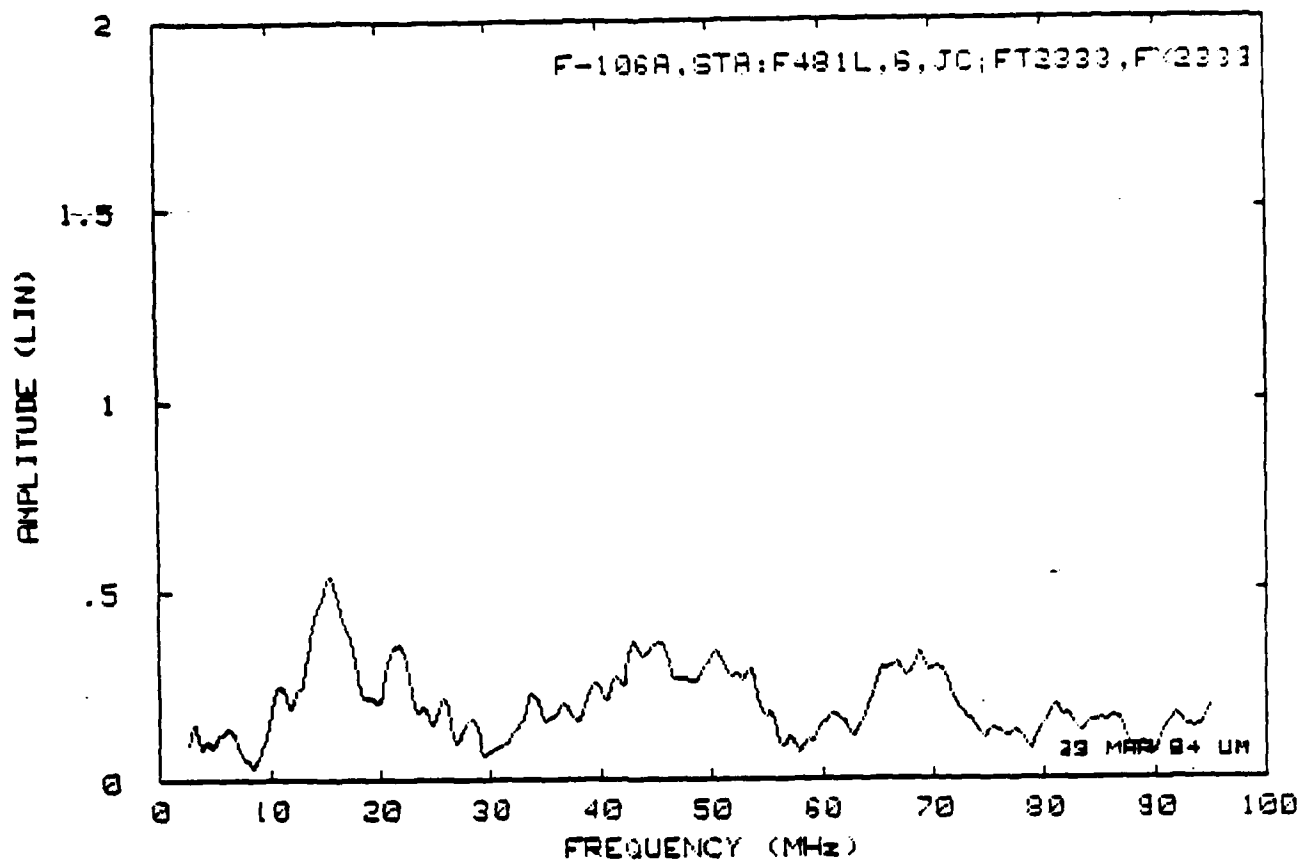


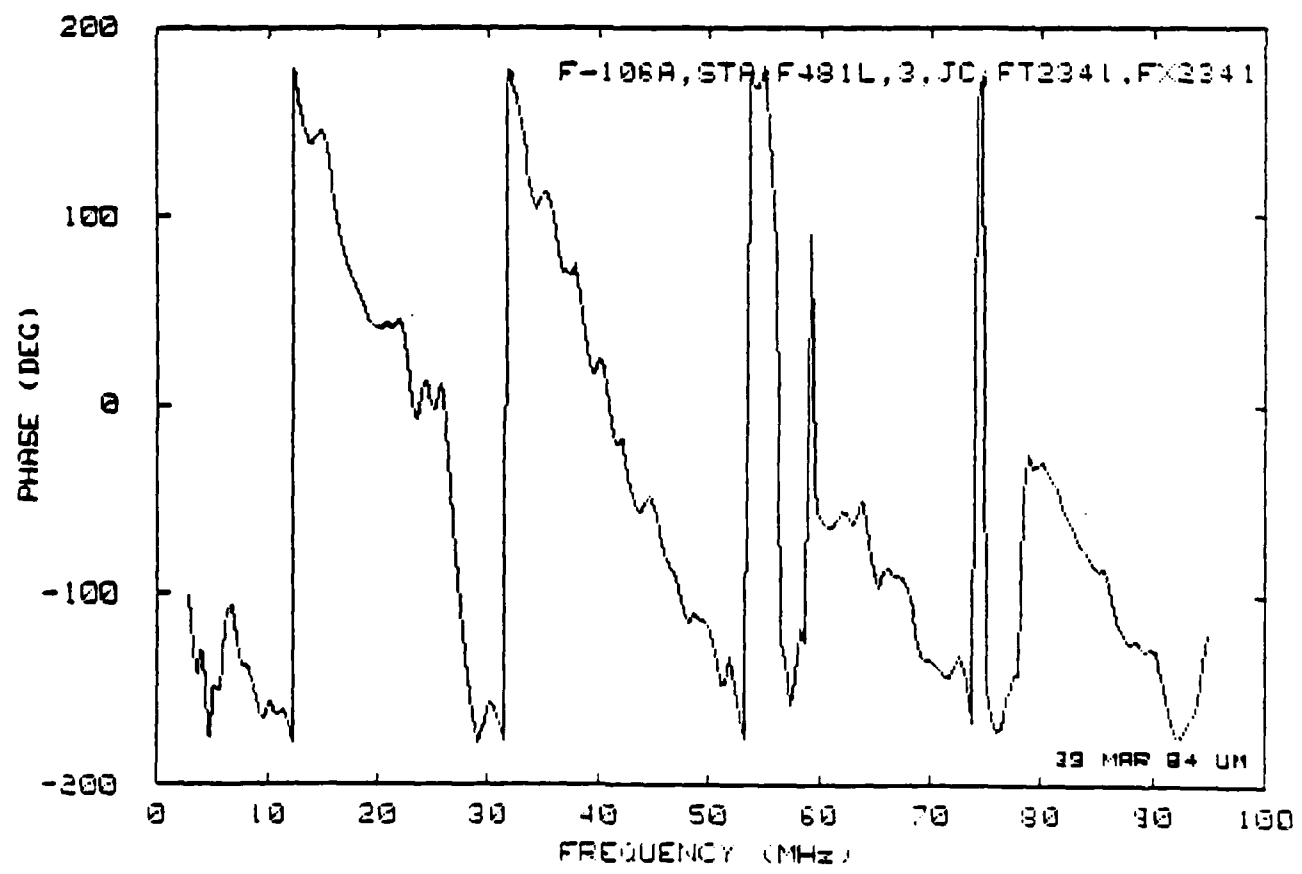
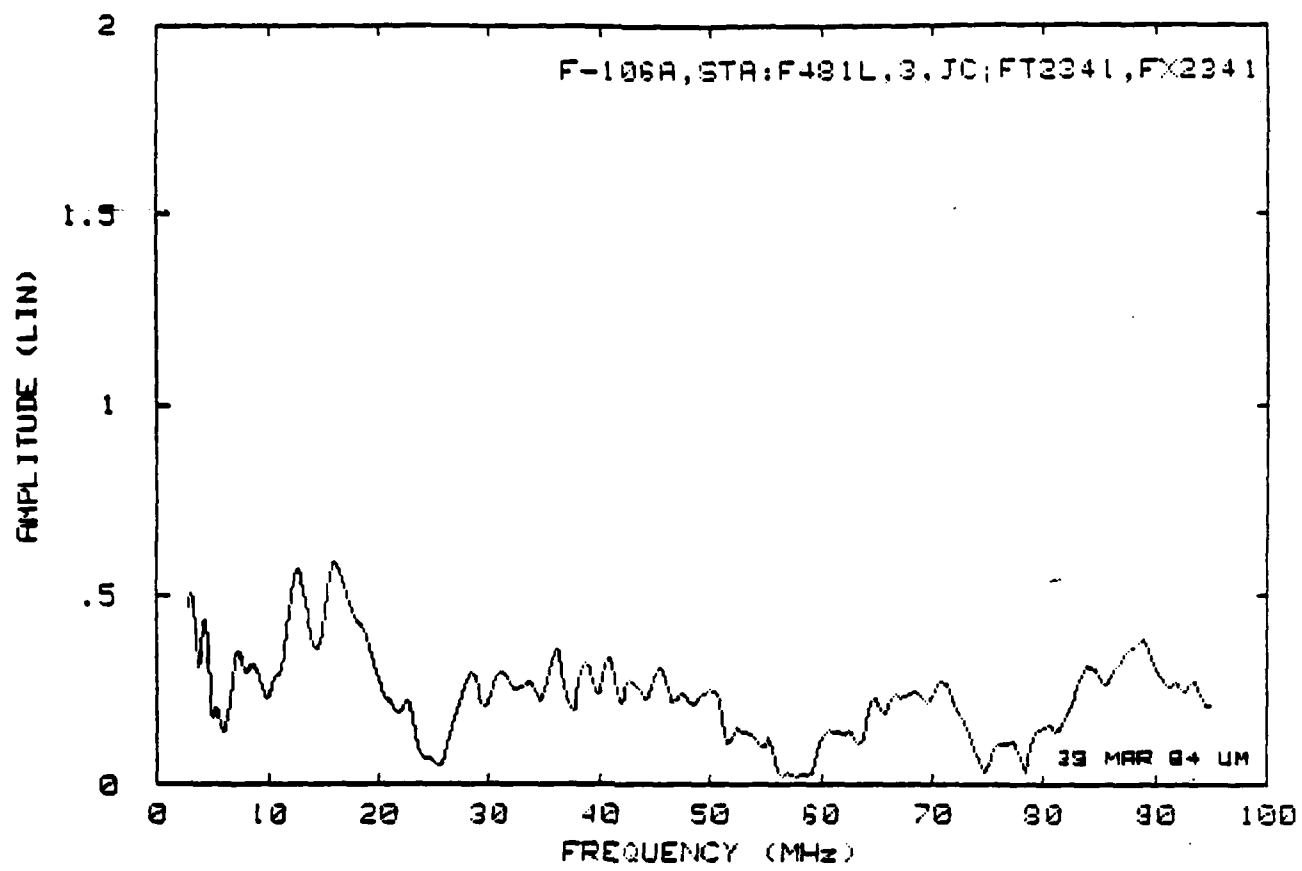


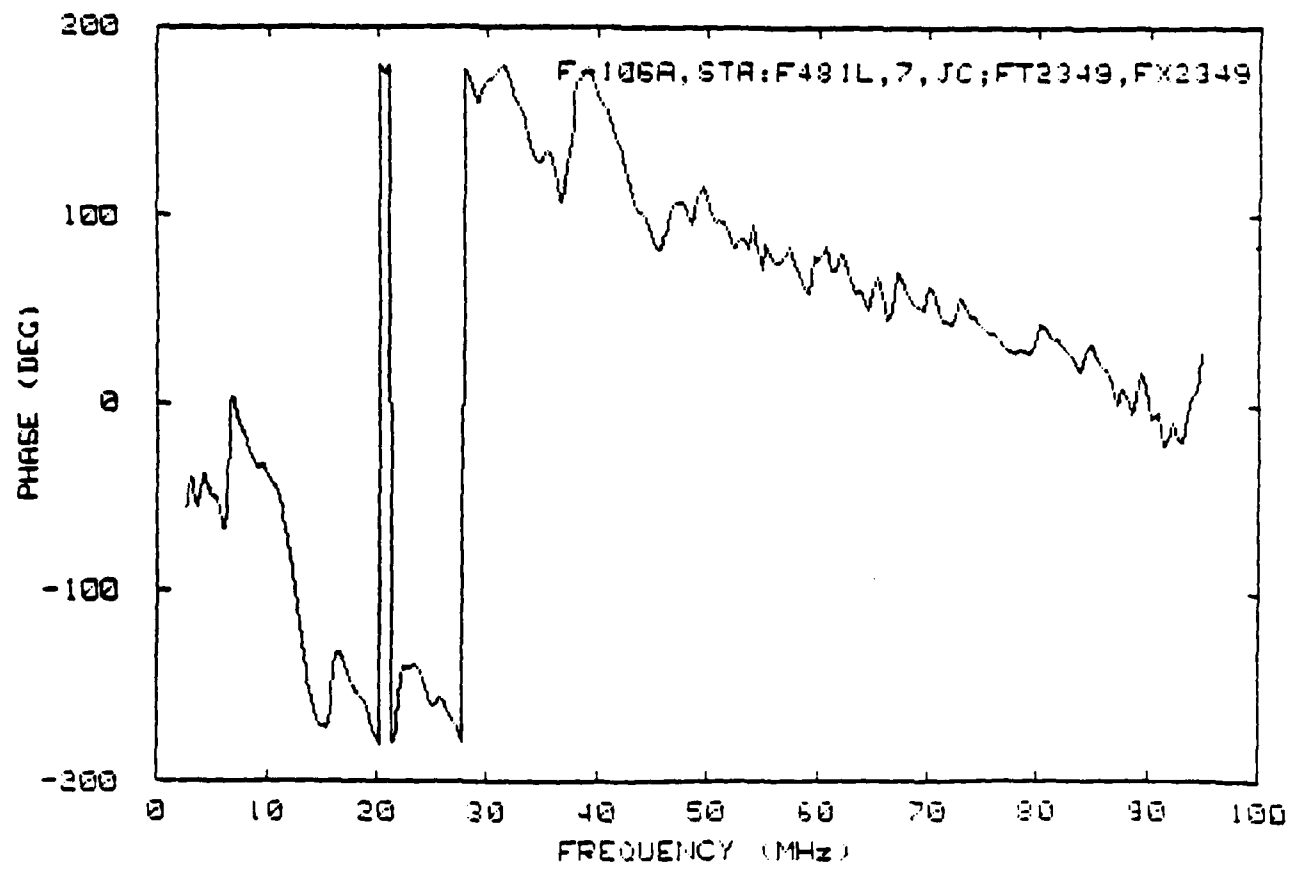
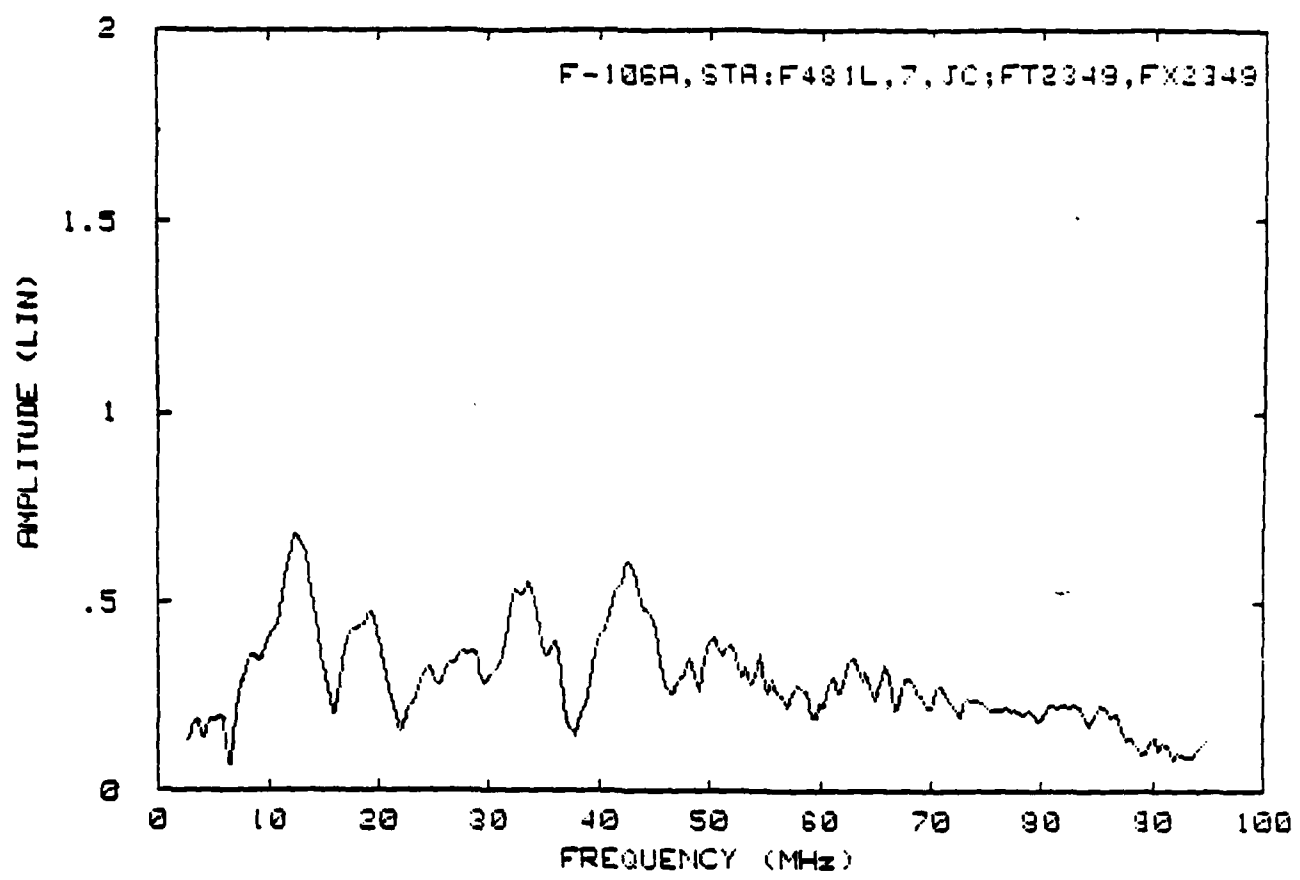


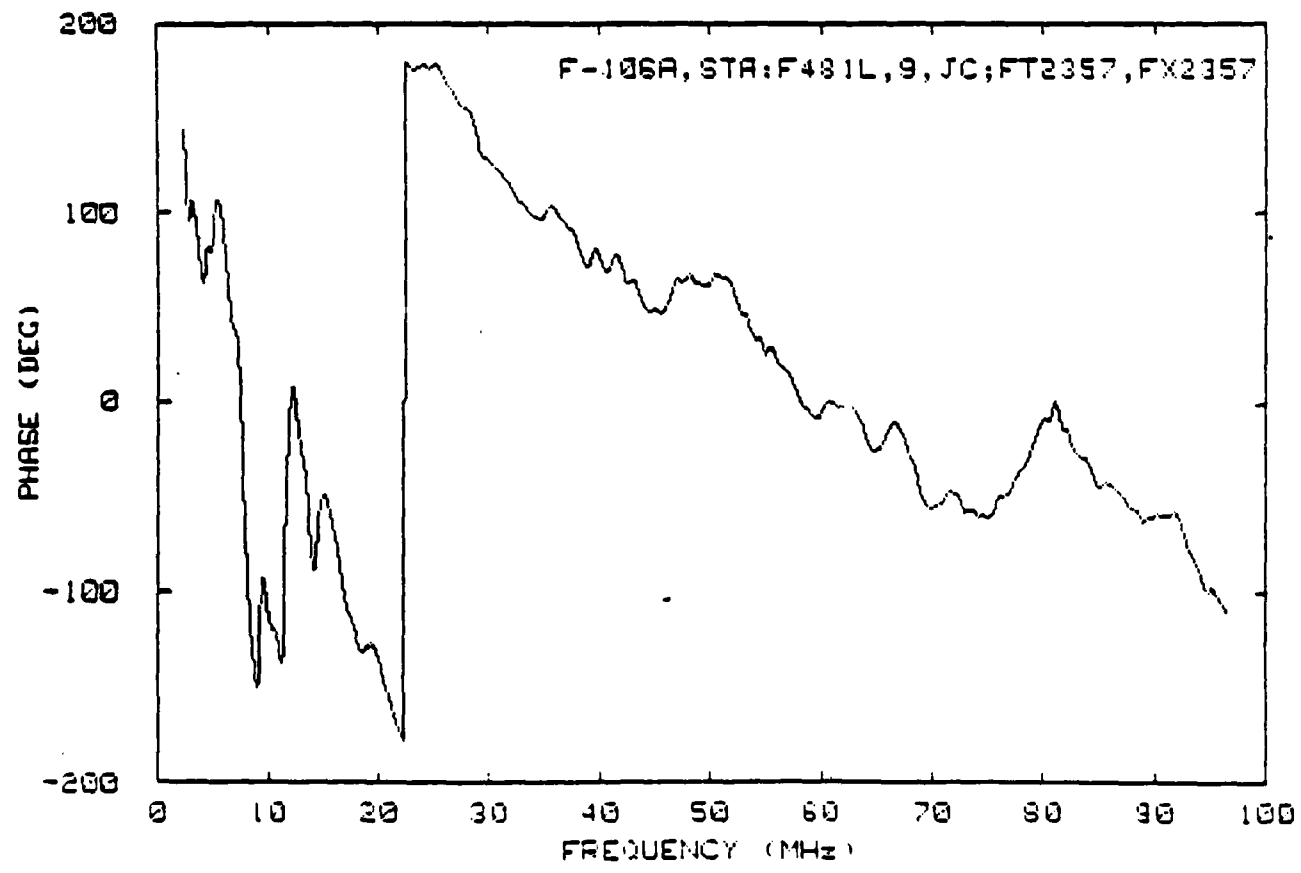
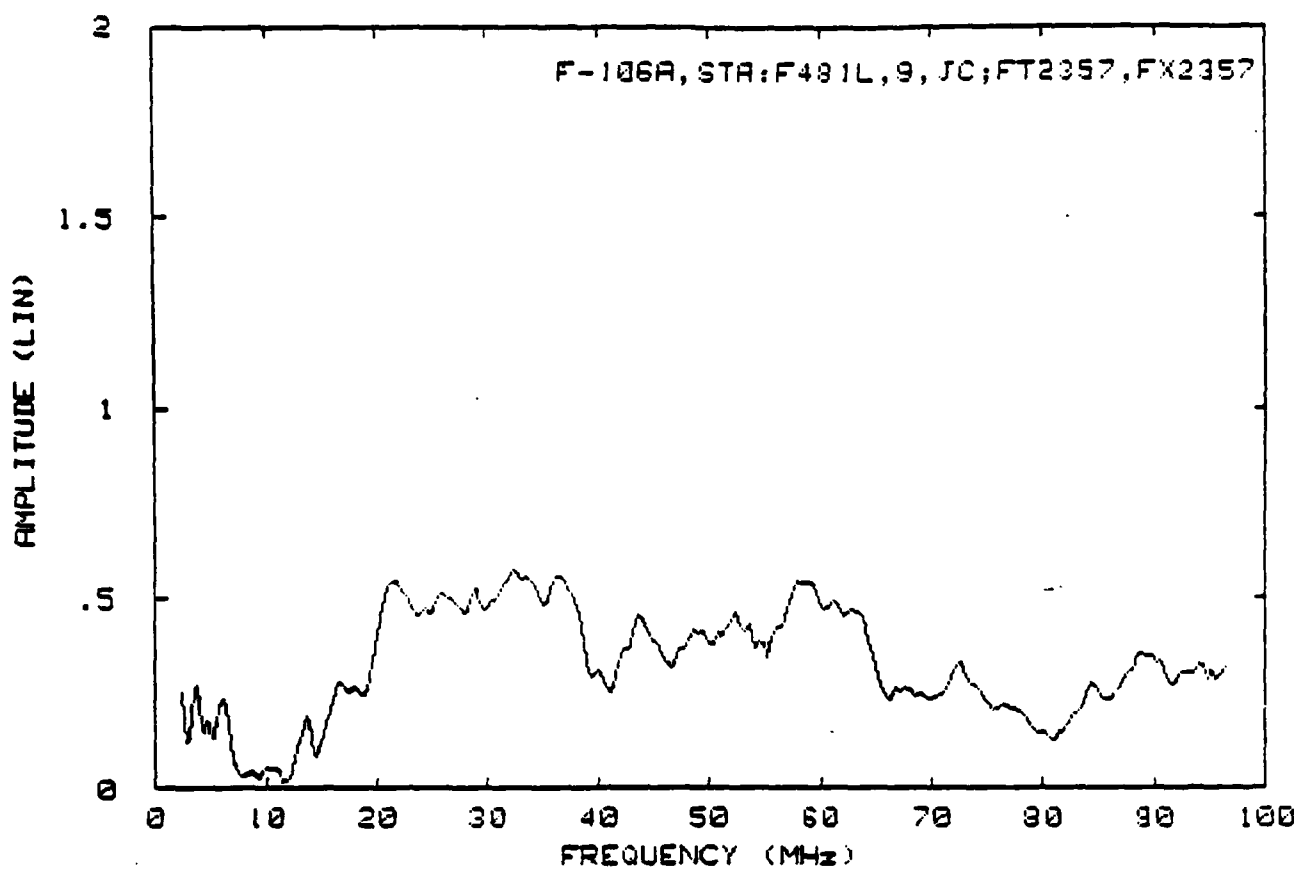


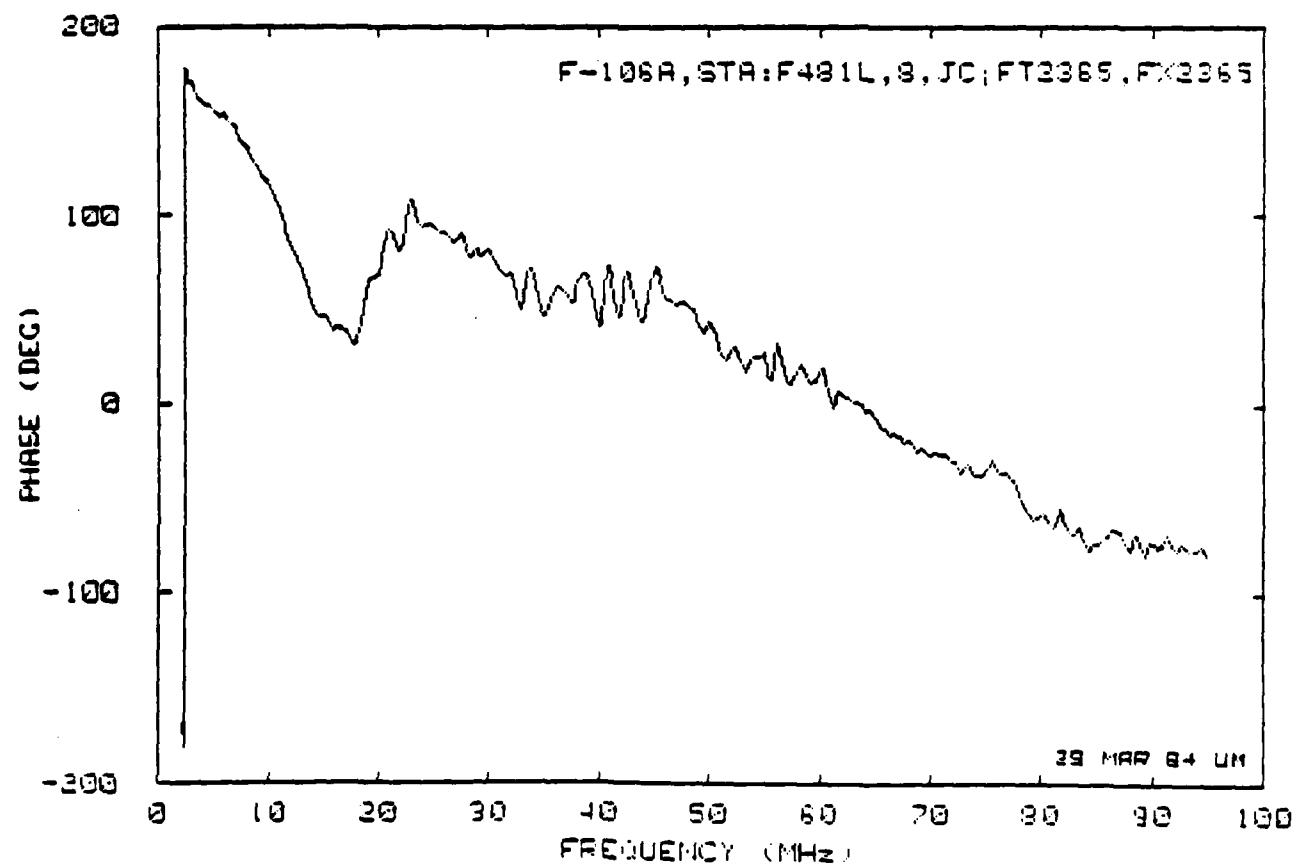
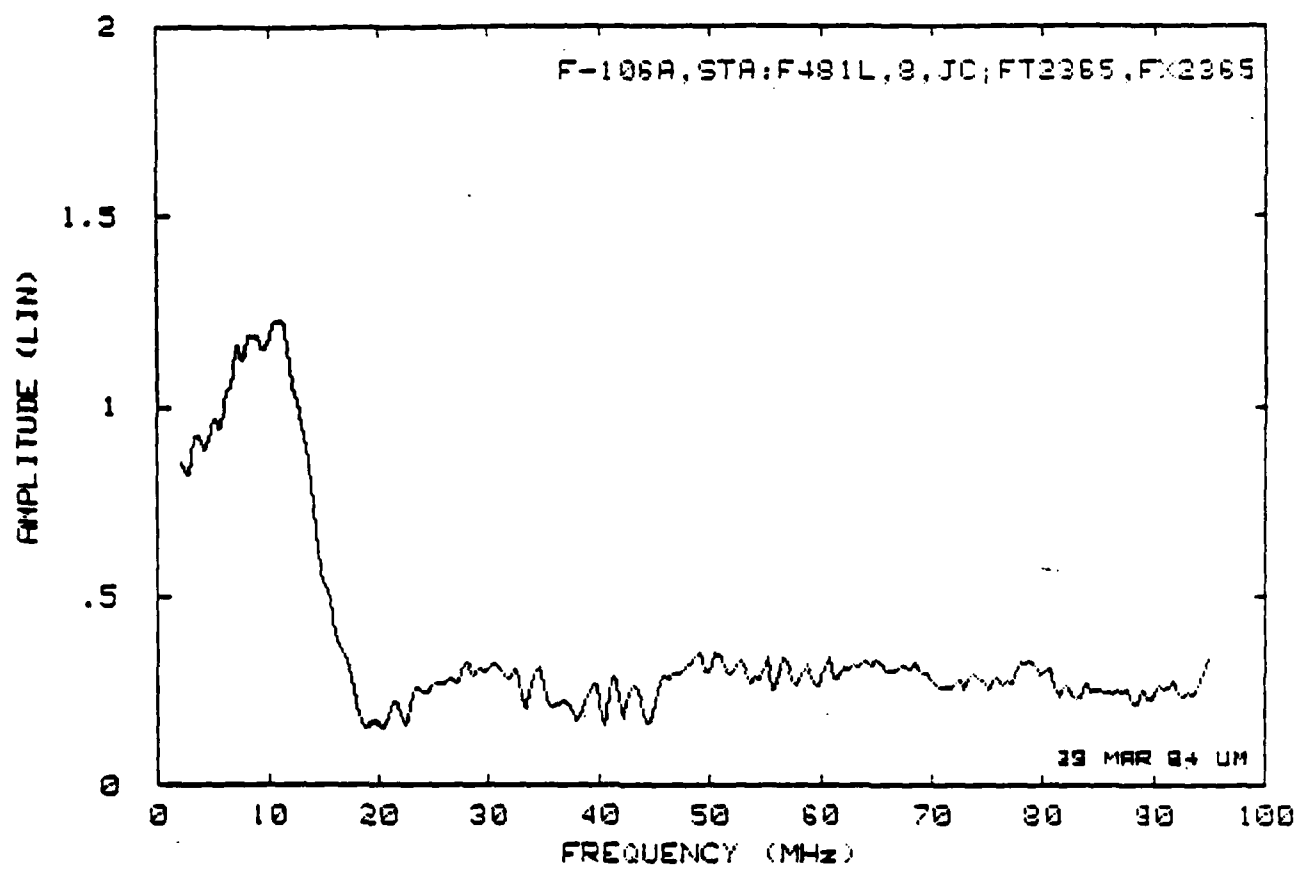


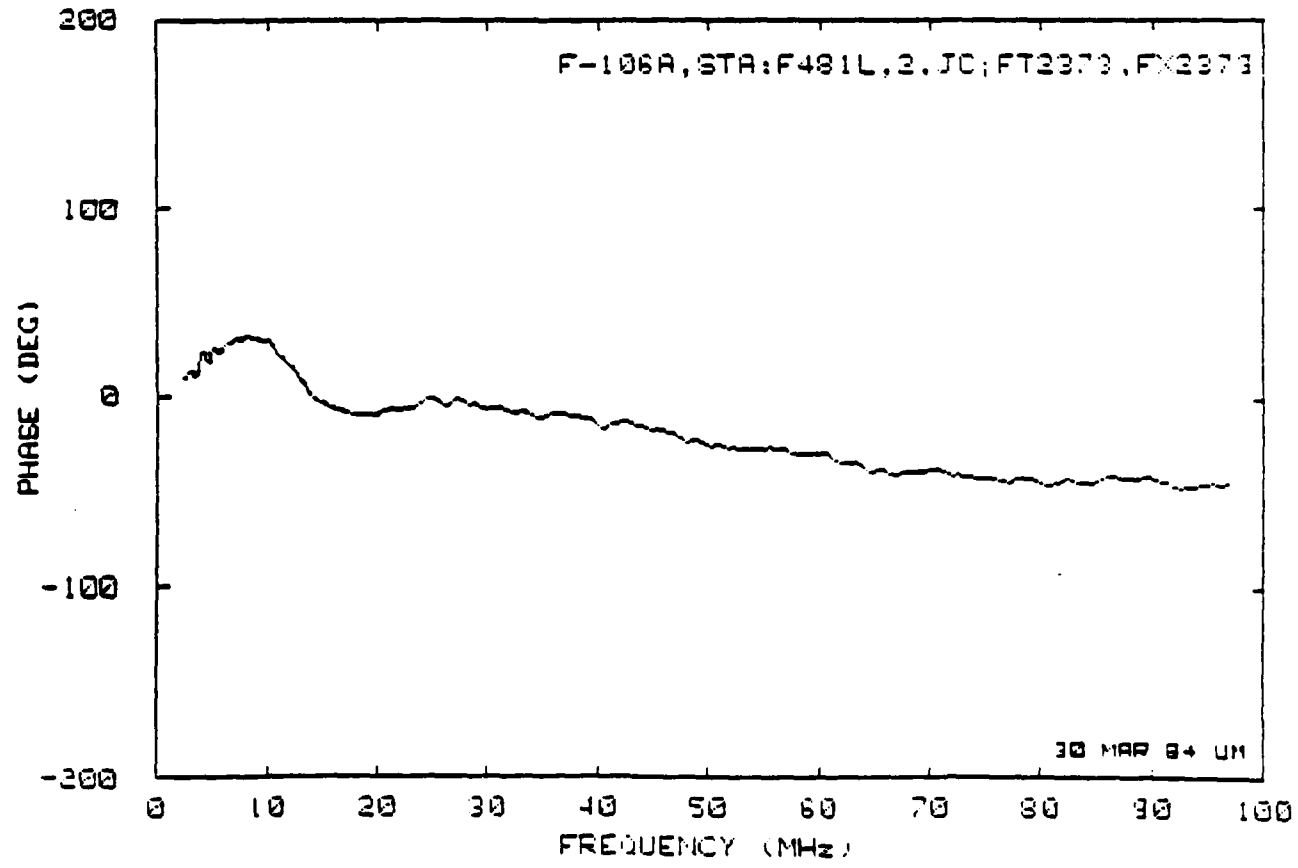
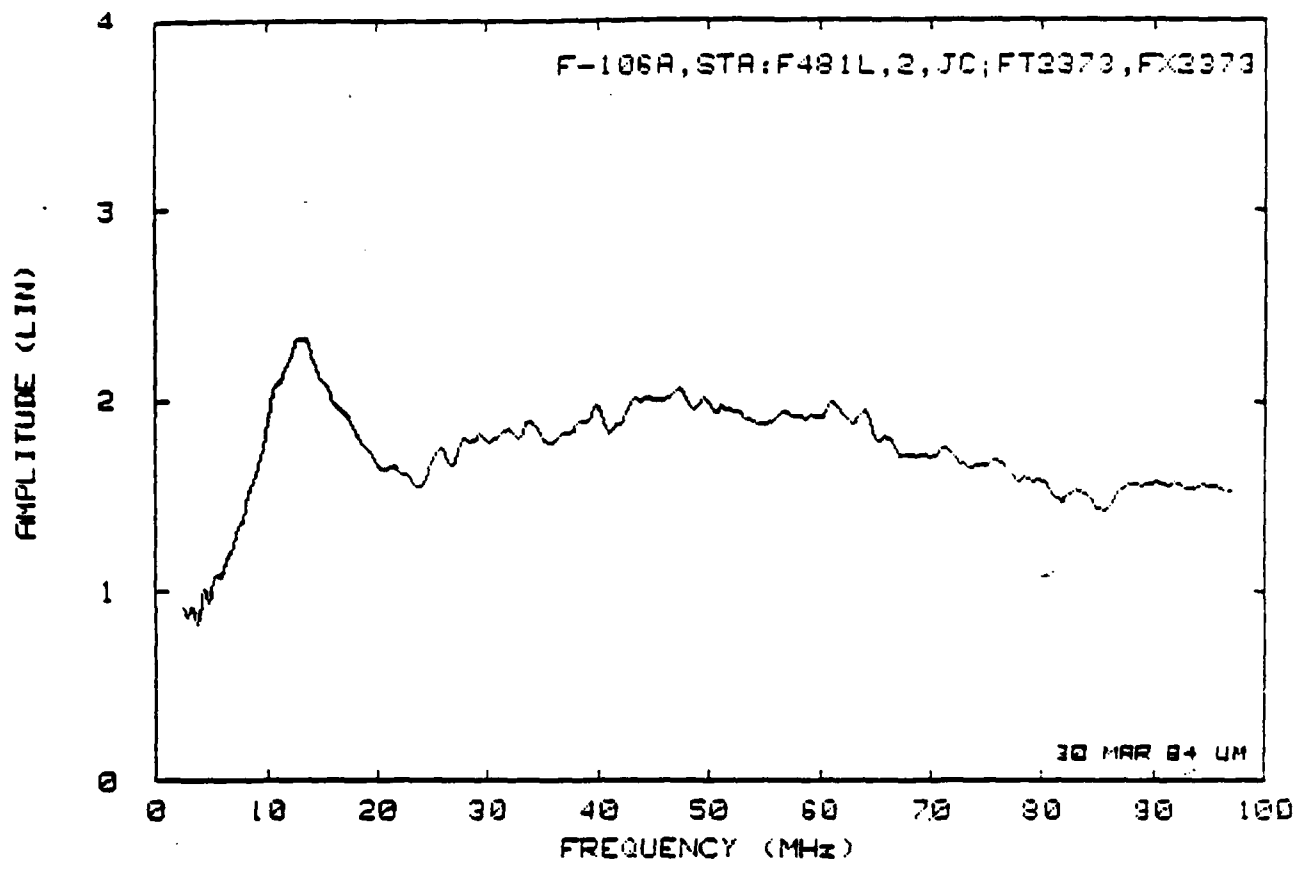


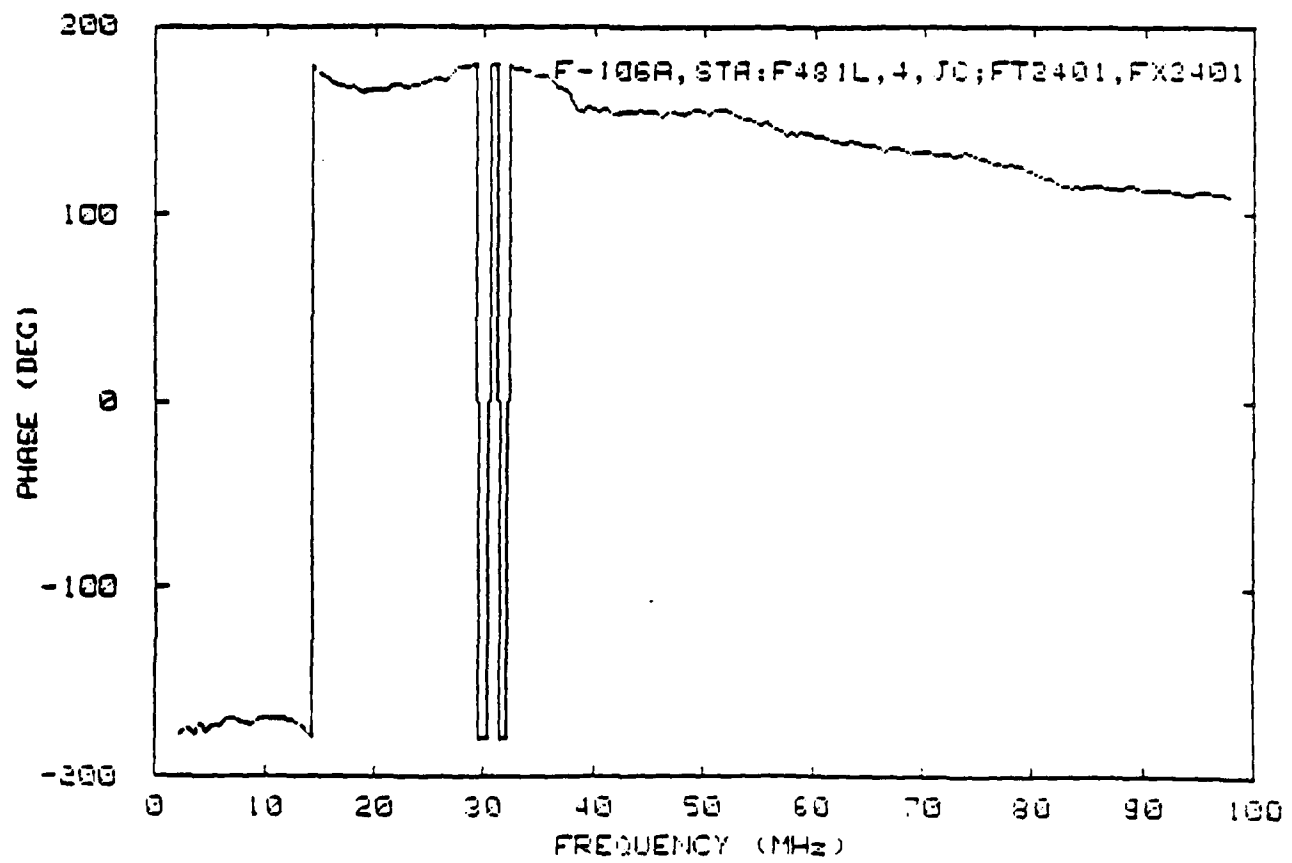
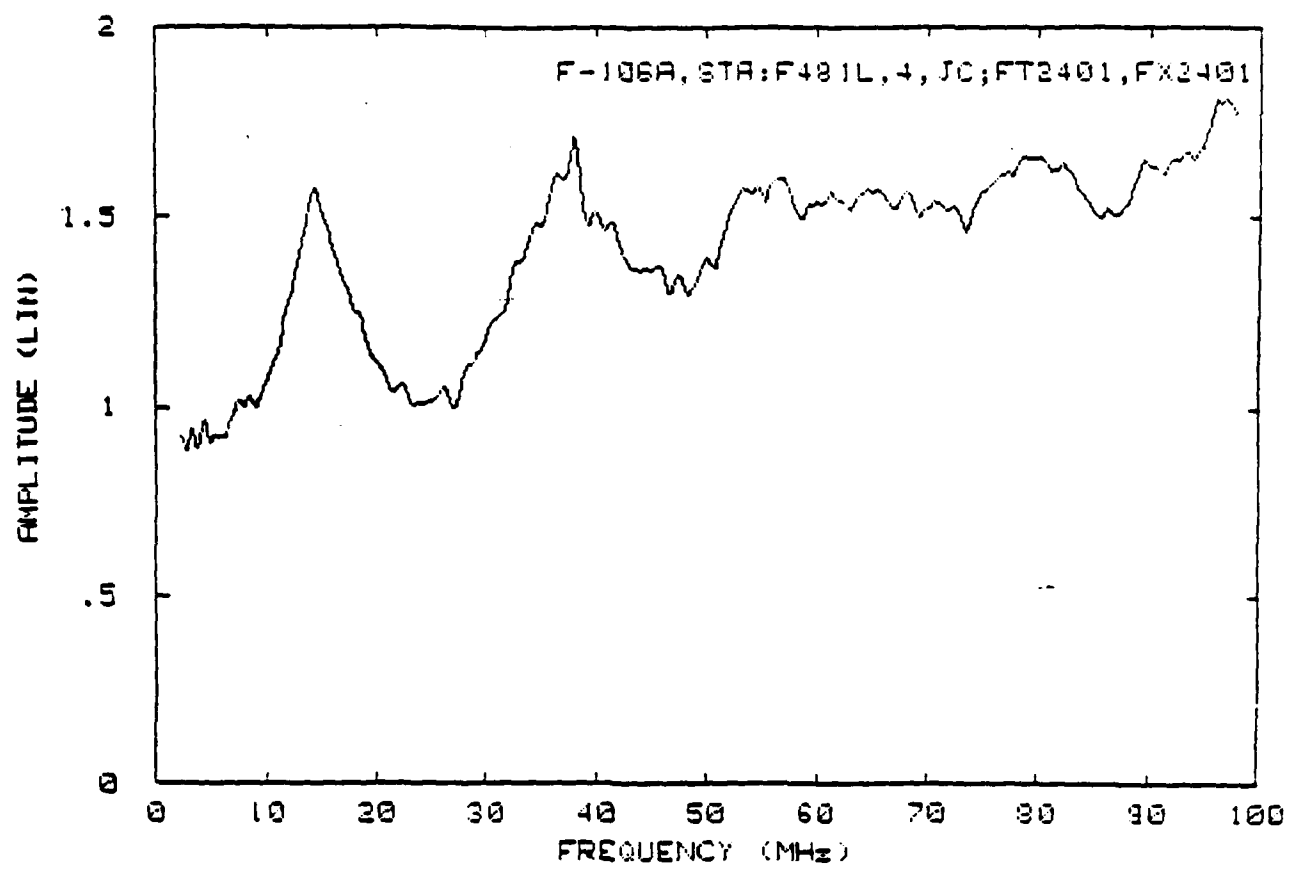


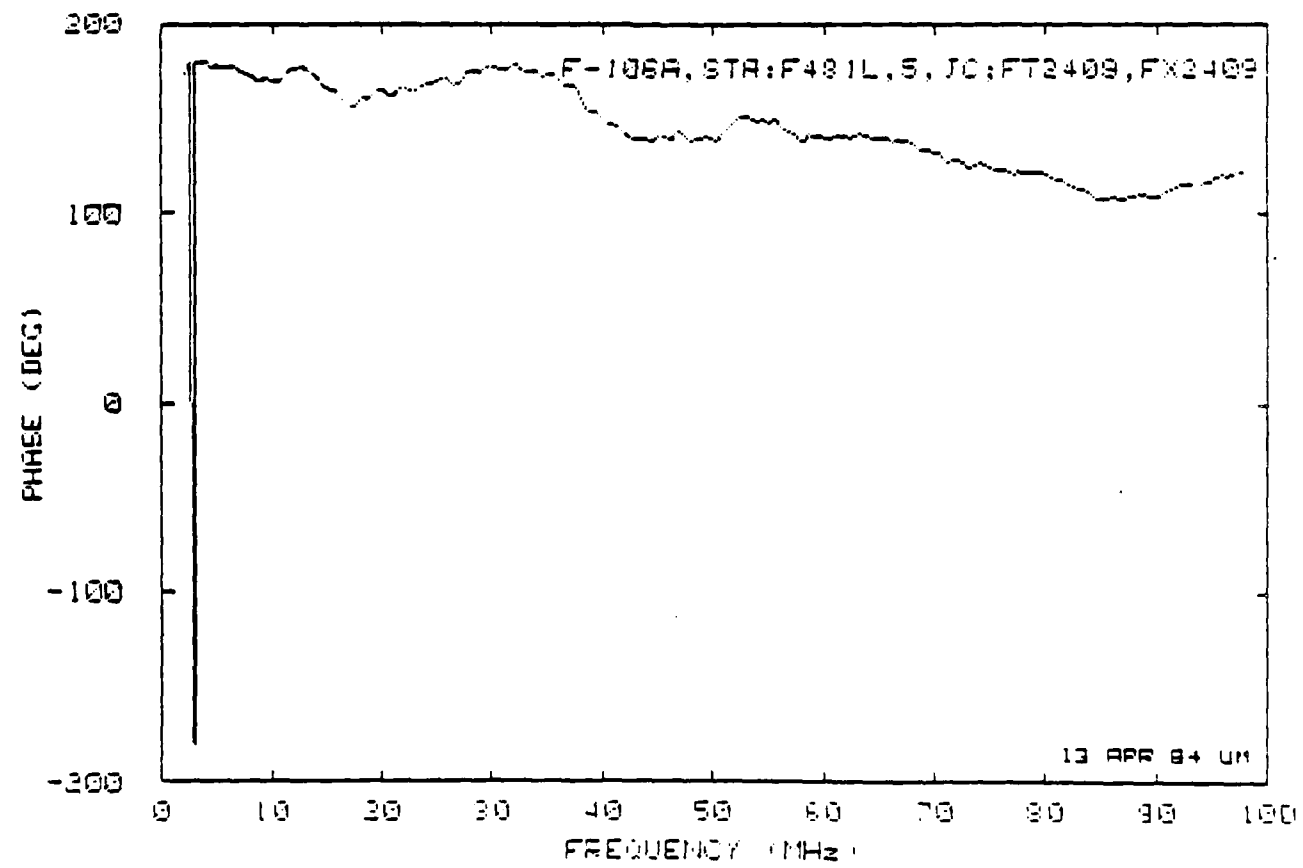
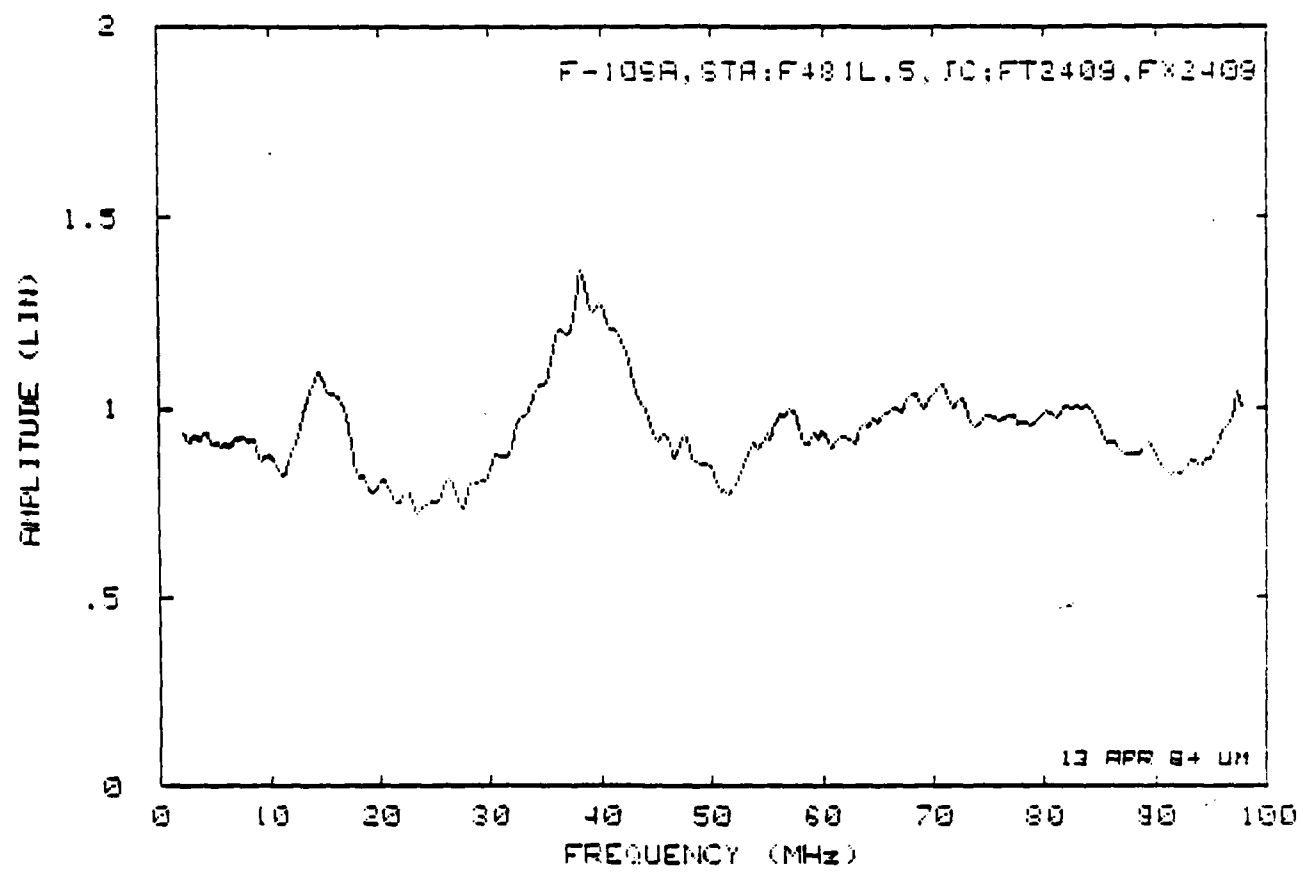


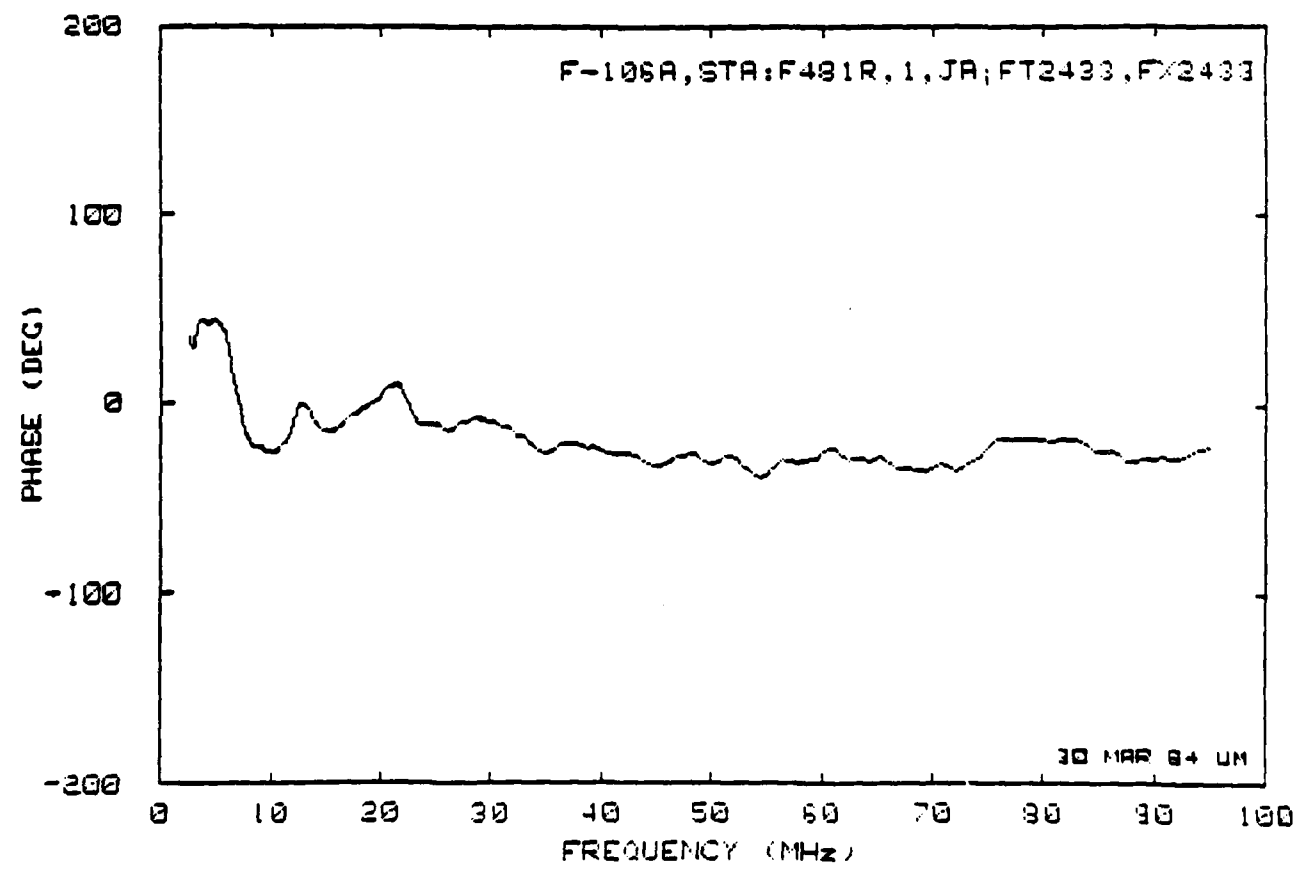
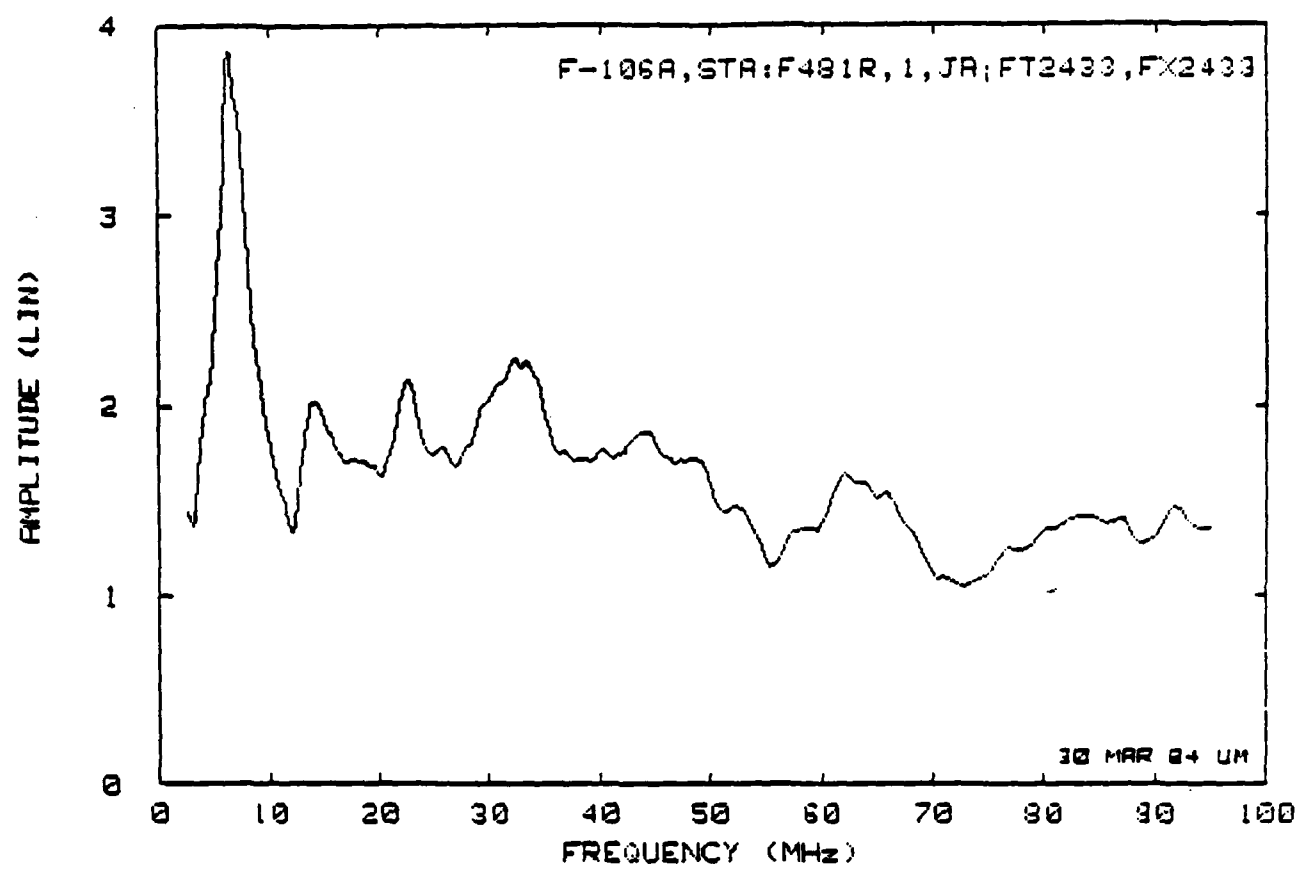


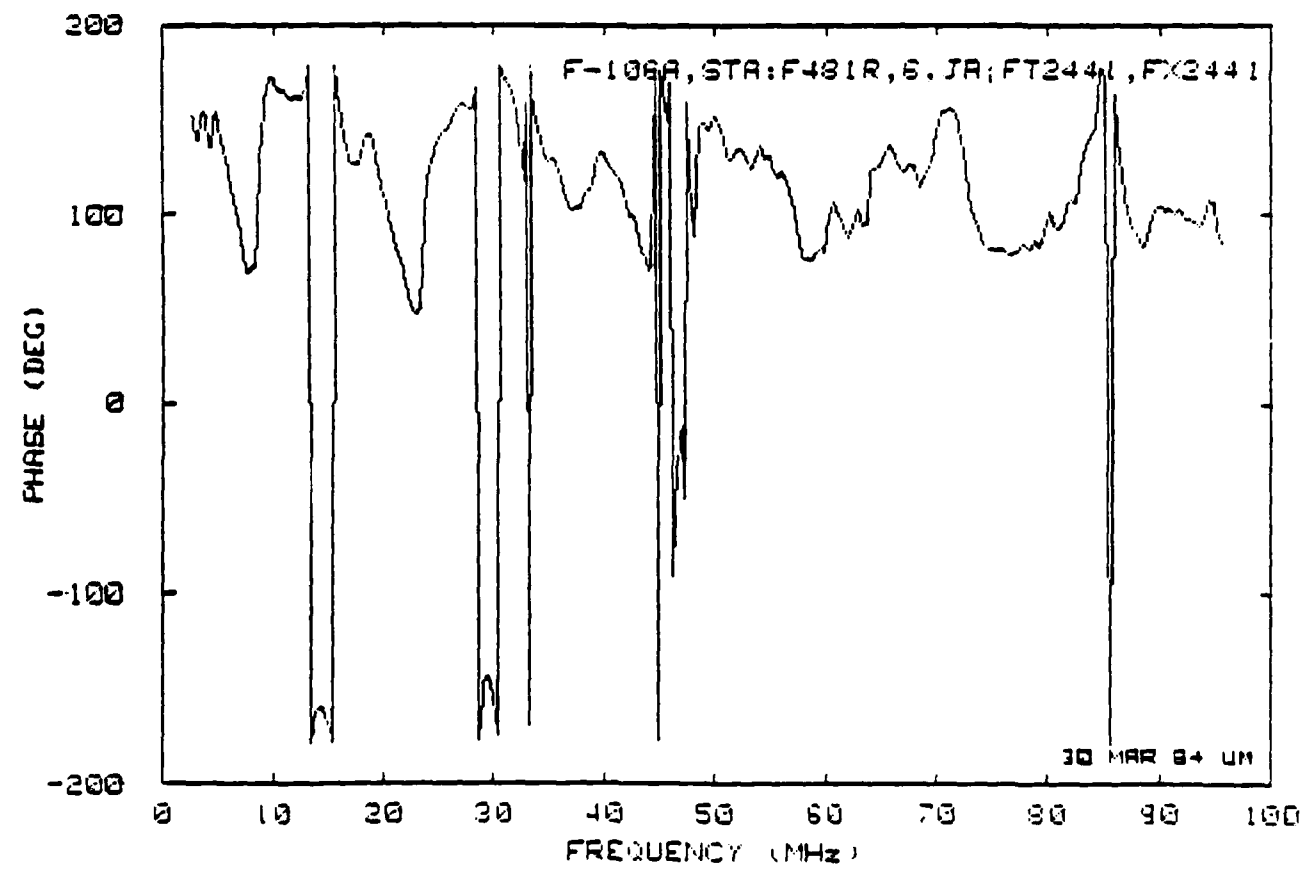
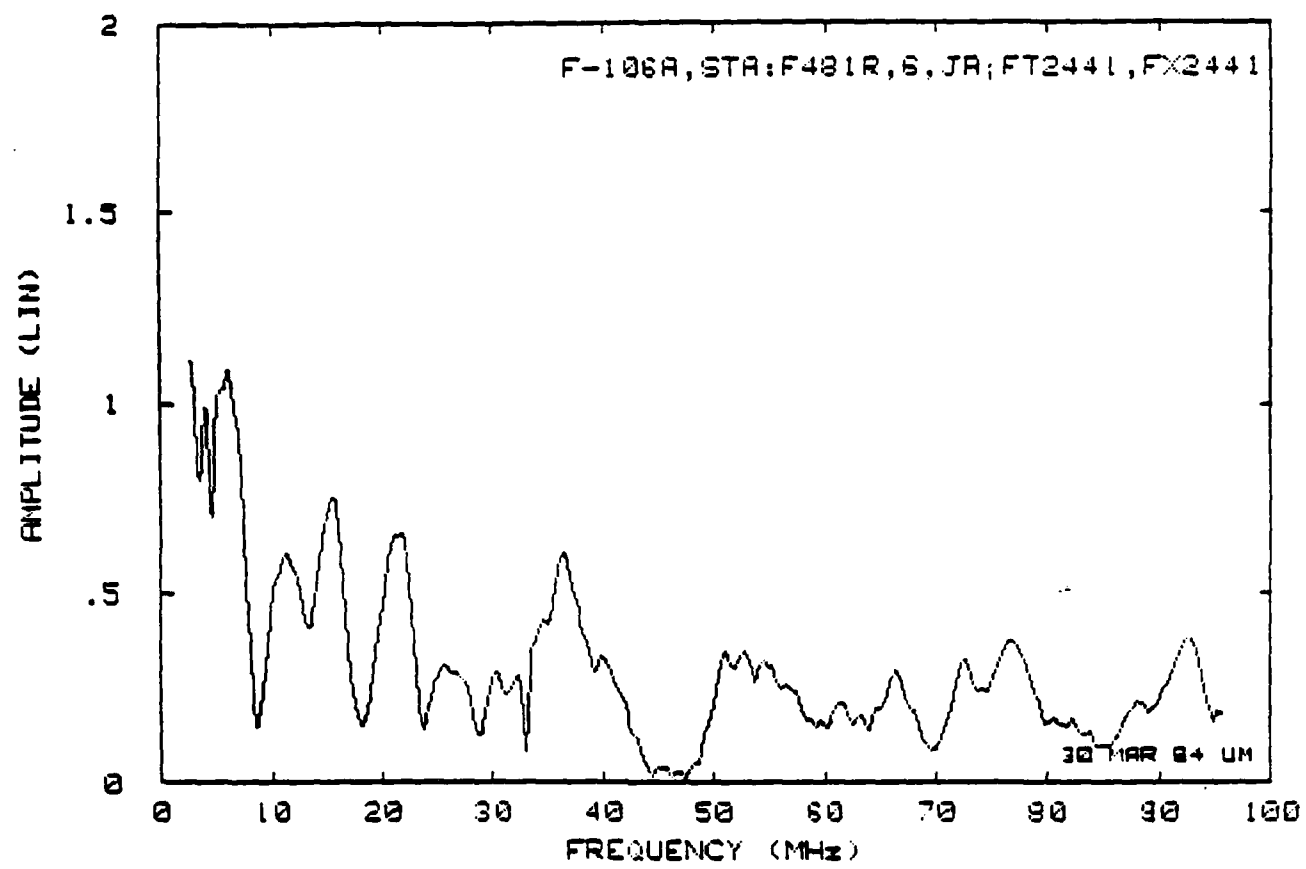


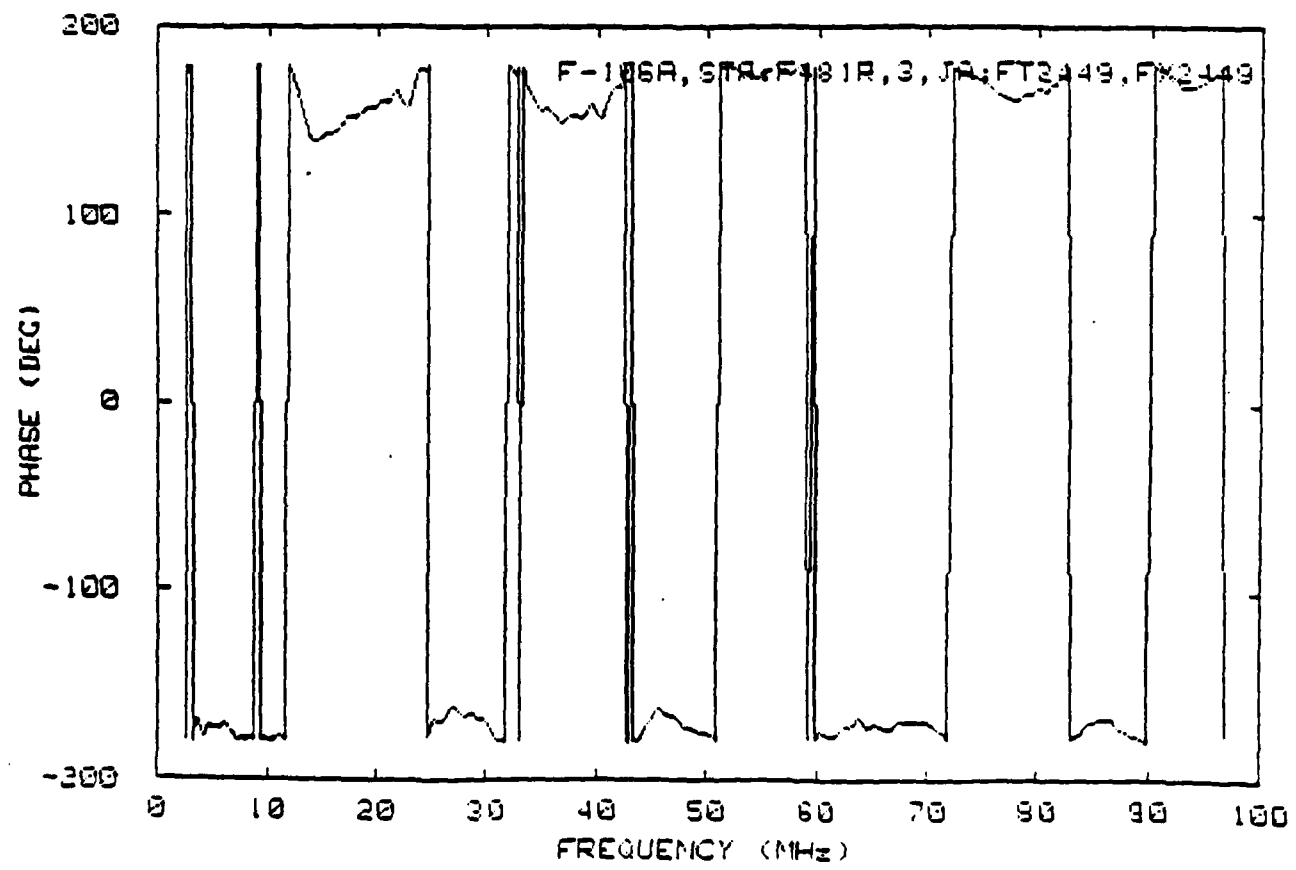
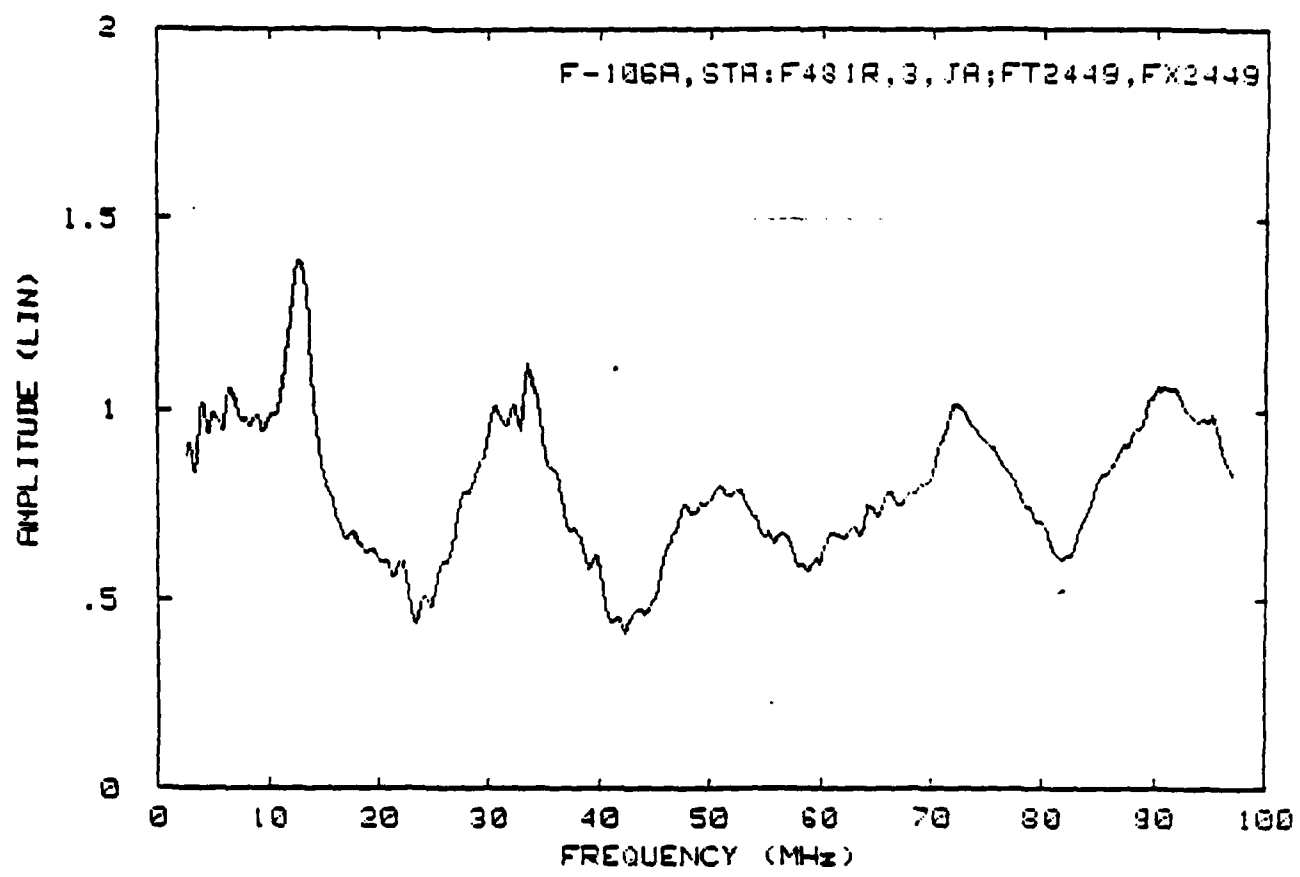


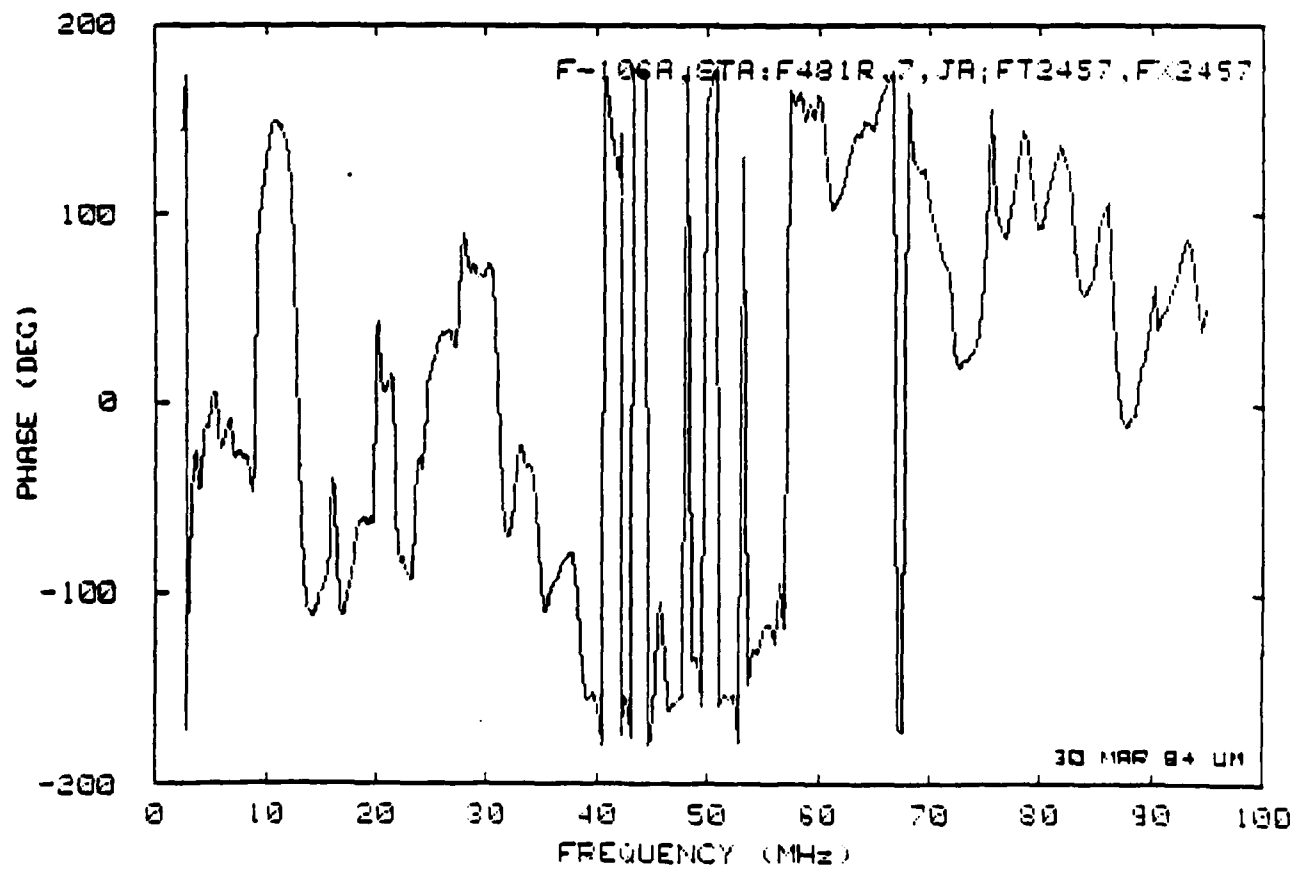
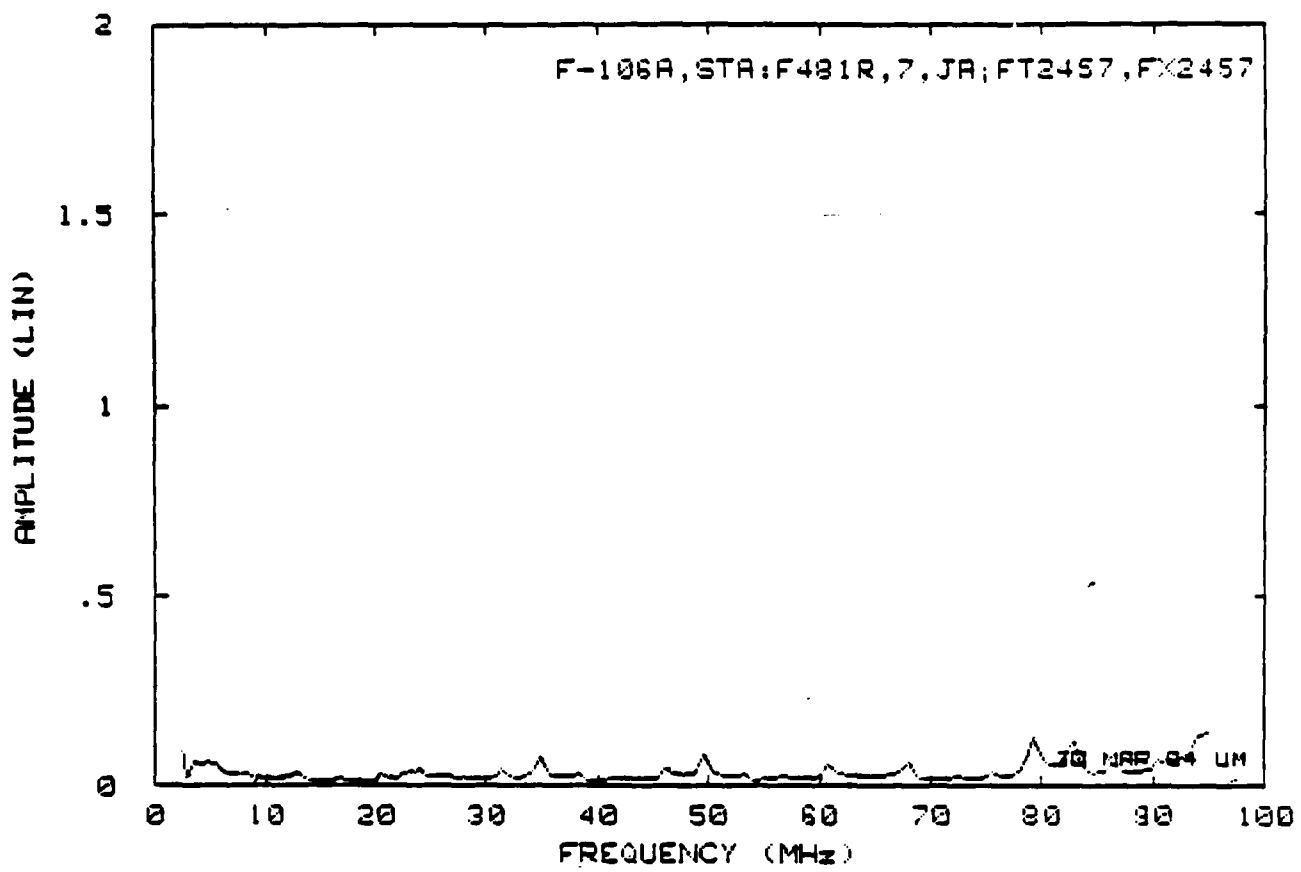


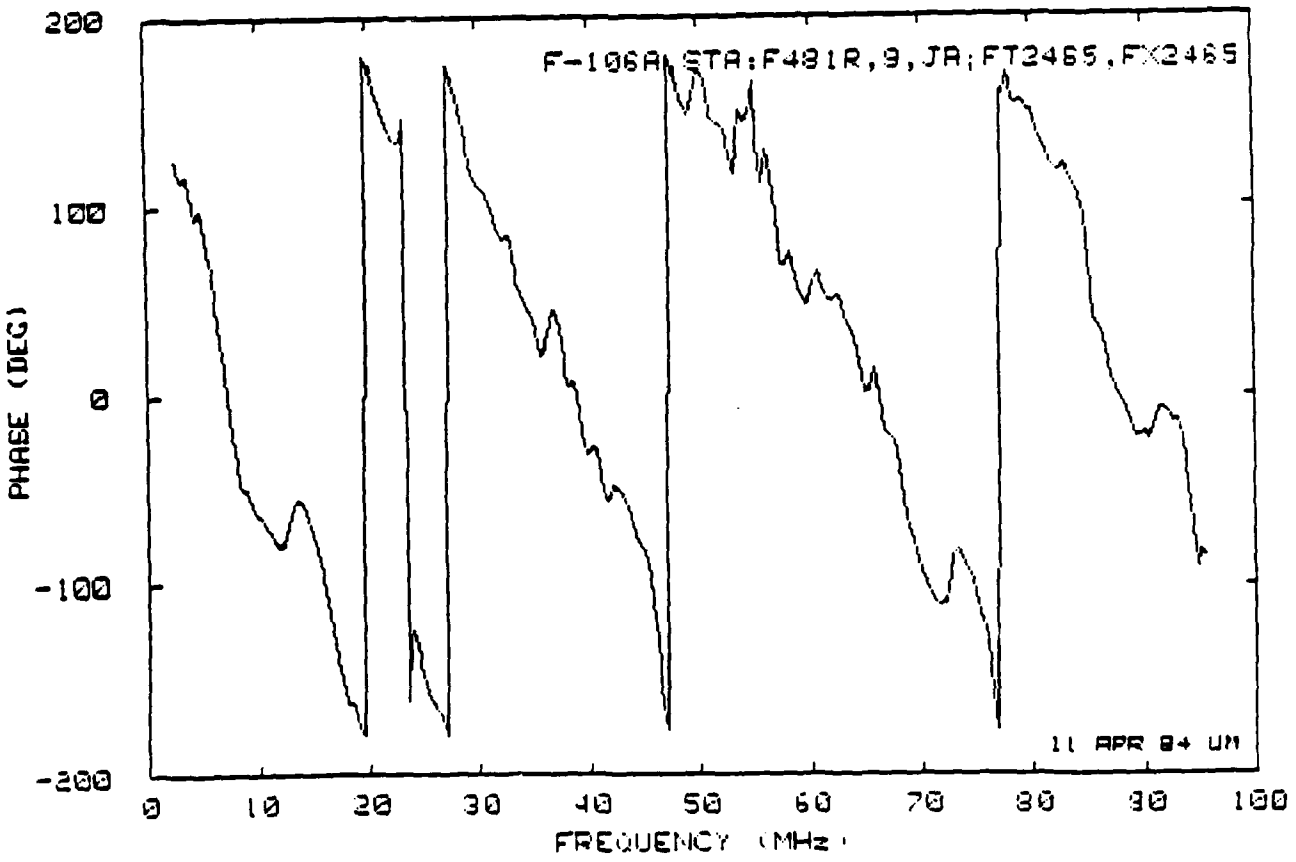
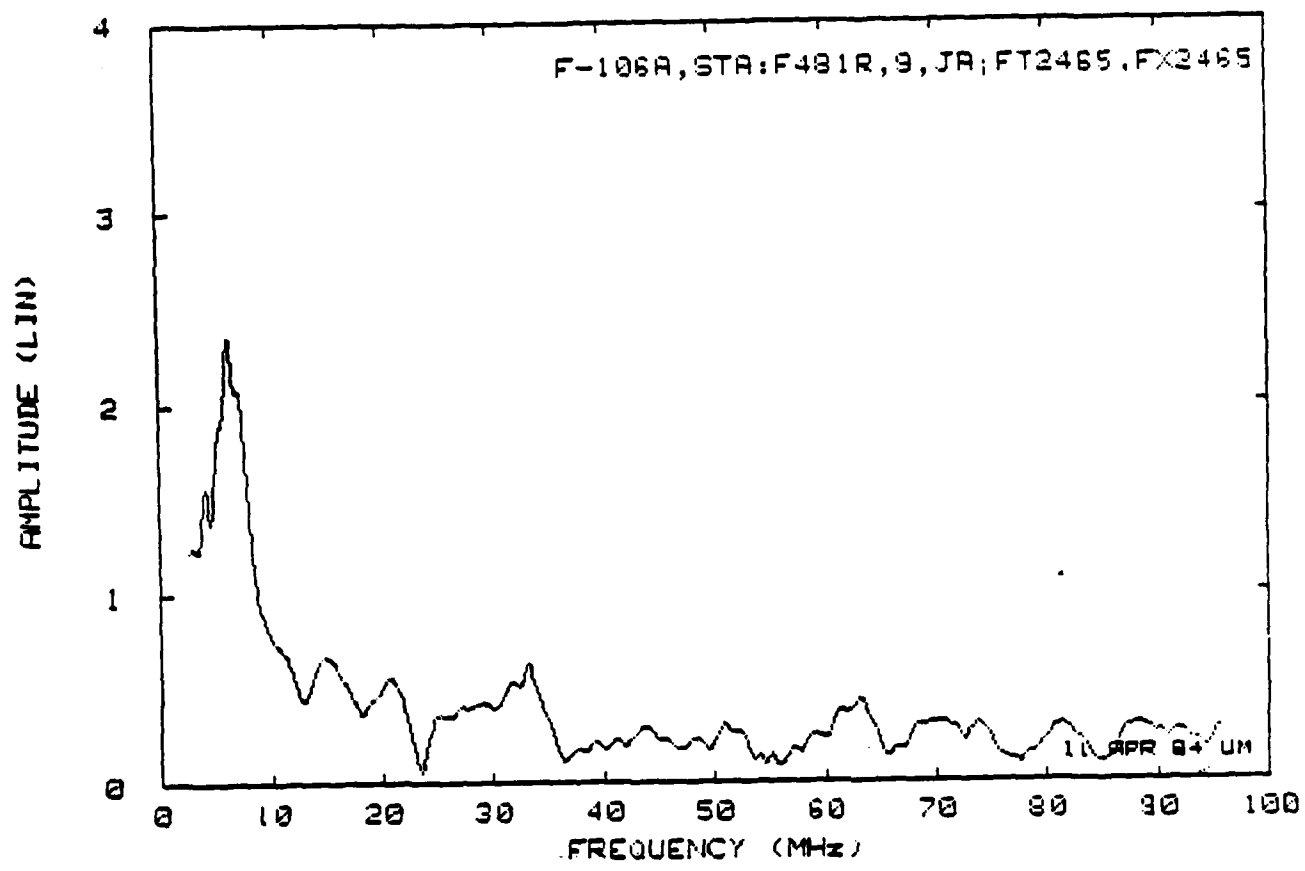


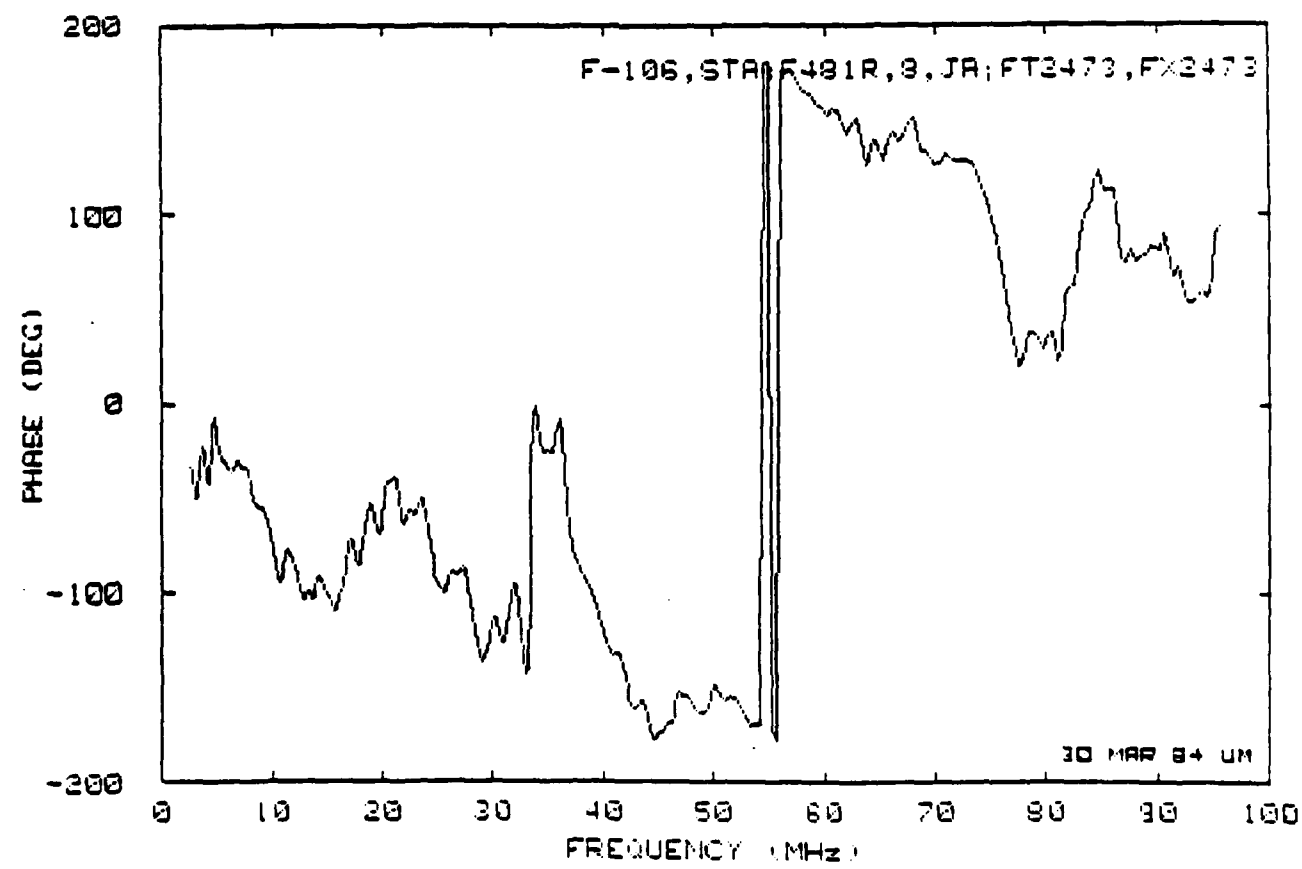
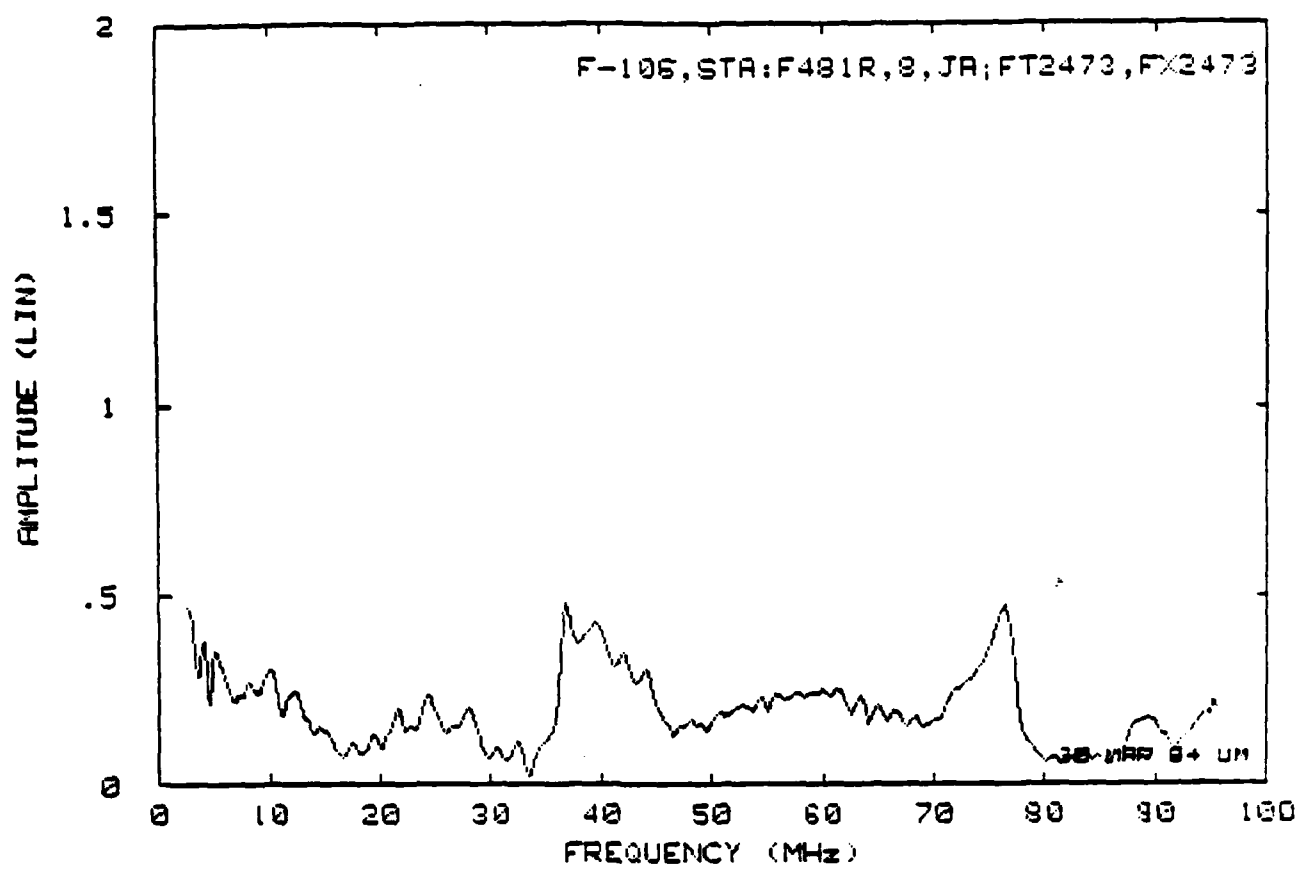


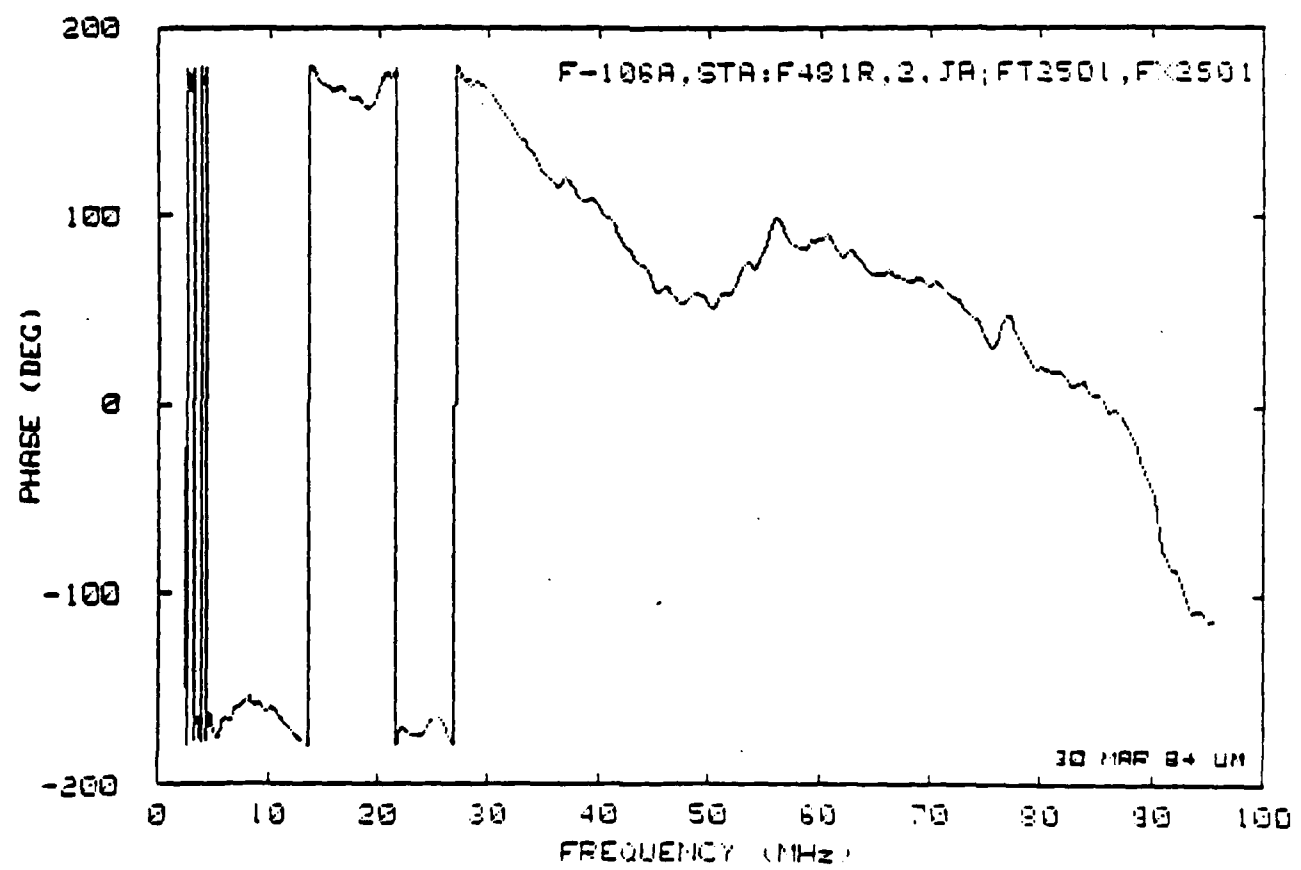
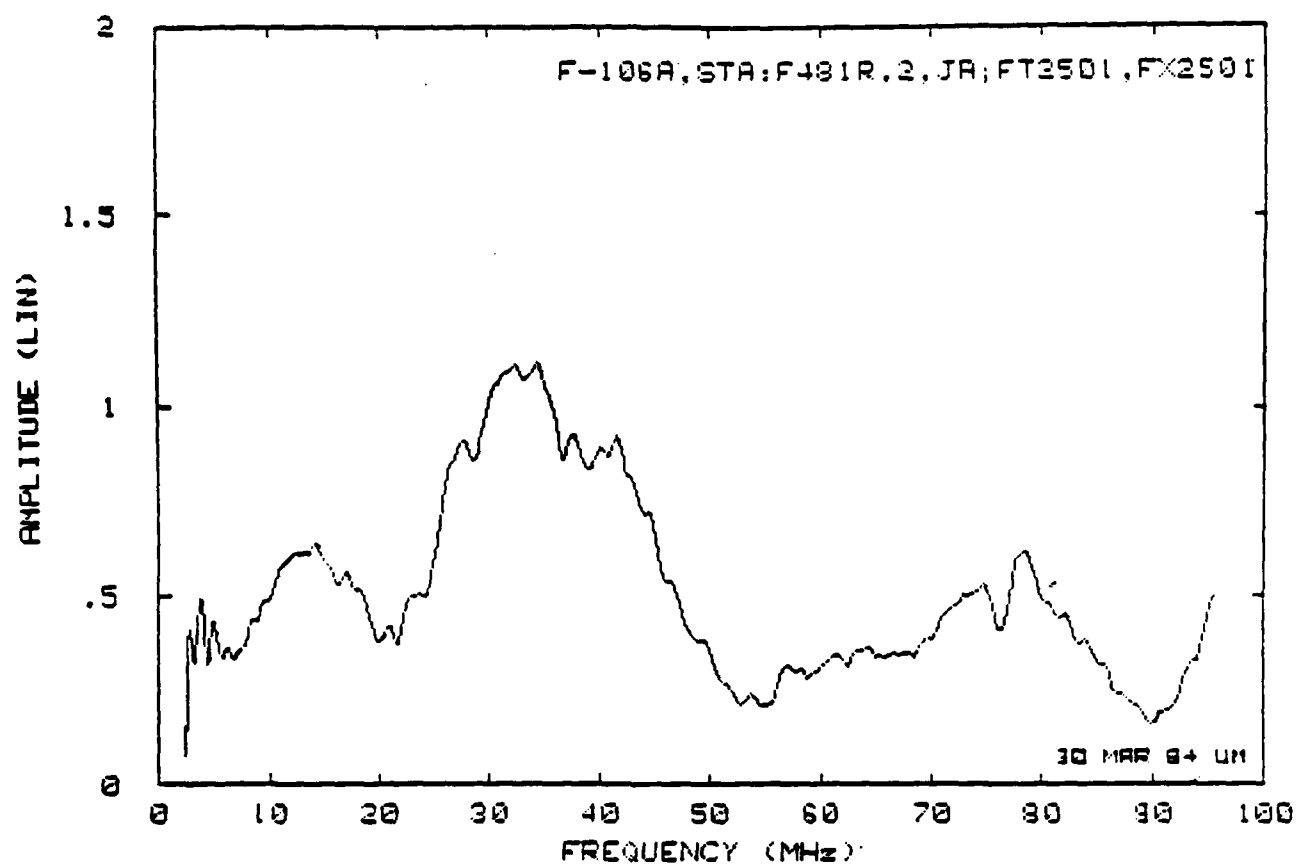


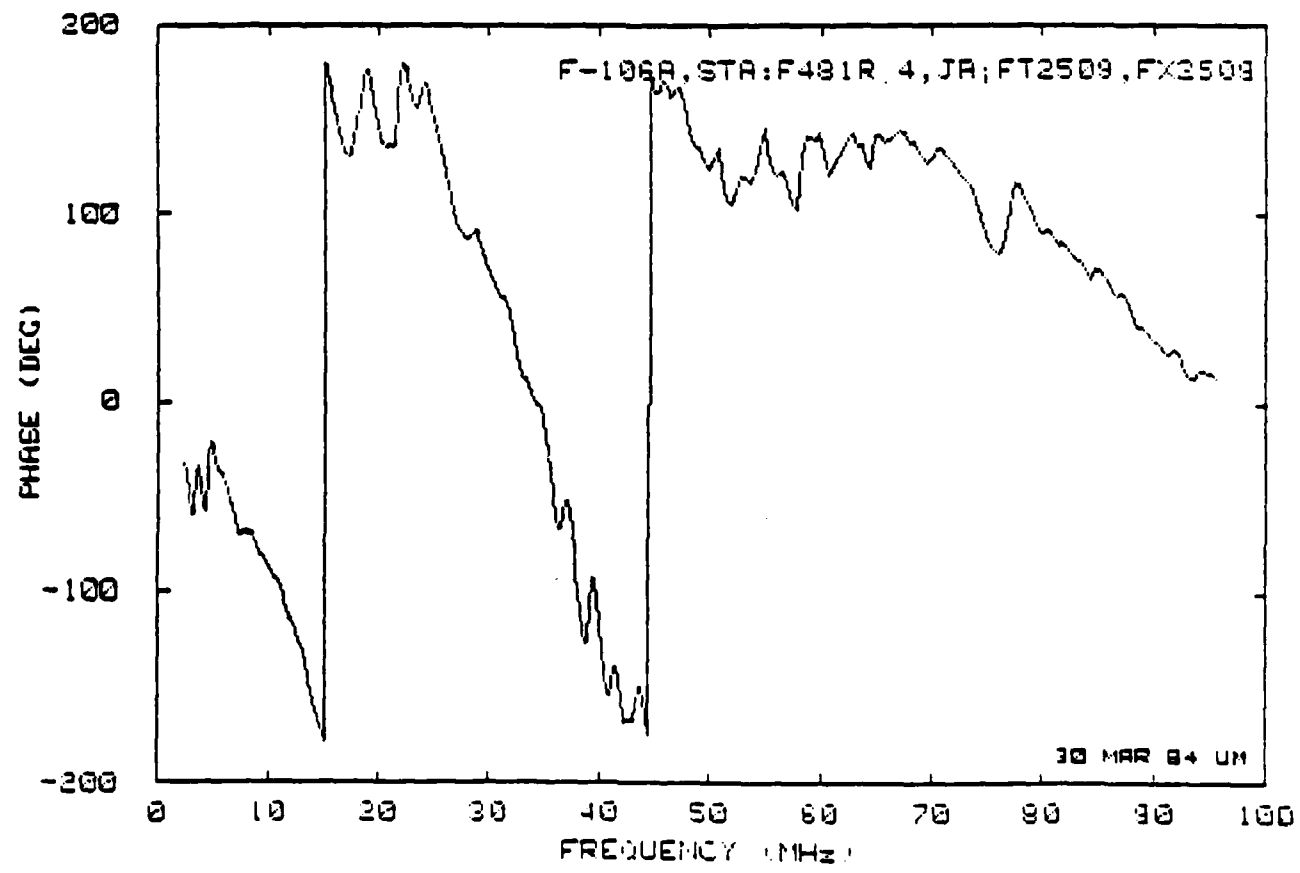
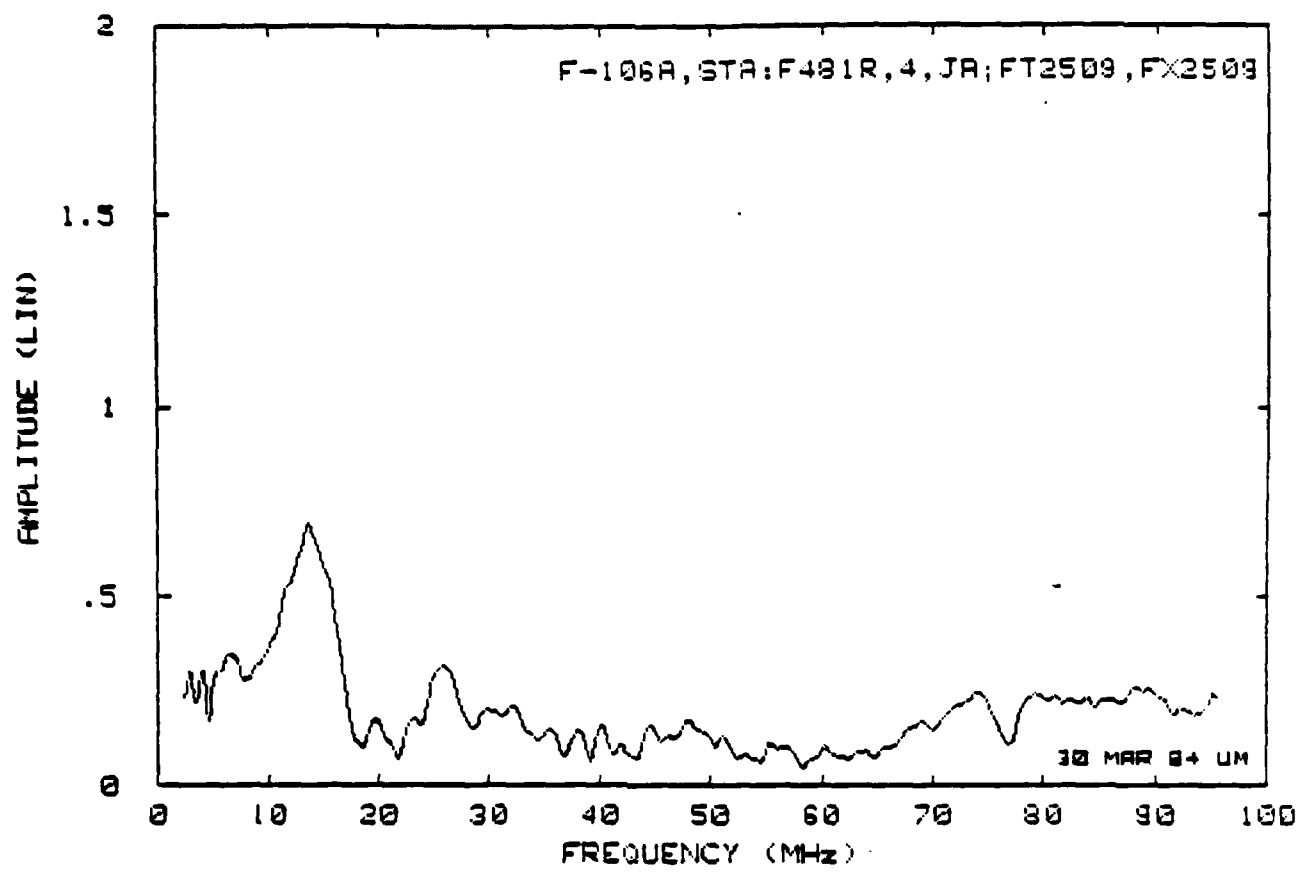


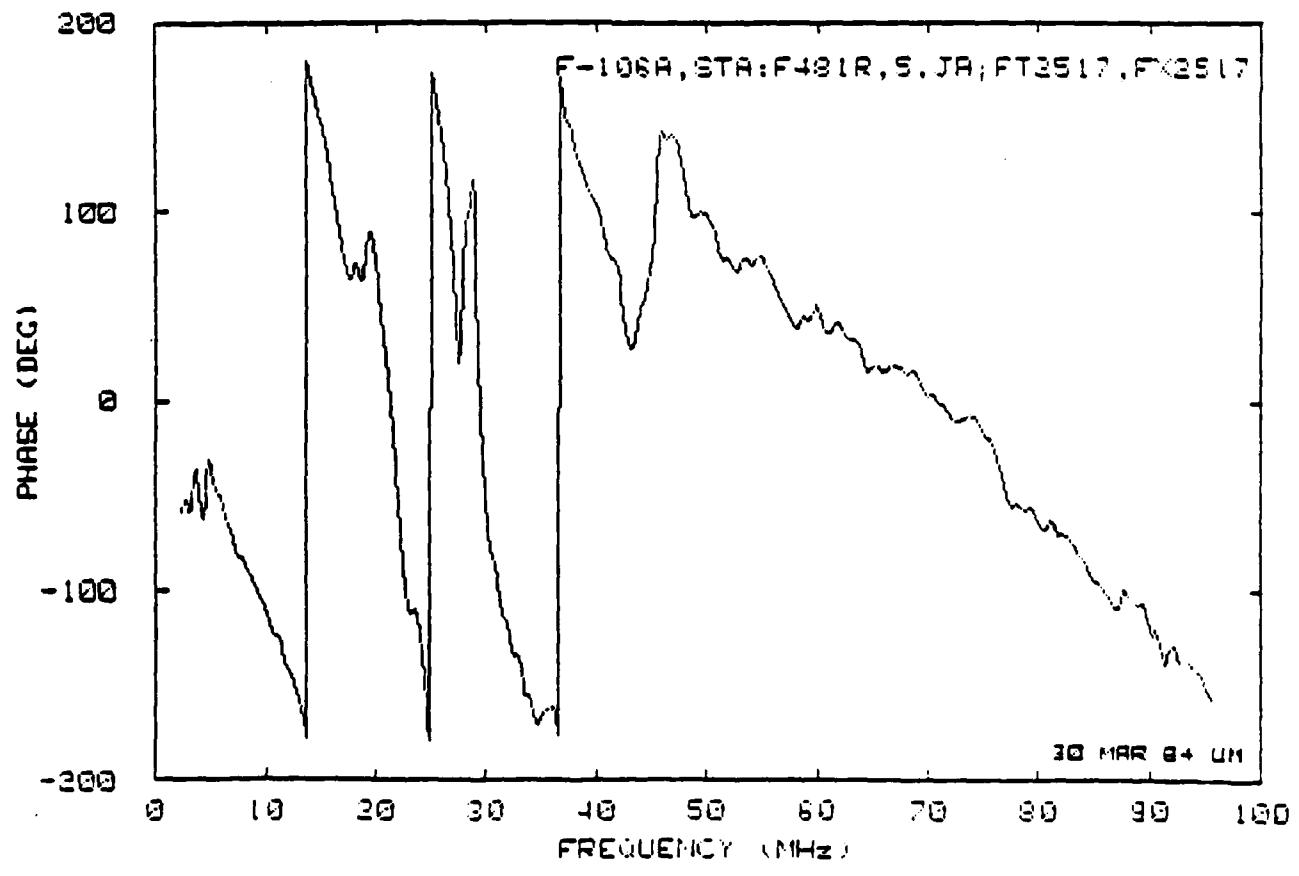
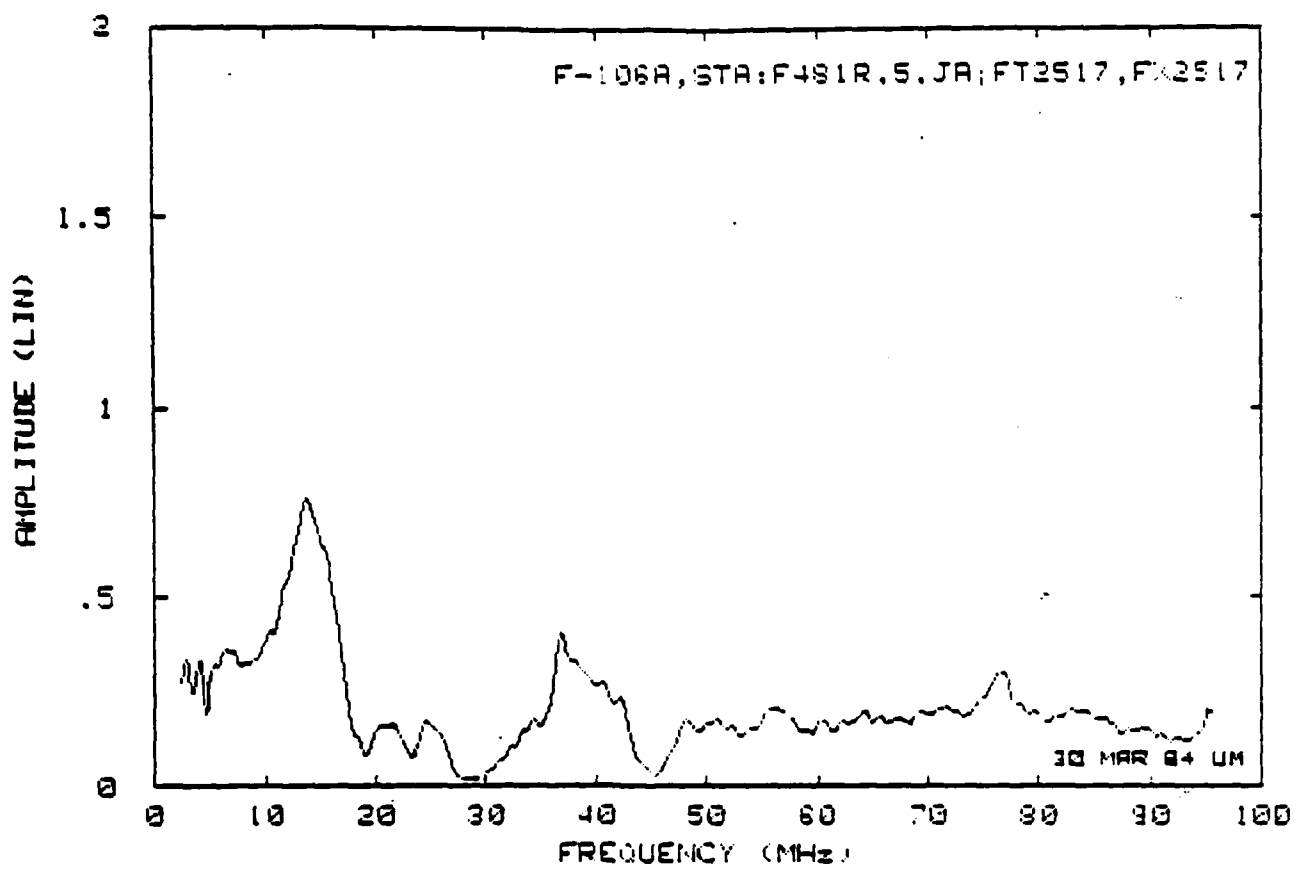












71/72

E AND D

10 - 8

DTTC